

1 **Glacial geomorphology of the Neutral Hills Uplands, southeast Alberta,**
2 **Canada: the process-form imprints of dynamic ice streams and surging ice**
3 **lobes**

4 David J. A. Evans¹, Nigel Atkinson² and Emrys Phillips³

5 1. Department of Geography, Durham University, South Road, Durham DH1 3LE, UK

6 2. Alberta Geological Survey, Twin Atria Building Suite 402, 4999-98 Avenue, Edmonton, Alberta, T6B 2X3,
7 Canada

8 3. British Geological Survey, The Lyell Centre, Research Avenue South, Edinburgh, EH14 4AP, UK

9

10 **Abstract**

11 The Neutral Hills Uplands of southern Alberta, Canada is an area of complex and varied glacial
12 landforms dominated by glacitectonic compressional structures but also containing expansive areas
13 of hummocky terrain and kame and kettle topography. It lies between the strongly streamlined
14 trunks of the former Central Alberta (CAIS) and Maskwa palaeo-ice streams of the SW Laurentide Ice
15 Sheet (LIS) and hence comprises an inter-ice stream regional moraine zone, constructed at around
16 15.5 cal ka BP. This study aimed to compile a regional map of the glacial geomorphology of the
17 central southeast Alberta in order to decipher the landform-sediment signatures of overprinted ice
18 stream margins in terrestrial continental environments, and to refine the palaeoglaciological
19 reconstructions for the southwest LIS. Detailed mapping from LiDAR and aerial imagery identifies
20 distinctive glacial landsystems diagnostic of the partial overprinting of cross-cutting ice stream
21 trunks and fast flow lobes. Widespread evidence of surge-diagnostic features indicates that the ice
22 streams experienced repeated flow instabilities, consistent with the broader scenario of a highly
23 dynamic and unstable SW LIS, characterised by markedly transitory and cross-cutting palaeo-ice
24 streams. The inter-ice stream moraine zone is characterised by spectacular glacitectonic
25 compression of bedrock, cupola hill construction and mega raft displacement but also displays
26 evidence of multi-phase stagnant ice melt-out, where partially overprinted surge lobes advanced
27 into large areas of buried glacier ice. Contemporaneous ice melting led to the widespread
28 development of glacier karst and the production of eskers at a range of scales, the largest of which
29 record deranged drainage patterns indicative of ice-walled channel sedimentation controlled by the
30 regional bedrock slope towards the northeast. These process-form regimes have created a
31 significant local relief that is a product of not only glacitectonic compression of bedrock but also the
32 creation and melting of a melange of ice and bedrock/sediment blocks of variable ice volume, which

33 are representative of former buried snout ice with a glacier karst system that was repeatedly
34 proglacially thrust due to surging. Widespread evidence for subglacial channel cutting is likely
35 strongly linked to the transitory, surging and cross-cutting nature of the palaeo-ice streams in the
36 region, whereby ice streams switched on and surged in response to the build-up, migration and
37 marginal outbursts of subglacial water reservoirs. In addition to the reduced basal friction caused by
38 the low permeability of the Cretaceous bedrock, pressurized groundwater and potentially also
39 shallow biogenic gas deposits were likely important to the process-form regimes of surging lobes of
40 soft-bedded ice streams in a region where ice flow was against an adverse bed slope; a scenario that
41 gave rise to a variety of enigmatic landforms such as doughnuts, doughnut chains, apparent blow-
42 out features and possible till eskers, as well as glacitectonic mega-rafts.

43 **Key words:** Palaeo-ice stream; inter-ice stream moraine; glacitectonics; hummocky terrain.

44

45 **1. Introduction**

46 The glacial geomorphology of the Canadian prairies of Alberta and Saskatchewan has been critical to
47 palaeoglaciological reconstructions of the southwestern Late Wisconsinan Laurentide Ice Sheet (LIS).
48 These reconstructions demonstrate that during full glacial and deglacial conditions, this sector of the
49 ice sheet was subject to ice streaming and the intermittent operation of surging lobes, which
50 promoted dramatic switches in ice flow directions (Clayton et al., 1985; Evans et al., 1999, 2008; Ó
51 Cofaigh et al., 2010; Margold et al., 2015; Atkinson et al., 2016; Fig. 1). The evidence for this complex
52 and dynamic behaviour is manifest in glacial landform-sediment assemblages and landsystems
53 arranged in large, arcuate ice-marginal subaerial depo-centres and moraines, lying downflow of
54 subglacially streamlined bedform corridors (Evans et al., 1999, 2008, 2012, 2014). This
55 palaeoglaciological signature has been likened to the terrestrial equivalent of ice stream/trough-
56 mouth fan systems of submarine settings (Evans et al., 2012), and on the prairies is representative of
57 marginal lobation and partial overprinting along the termini of fast ice flow corridors (Patterson,
58 1997, 1998; Colgan et al., 2003; Jennings, 2006; Evans et al., 2008; Ó Cofaigh et al., 2010; Margold et
59 al., 2015; Norris et al., 2018). The role of surging and changing basal thermal regimes in driving
60 spatial and temporal variability in landsystems associated with lobate ice stream margins are being
61 increasingly emphasised as higher resolution geomorphological mapping is undertaken (e.g.,
62 Mooers, 1990; Colgan et al., 2003; Evans et al., 2014, 2016a; Sookhan et al. 2018; Mulligan et al.
63 2019). Additionally, thinning and recession of these ice margins occurred down the adverse slope of
64 the regional drainage gradient, which promoted the development of large proglacial lakes, gave rise
65 to complex meltwater drainage patterns and ice-contact glacialfluvial features (Christiansen, 1979;
66 Kehew and Lord, 1986; Evans, 2000; Clayton et al., 2008; Utting et al., 2016). Also important are the
67 geomorphological implications of pressurised groundwater and possibly shallow gas in glacierized
68 Cretaceous bedrock terrains such as those of the Canadian prairies, where groundwater recharge
69 and over-pressurization of aquifers induced by ice sheet advance is thought to initiate substantial
70 blow-out features (cf. Mandl and Harkness, 1987; Bluemle, 1993; Boulton and Caban, 1995; Grasby
71 et al., 2000; Grasby and Chen, 2005; Lemieux et al., 2008).

72

73 Despite these improved reconstructions, a number of outstanding problems persist in the
74 interpretation of glacial landforms on the Canadian prairies, some of which have significant
75 longevity. For example, hummocky terrain and associated features like prairie mounds and
76 doughnuts (Gravenor and Kupsch, 1959) have been explained variously as the products of subglacial
77 pressing by passive deformation (Stalker, 1960; Eyles et al., 1999; Boone and Eyles, 2001), pingo

78 development (Bik, 1969), lake floor gas escape vents or lake ice features (Mollard, 2000), and
79 groundwater expulsion (Bluemle, 1993; Boulton and Caban, 1995; Evans, 2003; Evans et al., 2014).
80 Also, since the seminal work of Moran et al., (1980), glacitectonic processes have been widely
81 employed to explain a range of prairie landforms including hummocky terrain (e.g., Bluemle and
82 Clayton, 1984; Tsui et al., 1989; Evans, 2000; Evans et al., 2014). The role of glacitectonics is evident
83 at some classic sites (e.g., Mud Buttes; cf. Slater, 1927), which have been revisited to provide further
84 details into the nature of glacier-substrate interactions (Phillips et al., 2017). The range of alternative
85 explanations for glacial landforms on the Canadian prairies drives the need to critically examine the
86 wider and more diverse landform-sediment assemblages of the southwest LIS. Indeed, all these
87 explanations may play significant complementary roles in the development of the glacial
88 landsystems of the Canadian prairies, especially if the palaeoglaciological setting was, as widely
89 proposed, one of fast ice flow, changing basal thermal regimes, intermittently surging lobate ice
90 stream margins, and rapidly changing proglacial lake configurations.

91 One area that has been proposed as a former location of lobate and partly overprinted termini of
92 fast ice flow corridors is the Neutral Hills Uplands (Evans et al., 2008; Ó Cofaigh et al., 2010; Phillips
93 et al., 2017; Fig. 2), where complex glacial landform assemblages offer an opportunity to decipher
94 the patterns of deglacial ice sheet dynamics and their inter-relationships with regional topography,
95 climate and bedrock characteristics. The widespread juxtaposition in this area of enigmatic forms
96 such as prairie mounds, doughnuts, geometric ridge networks and hummocky terrain (Gravenor and
97 Kupsch, 1959; Mollard, 2000), in association with some of the most spectacular glacitectonic
98 features in North America (Hopkins, 1923; Slater, 1927; Aber et al., 1989; Fenton et al., 1993; Aber
99 and Ber 2007; Phillips et al., 2017), indicate that they likely emerge from a common, although
100 complex process-form regime and thereby constitute a specific glacial landsystem signature. The aim
101 of this study is therefore to compile a regional map of the glacial geomorphology of the central
102 portion of southeast Alberta, primarily the Neutral Hills Uplands, with the objective of deciphering
103 the landform-sediment signatures of overprinted lobate ice stream margins in terrestrial continental
104 environments, and to refine the palaeoglaciological reconstructions for the southwest LIS.

105

106 **2. Study area and methods**

107

108 The Neutral Hills Uplands comprises an area of glacitectonic constructional terrain which includes
109 the substantial composite ridges of the Neutral Hills (120 m high), Misty Hills (85 m high) and Nose
110 Hill (100 m high), as well as the more widely known cupola hill at Mud Buttes (50 m high) with its

111 well-exposed internal structures of intensely folded and thrust Late Cretaceous sandstones,
112 siltstones and mudstones (Figs. 2, 3, 4). These prominent landforms have long been recognized as
113 glacitected bedrock (Hopkins, 1923; Slater, 1927; Kupsch, 1962; Bayrock, 1967; Moran et al.,
114 1980; Shetsen, 1987, 1990; Evans et al., 2008; Phillips et al., 2017) and together form a suite of
115 landforms large enough to constitute a regional physiographic zone (Bostock, 1970a, b; Pettapiece,
116 1986). Geologically, the region is located in the south-central part of the Western Canada
117 Sedimentary Basin, which is characterised by fluvial and marine deposits associated with the
118 transgression of the Western Interior Seaway during the Late Cretaceous (Mossop and Shetsen,
119 1994). Previous work on the glacial landforms of the Neutral Hills Uplands includes surficial geology
120 mapping (Gravenor and Bayrock, 1955; Bayrock, 1958a, b, 1967; Shetsen, 1987, 1990; Kjeirsgaard,
121 1988) as well as local studies on the Mud Buttes and the large composite ridges of the Neutral and
122 Misty hills (Hopkins, 1923; Slater, 1927; Fenton et al., 1993; Phillips et al., 2017). The location of the
123 glacially thrust masses of the Neutral Hills Uplands has been related to LIS readvances against the
124 northernmost extension of the NW-SE orientated Missouri Coteau escarpment (Bretz, 1943; Evans et
125 al., 2008).

126

127 The geomorphology of the study area was mapped from a 15 m light detection and ranging (LiDAR)
128 bare-earth digital elevation model (DEM) specifically for more localised and larger scale detail and
129 the 30 m Shuttle Radar Topography Mission (SRTM) DEM for more regional trends. Features were
130 identified using their non-genetic, morphometric characteristics and then later assigned genetic
131 classifications. Reference was made to aerial photograph mosaics flown and compiled by the Alberta
132 Department of Lands and Forest in the 1950s, as well as Google Earth imagery. Also important were
133 archival maps of the glacial geology of the region, compiled by Gravenor and Bayrock (1955) and
134 Bayrock (1958a, b, 1967). This approach facilitated the identification and classification of ten types
135 of landform signature, each characterised by the occurrence and nature of linear or curvilinear
136 features or lineaments (sub-divided further according to parallel or non-parallel alignments),
137 conspicuous mounds with either rectilinear or rounded margins, hummocky terrain (including
138 distinctly patterned forms such as ridge-rimmed depressions or doughnuts and discontinuous
139 ridges), sinuous ridges and major channels and erosional cliffs or terraces.

140

141 The stratigraphy and sedimentology of the landforms was investigated wherever exposures were
142 available. As such exposures are relatively rare and/or ephemeral, archival material was utilised
143 wherever possible. Field exposures were recorded in scaled section sketches which included
144 information on primary sedimentary structures, bed contacts, sediment body geometry, sorting and

145 texture, as well as any pertinent data on clast macrofabric. These data were then used to
146 characterize lithofacies types and to allocate facies codes following the procedures of Evans and
147 Benn (2004). Clast macrofabrics were measured on samples of 30 or 50 clasts from diamictons using
148 A-axis orientation and dip, and plotted on Schmidt equal-area lower hemisphere diagrams using
149 Rockworks™. Contouring of the stereoplots represents standard deviations from the mean.

150

151 **3. Glacial geomorphology**

152

153 The glacial geomorphology map of southeast central Alberta, featuring the Neutral Hills Uplands, is
154 presented in Fig. 3 (see also Supplementary Information for high-resolution version). The ten types
155 of landform-sediment signature identified on this map are systematically described and interpreted
156 using typical example areas.

157

158 *3.1 Major glacitectonic thrust masses*

159 Both major glacitectonic thrust masses and lower amplitude lineaments and ridges (see section 3.2)
160 are recognised on the imagery as a series of closely spaced, parallel or sub-parallel, often sinuous
161 ridges and troughs. The ridges are the surface expressions of the crests of large-scale folds and/or
162 thrust-blocks and are clearly related to thrusting/glacitectonism of the underlying Cretaceous
163 bedrock and, to a lesser extent, pre-existing sediments (Fig. 4) (e.g., Kupsch, 1962; Christiansen and
164 Whitaker, 1976; Sauer, 1978; Moran et al., 1980; Bluemle and Clayton, 1984; Tsui et al., 1989;
165 Fenton et al., 1993). The intervening troughs demarcate the bounding thrust faults and synclinal
166 folds. A protocol for differentiating between glacitectonic ridges and similar looking recessional
167 push-moraines on the prairies was proposed by Evans et al. (2014). The large glacitectonic thrust
168 masses (composite ridges and hill-hole pairs, *sensu* Aber et al., 1989) of the region are well-
169 documented (e.g., Neutral Hills, Nose Hill, Misty Hills, Mud Buttes, Sharp Hills; cf. Shetsen, 1987,
170 1990; Fenton et al., 1993; Atkinson et al., 2014a, 2018; Fig. 2), consequently their surface expression
171 is easily recognised and mapped. Many prominent arcuate assemblages, for example in the Prospect
172 Valley area, document bedrock folding, detachment and displacement associated with readvances
173 and subsequent stagnation of Laurentide Ice Sheet lobes across existing Quaternary deposits (see
174 section 4). The orientation of these ridges is predominantly uni-directional and generally transverse
175 to the direction of applied stress (ice-push/glacier ice flow) and thereby can be used to delineate the
176 boundaries of individual thrust masses. However, multiple ridge orientations are also preserved in
177 some areas and record the presence of juxtaposed thrust masses or those with apparently
178 superimposed or overprinted glacitectonic signatures. In some areas, the overprinting is so extensive

179 that individual thrust masses cannot be delineated, but instead the landform patterns are mapped
180 as zones of lineaments and ridges (see section 3.2).

181

182 The juxtaposition of separate thrust masses and the overprinting of tectonic fabrics clearly records
183 repeated phases of glacitectorism which led to the construction of composite ridges and hill-hole
184 pairs. An excellent example occurs around the south shore of Killarney Lake, where a thrust mass has
185 been displaced to form the depression now occupied by this, and several other large lakes (Fig. 5a).
186 Mapped as thrust bedrock by Bayrock (1967), the surface crenulations of the main thrust mass are
187 orientated in two directions of NNW-SSE and WNW-ESE, both indicating displacement from the
188 source depression immediately to the north. Although the sequence of overprinting is difficult to
189 determine, it appears that the thrusting was initially from the NNE (phase 1) and probably coincided
190 with the detachment and transport of a ~18 km² bedrock raft 25 km further to the southwest, which
191 now forms a low hill between Fleeinghorse and Laurence lakes (Fig. 5a) and likely relates to flow at
192 the westernmost edge of Maskwa Ice Stream (cf. Norris et al., 2018). A subsequent phase of
193 compression from the ENE (phase 2) resulted in the development of ridges which crosscut the earlier
194 phase 1 thrust mass (Fig. 5a) as well as a series of densely-spaced crenulations aligned NNW-SSE on
195 the east shore of Killarney Lake (Fig. 5a) which continue northwards for some 13 km towards the
196 town of Chauvin, where they form part of the hill-hole pair now occupied by Reflex Lakes (Fig. 3).
197 The final phase of glacitectorism in the Killarney Lake area led to the formation of an arcuate set of
198 crenulations on the proximal side of the main thrust mass which cross-cut the earlier phase 2
199 landforms and are consistent with a direction of ice-push from the north and NNE (phase 3).

200

201 Outcrops through the Killarney Lake thrust mass are located on the summit and proximal slopes (KL1
202 and KL2; Fig. 5a) and expose a core of Quaternary sediment rather than bedrock (Fig. 5b). Section
203 KL1 reveals >1 m of laminated sands and fines with massive gravel lenses unconformably capped by
204 a 1.2 m thick matrix-supported diamicton that exhibits a lower pseudo-laminated and upper massive
205 appearance. This diamicton is in turn overlain by a massive, matrix supported diamicton with a more
206 clay-rich matrix. The contact of the two diamictons is sharp and is also marked by an attenuated lens
207 of mudstone derived from the local bedrock and which thickens to 1.1 m in mid-section and pinches
208 out to the right and left sides of the exposure. The diamictons are typical of the tills in the region.
209 Where pseudo-laminated, they have been derived by glacitectoric cannibalisation of underlying
210 glaciallacustrine deposits, here represented by the lower laminated deposits; vertical gradation to a
211 massive appearance reflects homogenisation in the deforming layer (Evans et al., 2006, 2012; Evans,
212 2018). A clast macrofabric from the lower Dml indicates an early glacier stress direction from 322°,

213 which corresponds with subtle fluting orientations to the north and east of the site (Fig. 3). The
214 emplacement and attenuation of the mudstone lens relates to a later phase of ice flow but a
215 macrofabric on the upper diamicton does not provide a clear sense of the shearing direction; it
216 instead displays high dip angles (average of 47°) typical of crevasse squeeze deposits (cf. Evans and
217 Rea, 2003; Evans, 2018). Section KL2 displays up to 4 m of pseudo-laminated diamicton within which
218 there is a <0.5 m layer of sheared and attenuated sand and silt laminae, glacitectonically interleaved
219 with the overlying and underlying diamicton (Fig. 5b). Repetition of the lower Dml and overlying
220 sheared sands, silts and diamict within the lower part of the section provide evidence of larger-scale
221 thrust-repetition and imbrication of the sequence. Importantly this lower imbricated sequence is
222 truncated by the base of the upper Dml (see Fig. 5b). The stress direction for this event is recorded in
223 a clast macrofabric from the lower part of the upper diamicton, which displays a weak easterly to
224 northeasterly dipping signature. The consistency of the lower fabrics from both Killarney Lake
225 sections is a record of early ice flow over glaciallacustrine deposits in the area, after which thrusting
226 displaced and attenuated glaciallacustrine deposits and bedrock. Of the thrust directions apparent in
227 the surface crenulations of the thrust mass, only the northeasterly imposed stress (phase 3) is
228 recorded in the upper till fabric.

229

230 A further example of overprinted tectonic fabrics is the assemblage of thrust masses comprising the
231 western Neutral Hills and the Nose Hill/Ribstone Creek area (Figs. 3, 5c). Here the predominant ice
232 flow direction and displacement is from north to south, but individual thrust masses recording this
233 displacement are superimposed on an older set of more subtle ridges recording glacitectonic stress
234 from the WNW or NW, which is consistent with the relative age and orientation of large-scale
235 flutings in the region (Ó Cofaigh et al., 2010; Atkinson et al., 2014b). Additionally, the most recent
236 thrust masses display arcuate ridge patterns and evidence of periclinal to dome-like folding of the
237 bedrock strata, created as they were displaced from up-ice depressions to form hill-hole pairs
238 (especially well illustrated by the thrust masses south of Sounding Lake and by Nose Hill; Fig. 5c).
239 Although the cores of these thrust masses are clearly bedrock, the relatively smaller ridges located
240 on their distal slopes are composed of deformed (folded and thrust) penecontemporaneous
241 Quaternary glacial deposits. Collectively, these glacitectonic landforms form an east-west aligned
242 assemblage which can be traced across the centre of the map area, which because it has not been
243 glacially overrun, must demarcate the limit of an ice sheet readvance. In contrast, the older, more
244 subtle ridges comprise elongate chains of hummocks, locally heavily incised and overprinted with
245 glacialfluvial landforms (see sections 3.6-3.8) and appear to have been developed mostly in
246 Quaternary deposits.

247

248 To the south of the Neutral Hills, complex overprinting of thrust masses is evident in the multiple
249 ridge orientations of the Misty Hills, Sharp Hills, Mud Buttes and Esther uplands (Figs. 2, 3). Here the
250 outermost (southern) thrust masses form an arcuate assemblage indicative of an ice lobe that
251 advanced towards the south and displacement of bedrock derived from the large topographic
252 depression now partially occupied by Grassy Island Lake and its subsidiaries (Fenton et al., 1993; Fig.
253 6). The subsequent displacement and partial rotation of thrust masses in the horizontal plane inside
254 the arcuate assemblage records further thrusting events, manifest in the construction and overriding
255 of the Mud Buttes cupola hill (Phillips et al., 2017; see section 3.3). Towards the east of the Misty
256 Hills complex lies a terrain with similar partially overprinted lineations but recognising the
257 boundaries of the individual thrust masses is difficult due to a discontinuous blanket of glacial
258 landforms and sediments (Grassy Island Moraine of Phillips et al., 2017) deposited during the final
259 downwasting of the ice lobe within the Grassy Island Lake depression (see section 4). The western
260 edge of the complex comprises a block with strongly N-S aligned ridges and furrows, which are
261 muted on their westernmost flank due to an overlying layer of till (Fig. 6). This till relates to a subtle
262 fluting alignment (see section 3.4) recording ice flow from the west and the construction of the
263 western thrust block at the margin of this flow event. The eastward displacement of the western
264 block was significant enough to superimpose N-S-trending glacial tectonic ridge pattern upon an
265 arcuate but predominantly E-W structural grain observed within the centre of the Misty Hills
266 complex.

267

268 Although these major thrust masses are mantled by discontinuous till veneers that predate a series
269 of later ice lobe readvances, they are clearly composed of Cretaceous bedrock. Nevertheless, ridges
270 and furrows on their summits locally contain features normally associated with sediment-cored
271 glacial landform-sediment associations. These include ridge-rimmed depressions or doughnuts
272 and isolated ponds reminiscent of kettle holes, as well as areas that have been subject to mass
273 movement and the production of apparent retrogressive flow scars (Fig. 7).

274

275 Like the doughnuts observed between recessional push moraines in other areas of the prairies
276 (Evans, 2003; Evans et al., 2014), those on the summits of the major thrust masses are often aligned
277 to form discontinuous chains within the tectonically controlled furrows (Fig. 7a). Previous
278 observations of such features on the proximal slopes of thrust masses (e.g. Dirt Hills, Saskatchewan)
279 have been attributed to the escape of over-pressurized groundwater or artesian escape vents, which
280 played a critical role in the large-scale displacement of bedrock and was then released through the

281 fractured thrust mass once glacier stress dropped (“extrusion moraines” of Boulton and Caban,
282 1995). Similar features have been reported from the immediate distal slopes of prairie-based
283 glacitectonic thrust masses, where they are termed hydrodynamic blowouts (Bluemle, 1993) and in
284 some cases eskers can emerge from source depressions, indicating that pressurised water created
285 tunnels beneath the glacier snout where it overrode the thrust mass (Bluemle and Clayton, 1984).

286

287 Modern analogues for this process have been reported from the distal slopes of composite ridges
288 created by glacier surging in Iceland, where pipes emerge from the moraine front and have clearly
289 discharged meltwater into channels on the foreland (Kjær et al., 2006). Not unrelated is Bik’s (1969)
290 theory that doughnuts might represent pingo scars, whereby groundwater emerging from
291 upwellings in the immediate proglacial zone has the potential to freeze in winter and construct icings
292 or afeis, such as occurs on glacier forelands in Svalbard (Gokhman, 1987; Hodgkins et al., 2004).
293 This process may be accentuated by supercooling due to rapid de-pressurization as groundwater
294 migrates from the subglacial system into the proglacial zone (cf. Cook and Knight, 2009).
295 Sedimentologically, all of these blowout or injection features would be recorded as clastic dykes or
296 hydrofracture infills (Mandl and Harkness, 1987; Le Heron and Etienne, 2005; van der Meer et al.,
297 2009; Phillips et al., 2013). Although groundwater is more widely cited as the cause of blowout
298 features, another potential driver in the Cretaceous strata of the prairies could be methane release
299 during the last deglaciation. Changing pressure and temperature regimes associated with the retreat
300 of the Scandinavian Ice sheet are proposed to have triggered dissociation of shallow gas hydrates
301 and the release of methane, resulting in widespread pockmarks on the floors of the North, Barents
302 and Norwegian seas (Cremiere et al., 2016; Mazzini et al., 2017). On the prairies, the influx of
303 meltwater from the LIS is proposed to have displaced brines that previously inhibited microbial
304 action within organic rich units of the Western Canada Sedimentary Basin, thereby triggering
305 methanogenesis and re-establishing conditions suitable for the formation of shallow biogenic gas
306 deposits (Grasby, 2013). Degassing of these deposits in terrestrial settings potentially produced
307 doughnut-shaped ring forms similar to those of blowouts associated with escape of pressurised
308 groundwater, since the preservation potential of constructional features would be higher than in
309 subaqueous environments.

310

311 Larger burst-out structures are evident on the crests and distal slopes of some large thrust masses,
312 the best example being on the eastern end of the eastern Neutral Hills (Fig. 7a). This feature
313 comprises a fan shaped assemblage of doughnut forms, which blanket and mostly mask the
314 structural lineaments, with an apex located at a discontinuous but deep channel through the thrust

315 mass summit occupied by a chain of ponds. An esker starts at the eastern side of the channel and
316 extends towards the ENE through the glactectonic ridges and furrows as an ice-margin parallel
317 feature directed by the topography emerging from the thinning snout (cf. Storrar et al. in press). The
318 esker likely represents a later stage of water release after near surface pressurised water was
319 initially driven through the thrust mass to emerge through artesian pipes and then via the surface as
320 a fan.

321

322 Isolated pits, often containing small ponds, are enclosed by cliffed or steep margins that cut across
323 the structural grain represented by the ridges and furrows (Fig. 7b). Larger pits, often occurring in
324 chains and bounded by fault scarps, also cut across structural ridges but appear to represent the
325 collapse of larger volumes of the thrust masses, especially around their lower margins (Fig. 7c).
326 These depressions most likely represent voids created by the melt-out of glacier ice and hence are
327 kettle holes but their occurrence on the summits of thrust bedrock masses is difficult to reconcile
328 with such an origin unless debris-covered stagnating ice was lying on the land surface prior to
329 proglacial thrusting. More extensive buried glacier ice is evidenced by the larger pits and associated
330 fault scarp boundaries. Where these occur on proximal slopes of thrust masses they are associated
331 with greater fragmentation of structural lineaments and more hummocky terrain and hence
332 represent melt-out of the glacier snout that overrode the back of the moraine. Where they lie on
333 distal slopes their boundaries/cliffed shorelines often tend to be rectilinear or arcuate and they
334 parallel the structural grain of the surrounding lineaments (Fig. 7c). This indicates that large bodies
335 of glacier ice were incorporated in the thrust mass and that they constituted thrust slices that later
336 melted out to form elongate depressions. The corollary is that, prior to thrusting by the readvancing
337 ice lobes, large areas of stagnating glacier ice occupied the prairie surface and these buried ice
338 masses likely contained glacialfluvial sediment assemblages such as eskers and kamiform features.

339

340 More enigmatic are conspicuous mass movement features that resemble large retrogressive flow
341 scars. They are often associated with melt-out pits and lie in and around the major thrust masses
342 where they appear to relate to mass failure in the oversteepened topography. One enormous
343 example, up to 40 m deep and hosting a large (1.4 km long) lake, lies on the distal slope of the west
344 end of the eastern Neutral Hills, immediately south of Sounding Lake (Fig. 7d). Here the
345 displacement of mass was towards the northeast to form an arcuate cliff and source depression and
346 a ridged, lobate failure mass with a leveed failure toe. As the volume of the failed mass appears to
347 equate to the size of the source depression, an ice melt-out origin is unlikely and hence failure may
348 have been triggered by pressurised groundwater driven from the thrust mass immediately to the

349 northwest of the site. Further similar features, more likely to relate to ice melt-out, occur
350 throughout the major thrust masses in the arc of composite moraine ridges that demarcate the
351 readvance margin of the Prospect Valley lobe to the north (see section 4).

352

353 *3.2 Short lineaments and ridges*

354 A range of short lineaments and ridge types are evident in the map area and conform generally to
355 the classifications of major transverse ridges (MTR) types 1 and 2 of Evans et al. (2014). In many
356 areas, differentiating MTR type 1 and 2 from the imagery is difficult, especially in the absence of
357 outcrops, and therefore the map unit is defined as “lineaments and ridges (including definite and
358 possible glacitectonic structures and areas of recessional push moraines)” (Fig. 3). The potential
359 occurrence of esker fragments in these assemblages is also acknowledged.

360

361 The MTR type 1 constitute corrugation patterns indicative of glacitectonic thrusting but, unlike those
362 reported by Evans et al. (2014), are not always fluted and hence many do not have the appearance
363 of unequivocally being glacially overrun (Figs. 8a, b). They are interpreted as the product of shallow,
364 thin-skinned folding and thrusting of bedrock or sediment and resemble, albeit with lower
365 amplitudes, the ridged and furrowed surfaces of the relatively deeper-seated major thrust masses
366 described above. Cross-cutting lineaments, similar to those identified in major thrust masses, record
367 superimposed or overprinted glacitectonic signatures, although individual thrust masses cannot be
368 delineated in areas of extensive overprinting. Instead, the landform patterns are mapped as zones of
369 lineaments and ridges (Fig. 8c). Large areas such as this are also characterised by ridge
370 fragmentation due to dense pitting and the occurrence of kettle holes whose margins dissect all
371 lineament sets. Although there is a hummocky appearance to these areas, the preservation of cross-
372 cutting lineaments indicates that pitting was due to melt-out after the tectonic grain was developed.
373 Hence it appears that large bodies of glacier ice were incorporated in the thrust masses as thrust
374 slices that later melted out to form elongate depressions. Similar to the kettle holes and melt-out
375 pits developed on the major thrust masses, these landform associations indicate that large areas of
376 stagnating glacier ice occupied the prairie surface prior to thrusting by readvancing ice lobes, and
377 glacialfluvial sediment assemblages such as eskers and hummocky kamiform features (cf. Eyles et al.,
378 1982) developed prior to and after thrusting.

379

380 The MTR type 2 are recessional push moraines similar to those developing at modern active
381 temperate glacier snouts (Fig. 8d) and only locally occur in the southern part of the map area. In
382 areas where ridge patterns are extensively overprinted and are not mapped as major thrust masses,

383 some of the ridges could represent recessional push moraines superimposed over glacitectonic
384 fabrics, especially if melt-out pits and kettle holes do not cross-cut all lineament sets. Alternatively,
385 the multiple ridge orientations record superimposed tectonic fabrics typical of complexly folded and
386 faulted strata (cf. Price and Cosgrove 1990; Hatcher 1995). A glacitectonic origin is favoured for
387 these linear, sub-parallel ridges rather than a minor recessional push moraine origin (*sensu* Benn and
388 Evans 2010), which tends to result in sinuous, crenulate or sawtooth and/or locally bifurcating
389 planforms that preserve the shape of the former receding ice margin (MTR type 2 of Evans et al.,
390 2014; cf. Boulton, 1986; Krüger, 1995; Evans and Twigg, 2002; Evans et al., 2016b, 2017; Chandler et
391 al., 2016).

392

393 *3.3 Conspicuous mounds and relatively higher topography (cupola hills and rubble terrain)*

394 Areas of smoothed, often fluted terrain that rise relatively abruptly above the surrounding prairie
395 surface are characterised by the presence of muted ridges or corrugations on their surface similar to
396 the sub-parallel lineations of thrust mass surfaces (Fig. 9). Such features have been reported
397 previously from prairie settings by Evans et al. (2014), who classify them as MTR type 1 and interpret
398 them as glacially overridden thrust masses or cupola hills (*sensu* Aber et al., 1989). Their arcuate or
399 lobate plan forms often indicate an ice-marginal origin, as demonstrated by the terrain immediately
400 north of the town of Coronation (Fig. 9a). A more elongate ridge lies immediately NE of Sounding
401 Lake and is adorned with flutings and geometric ridge networks created during the last phase of
402 subglacial streamlining of the area (Fig. 9b); its surface also contains pits indicative of ice melt-out,
403 similar to the ice-cored drumlins reported by Schomacker et al. (2006). A classic example of a cupola
404 hill is the Mud Buttes complex, where extensive exposures clearly demonstrate its multi-phase
405 glacitectonic origins (Phillips et al., 2017; Fig. 4c). More difficult to identify are overridden thrust
406 masses whose structural lineaments parallel the direction of the later overriding ice flow. One such
407 example occurs in the south of the map area and was initially displaced southwards from the
408 Sounding Creek depression. This was later overrun by ice flowing eastwards, as manifest in flutings
409 that cross the cupola hill summit as well as the adjacent prairie surface. On the cupola hill summit,
410 the underlying bedrock structures are apparent as sharp relief, narrow ridges that lie sub-parallel to
411 the more linear flutings (Fig. 9c).

412

413 Smaller upstanding masses of displaced bedrock are common throughout Alberta and have been
414 classified as “rubble terrain” by Fenton et al. (1993) or “aligned rubble” by Atkinson et al. (2018).
415 They comprise assemblages of small hills, often with rectilinear edges, that have been displaced
416 from a nearby source depression, but in contrast to hill-hole pairs the thrust mass has been

417 disaggregated down flow within narrow dispersal trains that typically parallel other ice flow features
418 such as flutings (Atkinson et al., 2018). The blocks are essentially mega-rafts (*sensu* Stalker 1973,
419 1976; Aber et al., 1989) and may be located only a short distance from fault-bounded or fracture-
420 bound source depressions, which are often visible as straight-edged lakes (Aber et al., 1989; Fenton
421 et al., 1993). A range of examples exist in the map area and include elongate assemblages that have
422 been widely dispersed from their likely source (e.g. southeast of Kirriemuir; Fig. 10a), isolated rafts
423 that lie within other landform suites but are identifiable by their surface morphology (Fig. 10b), and
424 incipient rafts that have been moved only a short distance from their fracture-bounded depressions
425 (Fig. 10c). At smaller scales certain flutings appear to be composed of chains of closely spaced mega-
426 rafts, here termed “rubble stripes” (Fig. 10d), where disaggregated bedrock has been differentially
427 displaced downflow and increasingly broken down into smaller fragments, and consequently
428 involved in grooving the glacier bed. Such fluting-like landforms are instructive in that they
429 demonstrate the juxtaposition of subglacial grooving as well as stoss-and-lee streamlining processes
430 in fluting production (see section 3.4).

431

432 Although the constituent blocks within rubble terrain are normally assumed to be bedrock,
433 exposures can reveal that the displaced and disaggregated materials comprise Quaternary deposits.
434 For example, at the Kirriemuir assemblage (Fig. 10a) a quarry exposure through one of the blocks
435 reveals a core composed of normally faulted, rhythmically bedded sands, silts and clays with gravel
436 lenses, coarsening upwards to horizontally bedded gravels and sandy gravels, which are in turn
437 deformed and truncated by a massive, matrix-supported diamicton with attenuated sand lenses and
438 stringers diagnostic of subglacial traction till (Evans et al., 2006; Evans, 2018; Fig. 10e). These
439 sediments are compatible with initial sedimentation in an ice-walled lake plain (Clayton and Cherry
440 1967; Clayton et al., 2008; see Section 3.7) which was later glacitectonically displaced and overrun by
441 ice flowing towards the SSE, as indicated by the subtle flutings running through the rubble
442 assemblage (Fig. 10a) and asymmetrical folds and low-angle extensional faults in the deformed
443 sediments (Fig. 10e); a clast macrofabric from the till on the southern edge of the block displays a
444 WSW dipping signature indicative of till plastering over the distal slope of the feature.

445

446 *3.4 Multiple parallel lineations (flutings and ice flow-aligned stripes)*

447 Areas of straight, parallel lineations represent subglacially streamlined terrain and comprise flutings
448 and elongate drumlins up to 14 km long. They occur in assemblages that represent flow sets aligned
449 at various orientations and thereby relate to sequential changes in ice flow directions. Flow sets
450 have been employed over the wider region of the Canadian prairies to demarcate the imprints of

451 palaeo-ice streams and their cross-cutting relationships (Ross et al., 2009; Evans et al., 1999, 2008,
452 2014; Ó Cofaigh et al., 2010; Atkinson et al., 2014a, b; Paulen and McClenaghan, 2015; Norris et al.,
453 2018) and in the map area represent the footprints of a number of lobate ice streams. The
454 appearance of variously orientated flutings in association with other ice-stream marginal landforms
455 enables establishing a relative chronology of events in the map area (see Section 4).

456

457 In the west, the bed of the Central Alberta Ice Stream (CAIS; cf. Evans et al., 2008) is recorded by
458 NNW-SSE aligned flutings (Fig. 11a) south of Coronation. These features comprise corridors of
459 grooved terrain, interspersed within bar-channel complexes of the “Coronation-Spondin scabland”
460 (Sjogren and Rains, 1995). Importantly, the grooves narrow downflow, coincident with an increase in
461 the number of progressively narrower positive relief flutings. Also significant in the area is the
462 development of hill-hole pairs, which exhibit subtle superimposed flutings (Fig. 11a). The sequence
463 of landform production in this area is evident from flutings cross-cutting the bar-channel complexes,
464 indicating that the water flow responsible for this scabland pre-dated the subglacial streamlining and
465 the production of the grooved corridors; indeed the more subtle flutings would not have survived
466 the fluvial erosion. The configuration of many of the bar-channel complexes also appear to have
467 been guided by the position of overridden thrust mass lineations. This detail, now evident in LiDAR
468 imagery, contradicts an earlier reconstruction that the CAIS ice stream footprint was cross-cut by the
469 flood features (cf. Evans et al., 2008), although the proposed subglacial origin of the fluvial erosion
470 remains valid. This sequence of events is compatible with the proposal by Evans et al. (2008) that
471 basal sliding rather than till deformation was driving fast ice flow in this area of thin till cover.
472 Specifically, ice-bed decoupling may have been initiated by the subglacial meltwater activity, which
473 itself was triggered by the sub-marginal decanting of ice-dammed lake waters from the receding LIS
474 margin further to the west. The fluting production during ice streaming appears to have been
475 developed at the up-ice end of the corridors by groove ploughing, with the southeastward narrowing
476 of the grooves indicating progressive down-ice comminution of the displaced block. As the grooves
477 begin at the overridden thrust moraine belt near Coronation (Fig. 9a), we propose that ploughing
478 was initiated by displaced bedrock mega-rafts, a process that is evident in the study area in the
479 widespread assemblages of rubble terrain and fluting-like rubble stripes. The creation of narrow
480 upstanding flutings in a down-ice direction within the groove corridors is attributed to the combined
481 effects of the stoss-and-lee deformation process (cf. Boulton, 1976; Rose, 1989; Benn, 1994) and
482 longitudinal erosion of grooves by the remaining fragments of the mega-rafts, together with the
483 accompanying lateral deformation/displacement of material to form the paraxial ridges (Atkinson et

484 al. 2018). Raft liberation within the groove corridors is evident also in the occurrence of streamlined
485 hill-hole pairs.

486

487 Further evidence demonstrating the importance of bedrock mega-rafts to fluting construction are
488 rubble stripes (Fig. 10d), where flow-parallel lineaments appear to be composed of chains of closely
489 spaced mega-rafts. Excellent examples occur along the footprint of a palaeo-ice stream in the north
490 of the map area (Fig. 11b), herein named the Fabyan-Amisk ice stream after the towns located in the
491 north and south of the footprint respectively; this former ice stream bed extends some 22 km north
492 of the map in Fig. 3. Large areas of the fluted ice stream bed contain disaggregated bedrock, with
493 blocks in various stages of down-ice transport and comminution. The hypothesized role of rubble
494 stripes and mega-rafts on the initiation of stoss-and-lee flutings as well as subglacial bed grooving
495 can be tested by identifying raft origins and linking the starting points of both positive and negative
496 relief flutings to those rafts. On the Fabyan-Amisk ice stream bed, the initiator clusters or partially
497 disaggregated thrust masses occur at the south margin of a large preglacial valley thalweg (Stalker
498 1961; Farvolden 1963; Andriashek, 2018), where glacitectonic dislocation is widely known to liberate
499 bedrock blocks (Tsui et al., 1989). Groove and mega-raft pairs also clearly illustrate the role of
500 grooving in subglacial landform evolution (Fig. 11c).

501

502 *3.5 Rectilinear ridges (geometric ridge networks)*

503 Geometric ridge networks (Bennett et al., 1996) are conspicuous landforms on the prairies and have
504 been widely reported (Flint, 1928; Sproule, 1939; Deane, 1950; Colton, 1955; Gravenor and Kupsch
505 1959; Atkinson et al., 2018). They have been described as straight or slightly arcuate till-cored ridges
506 that intersect at acute or right angles to form waffle, diamond, or box-shaped patterns and with
507 some intersections resembling hairpins or wishbones. These characteristics were initially attributed
508 to crevasse infills (Gravenor and Kupsch, 1959), with more recent studies on modern glacier
509 forelands classifying such features as crevasse squeeze ridges (CSRs) related to surge-type behaviour
510 (Sharp, 1985a, b; Bennett et al., 1996; Evans and Rea, 1999, 2003; Evans et al., 2007). These modern
511 analogues have been used to infer palaeo-ice stream surging on the Canadian prairies by Evans et al.
512 (1999, 2008, 2016a), where the arcuate, ice flow-transverse and subparallel sets of conjugate paired
513 ridges are created by subglacial sediment injection into full depth, mode 1 tensional crevasses
514 following the switch from surge to quiescence phases (cf. van der Veen, 1998a, 1998b; Rea and
515 Evans, 2011).

516

517 The geometric ridge networks of the map area have all the characteristics of CSRs (Fig. 12). They
518 occur across the full width of the various ice stream trunks or lobate footprints and predominantly
519 display arcuate, downflow-convex limbs similar to those reported by Evans et al. (1999, 2008), rather
520 than within discrete, relatively narrow corridors such as described by Evans et al. (2016a) within the
521 trunk of the Maskwa Ice Stream to the east of the map area (cf. Ross et al., 2009; Ó Cofaigh et al.,
522 2010; Norris et al., 2018; Fig. 1). They are everywhere intimately associated with long flutings
523 indicative of fast flow trunk zones (Fig. 3), such as on the bed of the CAIS to the west, in the footprint
524 of the Prospect Valley lobe (see section 4), and in the trunk zones of the Fabyan-Amisk (Fig. 11b) and
525 Eyehill Creek-Sounding Lake ice streams (see section 4). They also occur immediately inside arcuate
526 assemblages of thrust masses similar to their occurrence in modern surging glacier foreland records
527 (Sharp, 1985a, b; Evans and Rea, 1999, 2003; Evans et al., 2007), for example, north of Provost and
528 west of Wainwright (Fig. 3). The CSR field on the bed of the CAIS around the town of Brownfield
529 displays further features considered diagnostic of glacier surging such as zig-zag eskers (Fig. 12a;
530 Knudsen, 1995; Evans and Rea 1999, 2003; Evans et al., 2007).

531

532 Exposures through the CSRs in the region are rare but a road cut to the north of the map area, in the
533 CSR field around Lloydminster (the northern extension of CSRs of the Prospect Valley lobe) (Fig.
534 12b), provides some insight into their sedimentology. This exposure is cut through a single CSR and
535 displays a two tiered diamicton (till) sequence from which clast macrofabrics are generally weakly
536 aligned NNW-SSE, especially at the core of the ridge, but weaken significantly at the ridge flanks and
537 include some very high clast dip angles. Overall the clast dip angles are relatively high (averages
538 ranging 25-44°; Fig. 12c) and indicate a significant squeeze component in landform construction (26-
539 44° for modern Icelandic CSRs; cf. Evans and Rea, 2003; Evans, 2018). A clast fabric shape plot for the
540 Albertan and modern Icelandic CSR tills also reveals a range of fabric strengths (Fig. 12b) but
541 predominantly indicative of materials that have been subject to relatively low strains (Evans, 2018
542 and references therein).

543

544 *3.6 Sinuous ridges (eskers)*

545 Sinuous ridges in formerly glaciated terrains are indicative of glacialfluvial sedimentation in ice-walled
546 channels or tunnels and many have been previously mapped in the study area (Gravenor and
547 Bayrock, 1955; Bayrock, 1958a, b, 1967; Shetsen, 1987, 1990; Kjearsgaard, 1988; Atkinson et al.,
548 2018). Most eskers generally have narrow and often discontinuous, sharp-crested sinuous ridges but
549 the map area also contains some very large, flat-topped examples that pass laterally into flat-topped
550 hills (prairie mounds or plains plateaux of Gravenor and Kupsch, 1959; see section 3.7). These

551 unusually large landforms were previously partially identified in the area by Bayrock (1967). The
552 most impressive example spans the Sounding Lake depression and extends for over 90 km, with
553 parts of its flat summit reaching widths of 2 km (Fig. 13a). The main ridge of the Sounding Lake esker
554 displays a torturous alignment with predominant NW-SE and N-S trends and a conspicuous circular
555 deflection that forms part of a 180° change in direction at the eastern end, immediately north of the
556 lake. Additionally, the largely single crested main ridge is joined by tributaries and distributaries
557 composed of smaller multiple ridges. In the south, the most intricate feeder system emerges from
558 Neutral Valley and trends north-northeastwards, where it joins up the western elbows of the main
559 ridge before continuing northwards beyond the town of Metiskow. Additional braided esker
560 networks join the southern part of the main ridge from the Neutral Hills, on the west side of
561 Sounding Lake. These widen and converge to form large flat-topped ridges where they meet the
562 main ridge. A further branch of ridges trends northeastwards from the northern part of Sounding
563 Lake esker past the town of Cadogan. The two northern ends of the esker extend towards the
564 composite thrust moraine arc of the Prospect Valley lobe where readvance of the ice margin appears
565 to have compressed the esker into the moraine (see Section 4). Although they do not occupy deeply
566 incised valleys, these flat-topped esker ridges resemble Type 3, ice-walled canyon eskers (cf. Perkins
567 et al., 2016) which exhibit flat-crested segments resulting from lake sedimentation. This depositional
568 environment is compatible with our observations, particularly the close association between eskers
569 and ice-walled lake plains in the map area (Fig. 13c). The multiple sharp-crested tributary and
570 distributary eskers presumably represent the Type 1 subglacial eskers of Perkins et al. (2016), which
571 fed into and linked the ice-walled canyon eskers.

572

573 Because of its complex network of tributaries and distributaries and its overall deranged alignment,
574 palaeoflow directions in the Sounding Lake esker are difficult to assess. However, based upon the
575 assumption that esker networks will widen and coalesce and their crests will flatten to open out into
576 ice-walled lakes in a downstream direction, meltwater flow appears to have been from the Neutral
577 Hills and into the Sounding Lake-Eyehill Creek depression, flowing first towards the east and then
578 northwest and north after turning back on itself (Figs. 3, 13a). This somewhat counter-intuitive flow
579 direction was originally proposed by Shetsen (1987) after the mapping of Bayrock (1967). Meltwater
580 then likely developed a more direct route north-northeastwards from Neutral Valley towards
581 Metiskow, cutting off the more deranged and lengthy routeway towards the east. Hence meltwater
582 flowed back through the Neutral Hills after its summit had been exposed by downwasting ice, with
583 the earliest drainage direction being recorded by a W-E aligned esker network running along the
584 base of the proximal slope of the eastern block of the thrust moraine complex. The majority of the

585 drainage and glacial sedimentation was then concentrated along the large esker ridge. The
586 origins of the water must have been from the large expanse of stagnant ice lying immediately distal
587 to the Neutral Hills (see Section 3.9) as well as the numerous oversized and abandoned channels that
588 converged on the gaps through the thrust moraine complex from the south and discharged regional
589 meltwater decanting from proglacial lakes located to the west (see Section 3.10). In order to create
590 such large eskers in the Sounding Lake-Eyehill Creek depression, meltwater must have descended
591 into an extensive glacier body that still occupied this lowland terrain. Faint WNW-ESE flutings in the
592 depression, can be traced eastwards into a palaeo-ice stream footprint. This indicates that the area
593 was occupied by a late stage easterly-flowing ice mass which blocked northeasterly draining regional
594 meltwater, thereby giving rise to the creation of the large eskers and their tributaries.

595

596 A further extensive network of large flat-topped eskers with tributary and distributary branches
597 occurs 10 km south of Wainwright, and in the terrain adjacent to Ribstone Lake (Fig. 13b). The
598 largest features form a west-east orientated system in which a single, flat-topped ridge is fed by
599 tributaries converging from the southwest from the area north of Amisk, indicating that meltwater
600 initially drained northward along the Fabyan-Amisk ice stream bed, and subsequently flowed
601 eastward to join the main esker ridge after the ice stream had shut down. The main esker ridge then
602 fans out into a series of flat-topped distributaries that terminate at an expansive, flat and variably
603 pitted outwash on the distal edge of the Prospect Valley composite thrust moraine belt (Fig. 13b; see
604 Sections 3.8 and 4). This area appears to represent a former stagnant ice zone through which
605 englacial and subglacial drainage created tunnel fills/eskers beneath a contemporaneous
606 supraglacial to ice-contact outwash fan; the fan later locally collapsed to form isolated flat-topped
607 hills and to reveal the underlying eskers. Comparable depositional settings have been identified at
608 modern temperate glacier snouts (e.g., Price, 1969, 1982; Howarth, 1971; Evans and Twigg, 2002;
609 Storrar et al., 2015) but the size, low sinuosity and rapid lateral change from small sharp-crested
610 esker tributaries to a single, flat-topped esker terminating in a large area of buried glacier ice are
611 characteristics very similar to those of downstream ice tunnel unroofing and re-entrant creation
612 typical of jökulhlaup-fed systems (Russell et al., 2001a). Hence the Wainwright-Ribstone Lake esker is
613 interpreted as a jökulhlaup-generated esker. Indeed, kettle-like depressions in both the Wainwright-
614 Ribstone and the Sounding Lake-Eyehill Creek flat-topped eskers indicate that both systems could
615 have evolved by ice tunnel roof collapse during catastrophic discharges (Mokhtari Fard, 2002).

616

617 Numerous examples of minor eskers occur within areas of pitted or hummocky terrain, where they
618 are associated with flat-topped hills (Figs. 13c, d; see Sections 3.7-3.9). They appear as both

619 relatively continuous and discontinuous sinuous ridges and often link up with flat-topped hills. Linear
620 flat-topped hills are also observed forming continuations of esker ridges, indicating that englacial
621 and/or subglacial tunnels locally developed into supraglacial ice-walled channels. Together with the
622 associated hummocky and pitted topography, this constitutes a landform assemblage diagnostic of
623 glacier karst (cf. Clayton and Cherry, 1967; Clayton et al., 2008; Livingstone et al., 2010). The sinuous
624 features identified here as likely eskers have been previously classified as types of “disintegration
625 ridges” (e.g., Johnson and Clayton, 2003), although this term was also used by Gravenor and Kupsch
626 (1959) to include crevasse fills (geometric ridge networks). Sinuous chains of elongate doughnut
627 forms or rim ridges (cf. Gravenor and Kupsch, 1959; Parizek, 1969; Mollard, 2000) also occur in
628 association with these inferred eskers, in places running parallel with the sinuous ridges (Figs. 13c, d
629 and 14). Such features may relate to the process-form regime recognised on some modern glacier
630 forelands in Svalbard and Iceland in which freshly abandoned subglacial tunnels become the foci of
631 till squeezing from a deforming bed to form “till eskers” (Christoffersen et al., 2005; Larsen et al.,
632 2006; Evans et al., 2010, 2016b). In the case of an insufficient pressure differential and/or low till
633 supply, the squeezed material would not completely fill the tunnel, instead creating ridges along its
634 walls. The squeezing of till into tunnels and esker cores has been recognised previously by, for
635 example, Banerjee and McDonald (1975) and for the Canadian prairies by Burke et al. (2015). A
636 similar scenario was envisaged by Parizek (1969) to explain “bead-like ice-contact rings”, but rather
637 than a subglacial origin, he invoked the superimposition of ice-walled (supraglacial) channel fills on
638 the glacier bed. However, none of these interpretations account satisfactorily for chains of circular
639 forms or doughnuts, which we attribute on major thrust masses as piping orifices. A piping origin for
640 sinuous chains of doughnuts associated with eskers would imply the escape of pressurised
641 groundwater into low pressure abandoned subglacial tunnels or collapsed englacial tunnels, with
642 long chains being created by the up-ice migration of production zones similar to those envisaged for
643 normal eskers by Andersen (1931), Hebrand and Amark (1989), Hooke and Fastook (2007) and
644 Storrar et al. (2014a, b). Hence, we propose a hypothesis whereby doughnut chains evolved due to
645 the progressive activity of piping orifices along abandoned and/or collapsed tunnels. This is an
646 alternative but not incompatible model to the subglacial pressing envisaged by Stalker (1960), Eyles
647 et al. (1999) and Boon and Eyles (2001). Such a process could operate much like that of till esker
648 formation where the settling and concomitant floor-melting of a widening englacial tunnel or moulin
649 chain/ice-walled channel would create till ridges or doughnut chains by passive squeezing or
650 pressing.

651

652 In many locations, eskers are associated with channels, either lying within and/or forming linear
653 chains along them (Figs. 13c and d). In these settings, the channels are interpreted as subglacial
654 tunnel channels (see Section 3.10) that evolved due to the lateral migration of tunnels through weak
655 confining sediment and/or bedrock which was subsequently deposited in multiple esker ridges. This
656 is illustrated by complex and often meandering esker ridges contained within channels of variable
657 width and displaying arcuate cliff segments (Fig. 13d). Some tunnel channels contain segments that
658 constitute flat-topped ridges that rise above the walls of the channels, such as in the area around
659 Kinsella, just outside the western edge of the map area (Gravenor and Bayrock, 1956; Gravenor and
660 Kupsch, 1959; Fig. 13c). These features are presumably eskers that locally infilled channels as a result
661 of hydraulic jumps and hence prograded delta-like deposits that also aggraded upwards into the ice
662 base, similar to the tunnel channel and ice-walled channel infill reported by Russell et al. (2001a,
663 2007) and Burke et al. (2008) following the 1996 jökulhlaup at Skeidararjökull, Iceland. The
664 continuation of sinuous ridges (eskera) and doughnut chains across some tunnel channels at oblique
665 angles clearly indicates that either the channel was ice filled and/or the ridges/chains were
666 developed englacially or supraglacially (cf. Parizek, 1969).

667

668 *3.7 Flat-topped hills (mounds)*

669 Clusters of flat-topped hills or mounds occur in association with glacialfluvial landforms, especially
670 eskers and pitted terrain (Fig. 13c and d). Their close relationship with eskers, especially where
671 eskers grade into elongate or linear assemblages of flat-topped mounds, indicate that they
672 originated as the infillings of ice-walled channels or lakes, thereby constituting supraglacial eskers
673 and ice-walled lake plains (*sensu* Clayton and Cherry, 1967; Clayton et al., 2008) respectively. Also
674 visible in the map area are examples of rim ridges encircling flat-topped hills, features previously
675 described as rim-ringed moraine plateaux (Hoppe, 1952; Stalker, 1960) and given a genetic
676 classification of rim-ringed moraine-lake plateaux (Parizek, 1969). These ridge-rimmed mounds likely
677 represent “unstable ice-walled lake plains” (Clayton and Cherry, 1967), where insufficient debris was
678 available to fill the depression in the ice. In some cases, the lake infill was so thin that subglacial
679 forms can be viewed through the lake plain (Fig. 14). Some very large flat-topped hills occur in the
680 Sounding Lake-Eyehill Creek depression where they appear to be mostly disconnected from the
681 eastern part of the large esker (Fig. 3). Closer inspection reveals that there are a number of minor
682 eskers running between and alongside the hills and altogether these forms represent a drainage
683 system that flowed towards the northeast and east, likely bleeding off from the large esker via a
684 complex glacier karst network.

685

686 Smaller moulin infills have been envisaged by some researchers to account for doughnut forms
687 (*sensu* Clayton, 1967), also known as prairie mounds (Gravenor, 1955), rimmed kettles (Christiansen,
688 1956) and closed disintegration ridges (Gravenor and Kupsch, 1959). In such a depositional scenario
689 the doughnuts would effectively be small scale ice-walled lake plains created by the sloughing of
690 supraglacial material into small ice-walled depressions or sinkholes. Elsewhere, doughnut forms
691 appear to be linked to the construction of major thrust moraines (see Section 3.1), esker formation
692 (see Section 3.6) or hummocky terrain development (see Section 3.9), indicating that they likely have
693 polygenetic origins (cf. Mollard, 2000), the interpretive details of which need to be compatible with
694 their geomorphic context.

695

696 *3.8 Areas of pitted glacialfluvial deposits*

697 Only areas of predominantly flat terrain with largely isolated surface depressions can be confidently
698 classified as pitted glacialfluvial deposits based upon morphology alone. Elsewhere, almost total
699 collapse of buried ice cores renders the terrain similar to hummocky terrain. However, previous
700 mapping by Bayrock (1967) identified some hummocky areas where surficial materials were of
701 glacialfluvial origin and hence these locations can be classified as areas of pitted glacialfluvial deposits.

702

703 As discussed in Section 3.6, the most prominent area of pitted glacialfluvial deposits forms an
704 expansive, flat and variably pitted surface on the distal edge of the Prospect Valley composite thrust
705 moraine belt southeast of Wainwright (Fig. 13b). At its northern edge, significant collapse due to ice
706 melting is evidenced by the numerous water-filled depressions surrounding Ribstone Lake. The
707 occurrence of discontinuous sinuous ridges (eskers) in this area are interpreted as the products of
708 englacial and subglacial tunnel fills beneath a contemporaneous supraglacial to ice-contact outwash
709 fan. Similar extensive collapses and channel incisions appear at the southern edge of this fan, which
710 is fringed by arcuate lineaments that parallel the Prospect Valley moraine belt, which itself displays
711 extensive pitting indicative of glacitectonic thrusting of the ice-cored outwash. Drainage westwards,
712 contemporaneous with thrust moraine construction and over the top of pre-existing ice-cored
713 outwash associated with the Wainwright-Ribstone Lake esker (see Section 3.6), is evident in a series
714 of east-west aligned surface channels that deepen westward. A conspicuous sinuous chain of
715 elongate depressions trending south-north on the outwash surface (Fig. 13b) likely represent the
716 collapse of the material into a buried tunnel channel.

717

718 Some areas that appear to constitute pitted glacialfluvial materials represent types of glacitectonic
719 thrust masses, indicative of large areas of stagnating glacier ice juxtaposed with glacialfluvial

720 sediment-landform assemblages and highly disturbed bedrock, all of which were thrust by
721 readvancing ice lobes. Such process-form regimes are typical of modern surging glacier snouts
722 (Raymond et al., 1987; Evans and Rea, 1999, 2003; Schomacker et al., 2006; Evans et al., 2007, 2009;
723 Roberts et al., 2009; Evans, 2011). These are evidenced by two types of landform assemblage. Firstly,
724 substantial lakes with cliffed, often rectilinear or arcuate boundaries are representative of the melt-
725 out of extensive buried glacier ice and its overburden of glacialfluvial deposits juxtaposed with
726 bedrock rafts; these have all been proglacially thrust to form linear or arcuate ridges and
727 depressions that broadly parallel those of the more coherent thrust masses (i.e. bedrock) that were
728 pushed into them (Figs. 7c and 15a). Limited exposures through hummocks in this terrain reveal
729 significant deformation, thrust faulting and diapirism that has resulted in complex melanges of the
730 component materials (Fig. 15a). Secondly, areas of largely chaotically pitted Quaternary materials
731 but also displaying discontinuous lineaments (Fig. 15b) are likely representative of more fragmented
732 thrust masses developed in former supraglacial outwash that was initially overlying more extensive
733 buried glacier ice of variable thickness. A particularly prominent area of pitted thrust mass lies
734 directly south of the East Neutral Hills, at the eastern extremity of the Altario Moraine of Phillips et
735 al. (2017; see Section 3.9). This is a large, complex depression composed of multiple lakes and ponds
736 of various size and depth and draped by a veneer of glaciallacustrine sediment (Bayrock, 1967). The
737 southern rim of the complex, hereby named the “North Altario depression”, is composed of an
738 arcuate thrust mass that is fragmented by sinuous chains of large water-filled depressions. Linear
739 ridges also occur in the middle of the complex where they are surrounded by more chaotic mounds
740 and ponds (Fig. 15c). The extensive collapse of both the complex depression and the southern
741 bounding thrust mass, as evidenced by the many constituent depressions, indicates the melt-out of
742 a large ice body or glacier snout, which initially constructed the arcuate thrust mass from pre-
743 existing ice-cored deposits.

744

745 *3.9 Areas of hummocky terrain*

746 In contrast to hummocky topography resulting from the superimposition of glacialtectonic signatures
747 and ice melt-out (Fig. 8c) and chaotically pitted terrain displaying discontinuous lineaments (Fig.
748 15b), hummocky terrain lacks any clear linearity and contains the Types 1, 2 and 3 hummocks of
749 Evans et al. (2014). An excellent example of the juxtaposition of these terrains occurs within the
750 Veteran Moraine (Phillips et al., 2017) between Veteran and Nose Hill and the western Neutral Hills
751 (Figs. 8b and 16a). Although the southernmost part of the Veteran Moraine contains large and
752 densely spaced flat-topped hills interpreted as ice-walled lake plains (Fig. 16a), these are not
753 attributed to pitted glacialfluvial deposits, because the surrounding hummocks appear to lack sand

754 and gravel cores, being composed instead of clay-rich diamicton with sheared sand lenses (Bayrock,
755 1967; Fig. 16b). However, numerous discontinuous sinuous ridges (probable eskers) and large esker
756 networks do occur within the hummocks and link up with tunnel channels (Fig. 16a). At its southern
757 edge, the Veteran Moraine hummocks end abruptly at the margin of the faintly streamlined bed of
758 the CAIS (Fig. 16a). Modern drainage from this lower relief surface is clearly blocked by the
759 hummocky terrain, as indicated by lakes that have been impounded against the higher topography.
760 Eskers run into tunnel channels at the edge of the hummocky terrain, indicating that meltwater was
761 evacuated from under the margin of the CAIS. The juxtaposition of these two contrasting landform
762 assemblages indicates that large volumes of sediment accumulated within ice that lay outside of the
763 CAIS but south of the Neutral Hills thrust moraine complex. Although glacialfluvial landforms have
764 clearly developed within this hummocky terrain, large areas of chaotic hummocks and doughnuts as
765 well as highly fragmented sinuous ridges were constructed in sheared diamictons, a characteristic
766 widely identified in comparable landforms elsewhere on the prairies (e.g., Gravenor and Kupsch,
767 1959; Stalker, 1960; Parizek, 1969; Johnson and Clayton, 2003). Hence the Veteran Moraine must
768 have evolved from an extensive area of glacier karst that developed over and within till-cored
769 hummocks immediately east of the CAIS.

770

771 Another large expanse of hummocky terrain occurs within the Altario Moraine (Phillips et al., 2017),
772 directly south of the East Neutral Hills thrust complex. This moraine comprises an assemblage of
773 chaotic hummocks, short sinuous hummocky ridges, contiguous doughnut mounds (*sensu* Mollard,
774 2000), ice-walled lake plains, eskers and associated doughnut chains (see Section 3.6), tunnel
775 channels and scattered mega-rafts (Fig. 16c). Here, the hummocks are diamicton-cored (Bayrock,
776 1967) and locally vary from entirely chaotic to crudely aligned in sinuous chains; the chains are often
777 linked to form sinuous, dual crested ridges that grade laterally into eskers and ice-walled lake plains.
778 As with the hypothesized till eskers in Section 3.6, these associations favour a subglacial squeeze or
779 pressing origin (Stalker, 1960; Eyles et al., 1999; Boone and Eyles, 2001), as well as glacialfluvial tunnel
780 fills, especially where locally draped by supraglacial lake plain sediments.

781

782 The largest expanse of hummocky terrain occurs around Kinsella in the extreme northwest corner of
783 the map area, within the southern part of the regionally extensive Viking Moraine (Johnston and
784 Wickenden 1931; Bretz 1943). This area is characterised by an inset series of major channels (see
785 section 3.10 for further implications of this assemblage) and the prominent development of eskers
786 and ice-walled lake plains, the latter draping tunnel channels and hummocks (Fig. 16d). These record
787 the former existence of an expansive glacier karst within a lobate ice margin that abutted the

788 eastern edge of the CAIS (Figs. 13d and 14). Railway and road cuttings through the Viking Moraine
789 immediately east and west of the town of Kinsella, provide valuable insights into the cores and
790 possible origins of some of the hummocks (Fig. 16d). The exposures display stacked diamictons with
791 prominent SE-directed shear zones defined by attenuated sand lenses and sand-filled thrust planes.
792 In the west of the hummocky terrain (KW2, Fig. 16d) the thrusts dip towards the northwest. A
793 southeast directed sense of shear is also recorded by similar shear zones observed in the centre of
794 the hummocky terrain (KW, Fig. 16d). In this area the stacked diamictons also contain thrust-bound
795 rafts of mudstone. The upper Dmm within the section possesses a NW-SE aligned clast macrofabric;
796 consistent with the SE-directed sense of displacement on the thrust and shear zones. In contrast, the
797 macrofabric present within the lower Dmm of KW displays a steeply dipping, weakly easterly-aligned
798 signature more typical of crevasse squeeze processes (see Section 3.5). In the eastern part of the
799 hummocky terrain, an exposure displays an upper massive to laminated diamicton containing
800 attenuated sand lenses and sand-lined thrust faults dipping towards the northeast. The lenses
801 represent pre-existing sands which were deformed and emplaced into the diamicton during
802 thrusting. In contrast the sand-lined thrusts are thought to provide evidence that these glacitectonic
803 structures subsequently acted as fluid pathways allowing water-escape and deposition of the sand
804 lining. This is compatible with northerly and northeasterly aligned clast macrofabrics in both the
805 upper and lower diamictons at this site. The characteristics of the diamictons are indicative of a
806 subglacial origin for at least some of the hummock cores in this terrain (Evans, 2018 and references
807 therein). The opposing stress directions from the northwest and north-northeast in the west and
808 east parts of the hummocky terrain respectively are entirely compatible with its construction at the
809 coalescence zone of the CAIS and eastern ice lobes.

810

811 An important distinction should be made between the hummocks and ridges in the hummocky
812 terrain of the map area and those identified around the southern margin of the CAIS in southern
813 Alberta by Evans et al. (2014). The MTR Type 3 moraine ridges and Type 1-3 hummocks of southern
814 Alberta are arranged in arcuate zones located between MTR Type 2 moraines, collectively indicative
815 of changing sub-marginal thermal regimes during ice sheet marginal recession. In the Neutral Hills
816 Uplands, the hummocky terrain areas occur in large non-linear assemblages, more indicative of the
817 in situ stagnation of ice lobes, and contain greater numbers of glacial features. The latter include
818 eskers and possible eskers/till eskers (doughnut chains and short sinuous ridges) and ice-walled
819 plains that are aligned with tunnel channels, collectively indicating meltwater drainage flowing
820 oblique to former ice margins.

821

822 An unusual area of chaotic hummocky terrain lies within the Grassy Island Moraine (Phillips et al.,
823 2017) between Grassy Island Lake and the Misty Hills. This area comprises a complex range of
824 landforms including large kettle lakes, pitted glacialfluvial deposits, esker networks and ice-walled lake
825 plains juxtaposed with and partially draping glacitectonically thrust bedrock in the west and
826 hummocks containing heavily deformed stratified sediments and diamictos in the east (Fig. 6).
827 Overall, the Grassy Island Moraine appears to represent an extensive former stagnant ice zone
828 developed on the proximal slopes of the Misty Hills and Esther uplands thrust bedrock complex.

829

830 *3.10 Erosional channels, large terraces and cliffs*

831 The map area contains numerous prominent channels with many displaying cliffed margins
832 punctuated by modern landslides. These features have been termed “stream trenches” (Bayrock,
833 1958b; Gravenor and Ellwood, 1957) or “ice-walled channels” (Gravenor and Kupsch, 1959), and are
834 reported as being partly covered by till and hummocky terrain. They therefore either predate
835 glaciation, in the case of the thalwegs of bedrock valleys (cf. Stalker, 1961; Farvolden, 1963;
836 Andriashek, 2018), or more commonly, relate to subglacial and/or proglacial meltwater/spillway
837 incision. The Battle River occupies the largest of these trenches and its cliffed margins are largely
838 postglacial, although the upper slope along some stretches comprises an outer set of sediment
839 mantled preglacial cliffs which indicate that the modern river has re-occupied this earlier preglacial
840 river course (Fig. 17a). A number of large, steep-sided and flat bottomed, mostly relict channels
841 occur in the Hardisty area on the west side of the Battle River. These features are conspicuous by
842 rectilinear segments with sharp, obtuse corners and their tendency in places to join one another so
843 that they isolate polygonal-shaped areas of prairie surface. They constitute the southernmost extent
844 of a 150 km long series of largely N-S aligned and inset channels that stretch outside the northwest
845 corner of the map area. This regional channel system forms a wide arcuate assemblage fringing the
846 Viking Moraine (see section 3.9). Most of these channels appear mantled by glacialigenic sediment,
847 especially where they have not been re-occupied by deglacial and postglacial drainage. Evidence for
848 this includes muted cliff lines and drapes of hummocky terrain and eskers as well as enclosed,
849 elongate valley floor depressions, in places containing lakes. The latter characteristics in particular
850 indicate a subglacial origin for the valleys (cf. Brennand and Shaw, 1994; Ó Cofaigh, 1996; Kehew and
851 Kozlowski, 2007; Russell et al., 2007). Regionally, the channels widen southwards and also become
852 less parallel and more reticulate in the Hardisty area, where the isolated, polygonal-shaped prairie
853 surfaces display clear lineaments indicative of an overridden thrust moraine arc, initially constructed
854 by an ice lobe flowing from the NNW. Subsequent flow from the WNW is recorded by minor flutings
855 with clear stoss boulders, as well as N-S orientated lineaments on the northernmost polygonal-

856 shaped prairie surface (Fig. 17a). We hypothesize that the reticulate pattern of the channels in the
857 Hardisty area is controlled by the fracture patterns produced by early glacitectonic thrust mass
858 displacement, which were later exploited by both subglacial and deglacial meltwater drainage. This
859 remarkable channel network demarcates the drainage pathways developed along the coalescence
860 zone between the eastern margin of the CAIS and ice lobes flowing into the region from the east
861 (see section 4).

862

863 More subtle channels, identifiable as sinuous chains of elongate lakes that are partially obscured by
864 glacial depositional landforms are interpreted as subglacial tunnel channels (Patterson, 1994;
865 Clayton et al., 1999; Evans, 2000; Kehew and Kozlowski, 2007). Numerous examples occur within
866 every landform assemblage and are typically associated with eskers (see Section 3.6), whereby they
867 either lie in sinuous chains (Figs. 12a and 17b), run alongside one another (Fig. 17b) or the eskers lie
868 wholly within or overfill the channels (Figs 13c, d and 16a). The most spectacular subglacial drainage
869 network in the map area is that of the Coronation-Spondin scablands (Fig. 11a), which Sjogren and
870 Rains (1995) describe in significant detail as comprising anabranching channels with undulatory long
871 profiles and separating eroded residuals.

872

873 Typical of the Canadian prairies, numerous large relict channels cross-cut all glacial landforms and
874 hence are interpreted as spillways fed by water decanting from proglacial, ice-dammed lakes that
875 developed at the margins of the retreating LIS (cf. Elson, 1957; St Onge, 1972; Christiansen, 1979;
876 Kehew and Clayton, 1983; Kehew and Lord, 1986, 1987; Evans, 2000; Evans et al., 2006). The most
877 prominent of such features occupy the drainage basins of Loyalist, Monitor and Sounding creeks,
878 where multiple relict channels, in addition to those of the modern river courses, record the incision
879 of the upstanding glacitectonic thrust masses and the progradation of material removed from the
880 incisions to form channelled fans, especially in the Monitor Creek basin (Fig. 17c). The upper courses
881 of these spillway systems link to the Coronation-Spondin scabland to the west, indicating that
882 floodwater occupied the channels during and after the recession of the CAIS. The Monitor Creek
883 spillway feeds into the Eyehill Creek/Sounding Lake depression where its floodwaters appear to have
884 drained into stagnant ice in this area, contributing substantial amounts of sediment to the
885 construction of the large esker and ice-walled lake plains and other smaller eskers which record
886 drainage north and eastwards. Similarly, the Sounding Creek spillway appears to have drained into a
887 substantial area of stagnant ice occupying the Grassy Island Lake area, forming a chaotic hummocky
888 terrain of large kettle lakes, pitted glacial deposits, esker networks and ice-walled lake plains
889 juxtaposed with glacitectonic thrust masses and hummocks containing heavily deformed stratified

890 sediments and diamictos (the Grassy Island Moraine of Phillips et al., 2017; Figs. 6 and 17c). To the
891 north of this extensive former stagnant ice zone it appears that the water delivered by the Sounding
892 Creek spillway drained into the Monitor Creek system.

893

894 **4. Glacial landsystems and palaeoglaciological reconstructions**

895 Based upon the distribution of the landform-sediment assemblages described above (Fig. 3), the
896 Neutral Hills Upland and surrounding terrain can be classified according to a variety of landsystem
897 signatures (Fig. 18a), some of which have been previously identified by Phillips et al. (2017),
898 employing the mapping of Gravenor and Bayrock (1955), Bayrock (1958a, b, 1967), Shetsen (1987,
899 1990), Kjearsgaard (1988) and Fenton et al. (1993). Additionally, the area lies between the strongly
900 streamlined trunks of the Central Alberta and Maskwa palaeo-ice streams previously mapped by
901 Evans et al. (2008, 2014, 2016a), Ross et al. (2009), Ó Cofaigh et al. (2010) and Norris et al. (2018).
902 The extent of these ice streams, together with the later cross-cutting “Ice Stream 2” flow sets as
903 refined by Norris et al. (2018) are depicted in Figure 1, but this does not fully communicate the
904 remarkably complex ice dynamics of the Neutral Hills Upland and hence some modifications to this
905 palaeoglaciology based upon the new mapping presented here are now necessary (Fig. 18b). A series
906 of six ice flow events were proposed for the area by Phillips et al. (2017), which are now refined
907 using the cross-cutting relationships of various landsystem signatures.

908

909 The earliest landform imprints (pre-Event 1) appear to be the various examples of fluted or
910 streamlined lineaments or small areas of MTR Type 1 ridges which have been strongly overprinted
911 by subsequent vigorous ice stream or ice lobe advance (Fig. 18b). On the bed of the CAIS and on the
912 prairie surface between the reticulate channels of the Hardisty area, arcuate sets of lineaments
913 represent overridden thrust moraines constructed at the lobate margin of the advancing CAIS as it
914 flowed south and southeastwards. The thrust masses were later exploited by multiple phases of
915 thin-skinned glacitectonic raft displacement (Fig. 11c lower) and subglacial and deglacial meltwater
916 erosion (Fig. 17) at the migrating coalescence zone of the CAIS and eastern ice flow units. They also
917 appear to have been overprinted by more recent (Event 5) lobe advances. Further evidence for an
918 early southeasterly flow is represented by the overprinted tectonic fabrics in the western Neutral
919 Hills and the Nose Hill/Ribstone Creek area (Fig. 5b). A small area of NW-SE aligned flutings located
920 north of Chauvin has survived overprinting firstly by the Maskwa Ice Stream (Event 1) and then by
921 the Prospect Valley lobe (Event 5). This ice flow direction is recorded in the lowermost till in the area
922 (Fig. 5a).

923

924 Event 1 is the first ice flow trajectory for which a regional landform signature can be recognised and
925 is largely equated with the operation of the Maskwa palaeo-ice stream, directly east of the map
926 area. Overprinted N-S orientated flutings at the eastern edge of the CAIS footprint indicate that it
927 was also likely to have been operating at this time, after which the CAIS contracted to a narrower
928 but persistent fast flow zone throughout Events 2-4.

929

930 Events 2 and 3 involved the construction and modification respectively of the major thrust
931 complexes of the Neutral Hills Uplands. Contrary to the sequence of events proposed in previous
932 reconstructions (Evans et al., 2008; Phillips et al., 2017), it appears that these features pre-date the
933 operation of Ice Stream 2B of Ó Cofaigh et al. (2010; see below) and hence are not related to a late
934 stage deglacial surge activity but instead record surging by ice lobes flowing into the region from the
935 northeast. The implications of this are that the thrust masses were created within an inter-ice
936 stream, locally ice-cored, moraine zone (inter-corridor terrain of Evans, 2000; Evans et al., 2008),
937 where subsequent glacier overriding was restricted. Evidence of the latter is the narrow fast flow
938 corridor associated with later deformation events at the Mud Buttes (Phillips et al., 2017) and hence
939 designated here as Event 3 (Fig. 18b). There are three possible sub-phases to Event 2 (designated A-
940 C) as recorded in the thrust mass complexes. The extent of ice during Event 2A is demarcated by the
941 broad arc of bedrock-cored composite ridges comprising the Misty Hills, Sharp Hills and Esther
942 Uplands and inset by the Grassy Island Moraine. Typical of surge lobes, this landsystem comprises
943 outer thrust moraines and an inner zone of ice-cored hummocky terrain and extensively kettled
944 glacifluvial deposits (Evans and Rea, 1999, 2003; Schomacker et al., 2006; Evans et al., 2007, 2009).
945 Event 2B relates to the production of the Veteran and Altario moraines, which both constitute large
946 areas of formerly ice-cored terrain. The ice cores likely constituted buried glacier ice that persisted
947 across the landscape after earlier surges into the inter-ice stream zone. These assemblages of
948 extensive ice karst and glacifluvial deposits interspersed with bedrock and glacial sediment thrust
949 masses were then deformed by subsequent readvances/surges to form the rectilinear melt-out
950 depressions and heavily pitted thrust masses that are especially well-developed in the Veteran
951 Moraine around the Gooseberry Lake and Neutral Valley and the Altario depression of the Altario
952 Moraine. Event 2C is represented by a substantial readvance that resulted in the construction of the
953 prominent Neutral Hills and Nose Hill thrust-block moraines. The driving stress required to construct
954 these impressive glacial tectonic landforms could also have been responsible for thrusting of buried
955 glacier ice within the proglacial areas of the Veteran and Altario moraines. Finally, a potentially
956 further Event 2 fast flow corridor occurs further north, in the Wainwright area and records the
957 operation of a narrow ice stream flowing south-southeastwards with a flow set parallel to Event 2A.

958

959 Event 4 is recorded by the overprinting of the Maskwa palaeo-ice stream footprint by a NW-SE
960 flowing ice stream, previously designated Ice Stream 2B by Ó Cofaigh et al. (2010). They envisaged
961 this as an offshoot of Ice Stream 2A located further north and fed by the Battleford Valley fast flow
962 zone (Fig. 1). We have revised this reconstruction based upon our evidence for the Prospect Valley
963 lobe landsystem (see below). The flowset and end-moraine imprint of the Prospect Valley lobe is
964 clearly separate from, and overprints, that of Ice Stream 2B and hence we see no evidence for the
965 elbow shaped bifurcation that separates Ice Stream 2 into two flow units (Fig. 1). Instead, Ice Stream
966 2B is now considered to be a southeasterly flowing tributary of the ice streams that were operating
967 in the region to the east of the Maskwa ice stream after it had effectively shutdown (Buffalo Ice
968 Stream and James Lobe system; Ross et al. 2009; Margold et al. 2015). Indeed, not only the
969 shutdown of the Maskwa but also the narrowing and/or weakening of the CAIS could have facilitated
970 the westward propagation of the tributaries of the Buffalo/James Lobe ice stream system, as
971 proposed by Ross et al. (2009).

972

973 Ice Stream 2B also paralleled the Battleford River fast flow trunk (Ice Stream 2A of Ó Cofaigh et al.
974 2010) as well as the more southerly Ice Stream 2C of Norris et al. (2018; Fig. 18b). Our mapping
975 indicates that a contemporaneous southeasterly flowing ice stream also operated in the area
976 immediately south of Ice Stream 2B. The margin of this ice stream formed the southern limit of the
977 Veteran Moraine and modified the western edge of the Misty Hills thrust moraine complex. It also
978 streamlined the terrain to the south of the map area, where it eventually turned east-
979 northeastwards to join Ice Stream 2B and overprinted the Maskwa Ice Stream footprint. After Ice
980 Stream 2B had shutdown, it stagnated to develop a complex glacier karst and meltwater drainage
981 system that was augmented by drainage through the Neutral Hills thrust complex from the buried
982 ice in the Veteran and Altario moraines. It was also reworked into ice-cored thrust masses at its
983 western end and northern edge by the advance of subsequent lobate ice stream margins during
984 Event 5.

985

986 Event 5 is the most recent glacial geomorphic imprint identifiable in the study area. It comprises the
987 footprint and associated terminal moraines of two lobate ice streams, one of which, the Prospect
988 Valley lobe, created the most unequivocal surging glacier landsystem in the region (Fig. 19a). The
989 trunk zone of this surging lobe has been mapped previously by Evans et al. (1999) and Evans and Rea
990 (1999, 2003) and is remarkable for its extensive networks of crevasse squeeze ridges, which indicate
991 surges propagated up-ice for more than 100 km. Mapping presented here identifies the multi-lobate

992 terminal moraine complex constructed by the surge, an offshoot of which has been reported by
993 Evans et al. (2016a) to have excavated a hill-hole pair that cross-cuts the Maskwa palaeo-ice stream
994 footprint (Fig. 18b). The multi-lobate terminal moraine comprises composite ridges with extensive
995 evidence of ice melt-out (kettle holes and melt-out depressions), as well as numerous examples of
996 large failure scars and associated failed blocks resembling retrogressive flow complexes. At its
997 southern limit, the composite moraines appear to have been constructed from ice-cored glacial
998 materials rather than bedrock (cf. Bayrock, 1967), likely due to the impingement of the Prospect
999 Valley lobe on the stagnant ice and ice-cored glacial outwash of Ice Stream 2B. A modern
1000 analogue for this ice-cored surge moraine is that of the Skeiðarárjökull foreland in Iceland, created
1001 by a surge over dead ice in the late 19th century (Fig. 19b; Galon, 1973; Russell et al., 2001b).
1002 Because it is the best preserved lobate ice stream landform imprint in the study area, it provides
1003 the clearest evidence for the surging style of ice-marginal oscillations in the inter-ice stream moraine
1004 zones, most of which have otherwise been extensively overprinted.

1005

1006 The other clear Event 5 lobate ice stream imprint is located in the northwest corner of the map area
1007 (Fig. 18b) and was considered by Phillips et al. (2017) to relate to a much older event. However,
1008 based upon the higher resolution LiDAR imagery used in this study, the flutings within this imprint
1009 are clearly related to the later stages of south-southwesterly flow in the inter-ice stream zone and
1010 terminate at the broad arc of hummocky and ice-cored thrust terrain of the Viking Moraine (Fig.
1011 15b). A smaller flow set extending southeastwards from the eastern edge of the CAIS footprint into
1012 the western Viking Moraine records a further Event 5 fast flow imprint. Together, these Event 5 flow
1013 sets verify the macrofabric evidence from the hummocks of the Viking Moraine, confirming that this
1014 landform represents interlobate deposition of subglacial tills and bedrock rafts overprinted by
1015 complex glacial sediment-landform assemblages indicative of an extensive glacier karst.

1016

1017 Taken in its broader context of the southwest LIS, the distinctive landform-sediment assemblage of
1018 the Neutral Hills Uplands (Fig. 20) is diagnostic of the partial overprinting of fast flow lobes that
1019 operated in the area at the margins of, and between, the major regional Central Alberta and
1020 Maskwa palaeo-ice streams. Widespread evidence of surge-diagnostic features, especially crevasse
1021 squeeze ridges, proglacial thrust masses, extensive ice stagnation topography and occasional zig-zag
1022 eskers, indicate that these ice streams experienced repeated flow instabilities. This is particularly
1023 evident in the inter-ice stream moraine zone of the Neutral Hills Uplands where substantial belts of
1024 thrust masses, hummocky terrain and ice stagnation topography make up the long recognised
1025 regional moraine belts constructed at around 15.5 cal ka BP (Fig. 20; Wickenden, 1931; Bretz, 1943;

1026 Evans et al., 2008, 2014; cf. Margold et al., 2018 for dating control). The surge imprints of the
1027 Neutral Hills Uplands are typical of the broader scenario of a highly dynamic and unstable southwest
1028 LIS, characterised by markedly transitory and cross-cutting palaeo-ice streams. In the regional
1029 context of the juxtaposition of palaeo-ice stream beds with widespread tunnel channels and sub- to
1030 supraglacial drainage networks (cf. Patterson, 1997; Margold et al., 2015; Livingstone et al., 2016),
1031 such transitory and mobile ice stream behaviour is to be expected, especially given the role
1032 subglacial hydrology plays in the spatial and temporal variability of contemporary ice stream
1033 operation (e.g., Gray et al., 2005; Peters et al., 2007; Vaughan et al., 2008; Carter et al., 2013;
1034 Elsworth and Suckale, 2016; Siegfried et al., 2016). Moreover, modelling experiments by Lelandais et
1035 al. (2018) have indicated that ice streams can switch off when the drainage capacities of tunnel
1036 valleys are capable of suppressing subglacial water pressures. More importantly, in considering
1037 apparent ice stream surging, these modelling results demonstrate that ice streams switch on and
1038 accelerate in response to the build-up, migration and subsequent marginal outbursts of subglacial
1039 water reservoirs. This phase of basal decoupling is followed by deceleration when the subglacial
1040 drainage reorganizes into channels and creates tunnel channels and partial basal recoupling.

1041

1042 **Conclusions**

1043 A regional palaeoglaciology is now emerging from the study of the glacial geomorphology of the
1044 Canadian prairies. This features a highly dynamic southwest LIS, characterised by markedly transitory
1045 and cross-cutting palaeo-ice streams whose lobate margins are demarcated by large, arcuate ice-
1046 marginal moraine complexes (Fig. 20). Numerous overridden moraine arcs document the lobate
1047 margins during phases of more restricted ice cover, likely during ice sheet advance but in some
1048 instances related to recession. In the Neutral Hills Uplands, a distinctive landform-sediment
1049 assemblage is diagnostic of the partial overprinting of fast flow lobes that appear to have repeatedly
1050 surged into an inter-ice stream zone characterized by major moraine belts, the last surging dating to
1051 ≤ 15.5 cal ka BP.

1052 The geomorphology of the inter-ice stream moraine zone is characterised by spectacular
1053 glacetectonic compression of bedrock, cupola hill construction and mega raft displacement but also
1054 displays evidence of multi-phase stagnant ice melt-out where partially overprinted surge lobes
1055 advanced into large areas of buried glacier ice (Fig. 20). Contemporaneous ice melting within these
1056 ice bodies gave rise to the widespread development of glacier karst and the production of eskers at a
1057 range of scales, the largest of which record deranged drainage patterns indicative of ice-walled

1058 channel sedimentation controlled by the regional bedrock slope towards the northeast. The
1059 significant local relief created by the glacial geomorphology is likely a function of not only the
1060 glacitectonic compression of bedrock but also the production and melting of a melange of ice and
1061 bedrock/sediment blocks of variable ice volume, representative of buried snout ice often with well-
1062 developed or inherent glacier karst that is repeatedly proglacially thrust due to surging (Fig. 20).

1063 Widespread evidence for subglacial channel cutting is likely strongly linked to the transitory, surging
1064 and cross-cutting nature of the palaeo-ice streams in the region. This is compatible with modelling of
1065 ice stream operation whereby they switch on and accelerate in response to the build-up, migration
1066 and marginal outburst of subglacial water reservoirs. Also significant with respect to the role of
1067 subglacial meltwater networks is the impact of pressurized groundwater in a region where ice flow is
1068 against an adverse bed slope and hence a variety of enigmatic glacial landforms such as doughnuts,
1069 doughnut chains, apparent blow-out features and possible till eskers, as well as glacitectonic mega-
1070 rafts, might be best explained through a better understanding of the interaction between such
1071 pressurised sub-surface systems and the surging lobes of soft-bedded ice streams.

1072 **Acknowledgements**

1073 Thanks to Chris Orton, Durham University, for cartographic work, especially the compilation of the
1074 geomorphology map in Figure 3. Constructive comments by reviewers Martin Ross and Roger Paulen
1075 greatly helped us to clarify the contents of this paper.

1076 **References**

- 1077 Aber, J.S., Ber, A., 2007. Glaciotectonism. Development in Quaternary Science. Elsevier, Amsterdam.
1078 Aber, J.S., Croot, D.G., Fenton, M.M., 1989. Glaciotectonic Landforms and Structures. Kluwer,
1079 Dordrecht.
1080 Andersen, S.A., 1931. The waning of the last continental glacier in Denmark as illustrated by varved
1081 clays and eskers. *Journal of Geology* 39, 609-624.
1082 Andriashek, L.D., 2018. Thalwegs of bedrock valleys. Alberta Geological Survey. AER/AGS Digital
1083 Data 2018-0001.
1084 Atkinson, N., Utting, D.J., Pawley, S.M., 2014a. Glacial landforms of Alberta, Canada. Alberta
1085 Geological Survey. AER/AGS Map 604.
1086 Atkinson, N., Utting, D.J., Pawley, S.M., 2014b. Landform signature of the Laurentide and
1087 Cordilleran ice sheets across Alberta during the last glaciation. *Canadian Journal of Earth
1088 Sciences* 51, 1067-1083.
1089 Atkinson, N., Pawley, S.M., Utting, D.J., 2016. Flow-pattern evolution of the Laurentide and
1090 Cordilleran ice sheets across west-central Alberta, Canada: implications for ice sheet growth,
1091 retreat and dynamics during the last glacial cycle. *Journal of Quaternary Science* 31, 753-768.
1092 Atkinson, N., Utting, D.J., Pawley, S.M., 2018. An update to the glacial landforms map of Alberta.
1093 Alberta Geological Survey. AER/AGS Open File Report 2018-08.
1094 Banerjee, I., McDonald, B.C., 1975. Nature of esker sedimentation. In: Jopling, A.V., McDonald, B.C.

- 1095 (eds.), Glaciofluvial and Glacilacustrine Sedimentation. SEPM: Oklahoma; 304–320.
- 1096 Bayrock, L.A., 1958a. Glacial Geology, Alliance-Brownfield District, Alberta. Preliminary Report 57-2.
- 1097 Research Council of Alberta.
- 1098 Bayrock, L.A., 1958b. Glacial Geology, Galahad-Hardisty District, Alberta. Preliminary Report 57-3.
- 1099 Research Council of Alberta.
- 1100 Bayrock, L.A., 1967. Surficial Geology of the Wainwright Area (East Half), Alberta. Report 67-4.
- 1101 Research Council of Alberta.
- 1102 Benn, D.I., 1994. Fluted moraine formation and till genesis below a temperate glacier:
1103 Slettmarkbreen, Jotunheimen, Norway. *Sedimentology* 41, 279–292.
- 1104 Benn, D.I., Evans, D.J.A. 2010. *Glaciers and Glaciation*. Hodder Education, London.
- 1105 Bennett, M.R., Hambrey, M.J., Huddart, D., Ghienne, J.F., 1996. The formation of a geometrical ridge
1106 network by the surge-type glacier Kongsvegen, Svalbard. *Journal of Quaternary Science* 11,
1107 437-449.
- 1108 Bik, M.J.J., 1969. The origin and age of the prairie mounds of southern Alberta, Canada. *Biuletyn*
1109 *Peryglacjalny* 19, 85–130.
- 1110 Bluemle, J.P., 1993. Hydrodynamic blowouts in North Dakota. In: Aber, J.S. (Ed.), *Glaciotectonics and*
1111 *Mapping Glacial Deposits*. Canadian Plains Research Centre, University of Regina, pp. 259–
1112 266.
- 1113 Bluemle, J.P., Clayton, L., 1984. Large-scale glacial thrusting and related processes in North Dakota.
1114 *Boreas* 13, 279–299.
- 1115 Boone, S.J., Eyles, N., 2001. Geotechnical model for great plains hummocky moraine formed by till
1116 deformation below stagnant ice. *Geomorphology* 38, 109–124.
- 1117 Bostock, H.J., 1970a. Physiographic Regions of Canada. Geological Survey of Canada. Map 1254A,
1118 scale 1:5 000 000.
- 1119 Bostock, H.J., 1970b. Physiographic subdivisions of Canada. In: Douglas, R.J.W. (ed.), *Geology and*
1120 *Economic Minerals of Canada*. Geological Survey of Canada, Economic Geology Report 1, pp.
1121 11-30.
- 1122 Boulton, G.S., 1976. The origin of glacially fluted surfaces: observations and theory. *Journal of*
1123 *Glaciology* 17, 287–309.
- 1124 Boulton, G.S., 1986. Push moraines and glacier contact fans in marine and terrestrial environments.
1125 *Sedimentology* 33, 677–698.
- 1126 Boulton, G.S., Caban, P., 1995. Groundwater flow beneath ice sheets, part II: Its impact on glacier
1127 tectonic structures and moraine formation. *Quaternary Science Reviews* 14, 563-587.
- 1128 Brennand, T.A., Shaw, J., 1994. Tunnel channels and associated landforms, southcentral Ontario:
1129 their implication for ice-sheet hydrology. *Canadian Journal of Earth Sciences* 31, 505-522.
- 1130 Bretz, J.H., 1943. Keewatin end moraines in Alberta, Canada. *Geological Society of America Bulletin*
1131 54, 31-52.
- 1132 Burke, M.J., Brennand, T.A., Sjogren, D.B., 2015. The role of sediment supply in esker formation and
1133 ice tunnel evolution. *Quaternary Science Reviews* 115, 50-77.
- 1134 Carter, S.P., Fricker, H.A., Siegfried, M.R., 2013. Evidence of rapid subglacial water piracy under
1135 Whillans Ice Stream, West Antarctica. *Journal of Glaciology* 59, 1147–1162.
- 1136 Chandler, B.M.P., Evans, D.J.A., Roberts, D.H., 2016. Characteristics of recessional moraines at a
1137 temperate glacier in SE Iceland: Insights into patterns, rates and drivers of glacier retreat.
1138 *Quaternary Science Reviews* 135, 171–205.
- 1139 Christiansen, E.A., 1956. Glacial geology of the Moose Mountain area, Saskatchewan. Saskatchewan
1140 Department of Mineral Resources, Report 21, 35p.
- 1141 Christiansen, E.A., 1979. The Wisconsinan deglaciation of southern Saskatchewan and adjacent

- 1142 areas. *Canadian Journal of Earth Sciences* 16, 913-938.
- 1143 Christiansen, E.A., Whitaker, S.H., 1976. Glacial thrusting of drift and bedrock. In: Leggett, R.F.
1144 (ed.), *Glacial Till*. Royal Society of Canada, Special Publication 12, pp. 121-130.
- 1145 Christoffersen, P., Piotrowski, J.A., Larsen, N.K., 2005. Basal processes beneath an arctic glacier and
1146 their geomorphic imprint after a surge, Elisebreen, Svalbard. *Quaternary Research* 64, 125–
1147 137.
- 1148 Clayton, L., Cherry, J.A., 1967. Pleistocene Superglacial and Ice Walled Lakes of West central North
1149 America. *Miscellaneous Series* 30. North Dakota Geological Survey, pp. 47-52.
- 1150 Clayton, L., Attig, J.W., Ham, N.R., Johnson, M.D., Jennings, C.E., Syverson, K.M., 2008. Ice-walled-
1151 lake plains: implications for the origin of hummocky glacial topography in middle North
1152 America. *Geomorphology* 97, 237-248.
- 1153 Clayton, L., Teller, J.T., Attig, J.W., 1985. Surging of the south- western part of the Laurentide ice
1154 sheet. *Boreas* 14, 235-241.
- 1155 Clayton, L., Attig, J.W., Mickelson, D.M., 1999. Tunnel Channels Formed in Wisconsin during the Last
1156 Glaciation. *Geological Society of America (Special Paper)* 337, pp. 69-82.
- 1157 Colgan, P.M., Mickelson, D.M., Cutler, P.M., 2003. Ice marginal terrestrial landsystems: southern
1158 Laurentide Ice Sheet margin. In: Evans, D.J.A. (Ed.), *Glacial Landsystems*. Arnold, London, pp.
1159 111–142.
- 1160 Colton, R.B., 1955. *Geology of the Wolf Point quadrangle, Montana*. USGS, Geology Quadrangle
1161 Map.
- 1162 Cook, S.J., Knight, P.G., 2009. Glaciohydraulic supercooling. *Progress in Physical Geography* 33,
1163 705-710.
- 1164 Crémière, A., Lepland, A., Chand, S., Sahy, D., Condon, D.J., Noble, S.R., Martma, T., Thorsnes, T.,
1165 Sauer, S., Brunstad, H., 2016. Timescales of methane seepage on the Norwegian margin
1166 following collapse of the Scandinavian Ice Sheet. *Nature Communications* 7:11509.
- 1167 Deane, R.E., 1950. Pleistocene geology of the Lake Simcoe District, Ontario. *Memoir* 256. Geological
1168 Survey of Canada, Ottawa.
- 1169 Elson, J.A., 1957. Souris basin glacial lakes, southwestern Manitoba. *Abstract, Geological Society of*
1170 *America* 68, 1722.
- 1171 Elsworth, C. W., Suckale, J., 2016. Rapid ice flow rearrangement induced by subglacial drainage in
1172 West Antarctica. *Geophysical Research Letters* 43, 697–707.
- 1173 Evans, D.J.A., 2000. Quaternary geology and geomorphology of the Dinosaur Provincial Park area
1174 and surrounding plains, Alberta, Canada: the identification of former glacial lobes, drainage
1175 diversions and meltwater flood tracks. *Quaternary Science Reviews* 19, 931–958.
- 1176 Evans, D.J.A., 2003. Ice-marginal terrestrial landsystems: active temperate glacier margins. In:
1177 Evans, D.J.A. (Ed.), *Glacial Landsystems*. Arnold, London, pp.12–43.
- 1178 Evans, D.J.A., 2011. Glacial landsystems of Satujökull, Iceland: a modern analogue for glacial
1179 landsystem overprinting by mountain icecaps. *Geomorphology* 129: 225-237.
- 1180 Evans, D.J.A., 2018. *Till: A Glacial Process Sedimentology*. Wiley-Blackwell, Chichester: 390p.
- 1181 Evans, D.J.A., Benn, D.I., 2004. Facies description and the logging of sedimentary exposures. In:
1182 Evans, D.J.A., Benn, D.I. (Eds.), *A Practical Guide to the Study of Glacial Sediments*. Arnold,
1183 London, pp. 11–51.
- 1184 Evans, D.J.A., Rea, B.R., 1999. The geomorphology and sedimentology of surging glaciers: A land-
1185 systems approach. *Annals of Glaciology* 28, 75-82.
- 1186 Evans, D.J.A., Rea, B.R., 2003. Surging glacier landsystem. In: Evans, D.J.A. (Ed.), *Glacial Landsystems*.
1187 Arnold, London, pp. 259–288.
- 1188 Evans, D.J.A., Twigg, D.R. 2002. The active temperate glacial landsystem: a model based on

- 1189 Breiðamerkurjökull and Fjallsjökull, Iceland. *Quaternary Science Reviews* 21, 2143-2177.
- 1190 Evans, D.J.A., Clark, C.D., Rea, B.R., 2008. Landform and sediment imprints of fast glacier flow in the
1191 southwest Laurentide Ice Sheet. *Journal of Quaternary Science* 23, 249–272.
- 1192 Evans, D.J.A., Ewertowski M., Orton, C., 2016b. Fláajökull (north lobe), Iceland: active temperate
1193 piedmont lobe glacial landsystem. *Journal of Maps* 12, 777-789.
- 1194 Evans, D.J.A., Ewertowski, M., Orton, C., 2017. Skaftafellsjökull, Iceland: glacial geomorphology
1195 recording glacier recession since the Little Ice Age. *Journal of Maps* 13, 358-368.
- 1196 Evans, D.J.A., Hiemstra, J.F., Boston, C.M., Leighton, I., Ó Cofaigh, C., Rea, B.R., 2012. Till stratigraphy
1197 and sedimentology at the margins of terrestrially terminating ice streams: case study of the
1198 western Canadian prairies and high plains. *Quaternary Science Reviews* 46, 80–125.
- 1199 Evans, D.J.A., Lemmen, D.S., Rea, B.R., 1999. Glacial landsystems of the southwest Laurentide Ice
1200 Sheet: modern Icelandic analogues. *Journal of Quaternary Science* 14, 673–691.
- 1201 Evans, D.J.A., Nelson, C.D., Webb, C., 2010. An assessment of fluting and till esker formation on the
1202 foreland of Sandfellsjökull, Iceland. *Geomorphology* 114, 453–465.
- 1203 Evans, D.J.A., Phillips, E.R., Hiemstra, J.F., Auton, C.A., 2006. Subglacial till: formation,
1204 sedimentary characteristics and classification, *Earth Science Reviews* 78, 115-130.
- 1205 Evans, D.J.A., Storrar, R.D., Rea B.R. 2016a. Crevasse-squeeze ridge corridors: diagnostic features of
1206 late-stage palaeo-ice stream activity. *Geomorphology* 258, 40-50.
- 1207 Evans, D.J.A., Twigg, D.R., Rea B.R., Orton, C. 2009. Surging glacier landsystem of Tungnaárjökull,
1208 Iceland. *Journal of Maps* 2009: 134-151.
- 1209 Evans, D. J. A., Twigg, D.R., Rea, B.R., Shand, M., 2007. Surficial geology and geomorphology of the
1210 Brúarjökull surging glacier landsystem. *Journal of Maps* 3:1, 349-367.
- 1211 Evans, D.J.A., Young, N.J.P., Ó Cofaigh, C. 2014. Glacial geomorphology of terrestrial-
1212 terminating fast flow lobes/ice stream margins in the southwest Laurentide Ice Sheet.
1213 *Geomorphology* 204: 86-113.
- 1214 Eyles, N., Boyce, J.I., Barendregt, R.W., 1999. Hummocky moraine: sedimentary record of stagnant
1215 Laurentide Ice Sheet lobes resting on soft beds. *Sedimentary Geology* 123, 163–174.
- 1216 Eyles, N, Sladen, J.A., Gilroy, S., 1982. A depositional model for stratigraphic complexes and facies
1217 superimposition in lodgement tills. *Boreas* 11, 317-333.
- 1218 Farvolden, R.N., 1963. Bedrock channels of southern Alberta. *Research Council of Alberta Bulletin*
1219 12, 63–75.
- 1220 Fenton, M.M., Langenberg, W., Pawlowicz, J., 1993. Glacial deformation phenomena of east-central
1221 Alberta in the Stettler-Coronation region. Field trip B-1, Guidebook. Geological Association of
1222 Canada/Mineralogical Association of Canada, 46 pp.
- 1223 Fenton, M.M., Waters, E.J., Pawley, S.M., Atkinson, N., Utting, D.J., McKay, K., 2013. Surficial Geology
1224 of Alberta. Alberta Geological Survey AER/AGS Map 601.
- 1225 Flint, R.F., 1928. Eskers and crevasse fillings. *American Journal of Science* 15, 410-16.
- 1226 Galon, R., 1973b. Geomorphological and geological analysis of the proglacial area of Skeiðarárjökull.
1227 *Geographica Polonica* 26, 15-56.
- 1228 Gokhman, V. V. 1987. Two types of intraglacial meltwater regime for the Bertil Glacier, Svalbard.
1229 *Polar Geography and Geology* 11, 241-248.
- 1230 Grasby, S.E., Osadetz, K., Betcher, R., Render, F. 2000. Reversal of the regional-scale flow system
1231 of the Williston basin in response to Pleistocene glaciation. *Geology* 28, 635–638.
- 1232 Grasby, S.E., Chen, Z., 2005. Subglacial recharge into the Western Canada Sedimentary Basin -
1233 impact of Pleistocene glaciation of basin hydrodynamics. *Geological Society of America*
1234 *Bulletin* 117, 500-514.
- 1235 Grasby, S.E., 2013. Pickled shale gas play – How continental glaciation drives biogenic gas formation.

- 1236 GeoConvention. Canadian Society of Petroleum Geologists, Calgary.
- 1237 Gravenor C.P., Bayrock L.A. 1955. Glacial Geology, Coronation District, Alberta. Preliminary Report
1238 55-1. Research Council of Alberta, 38pp.
- 1239 Gravenor, C.P., Kupsch, W.O., 1959. Ice disintegration features in western Canada. *Journal of*
1240 *Geology* 67, 48-64.
- 1241 Gravenor, C.P., Ellwood, R.B., 1957. Glacial geology, Sedgewick District, Alberta. Alberta Research
1242 Council, Preliminary Report 57-1.
- 1243 Gray, L., Joughin, I., Tulaczyk, S., Spikes, V. B., Bindschadler, R., Jezek, K., 2005. Evidence for
1244 subglacial water transport in the West Antarctic Ice Sheet through three-dimensional
1245 satellite radar interferometry. *Geophysics Research Letters* 32, L03501,
1246 <https://doi.org/10.1029/2004GL021387>, 2005.
- 1247 Hatcher, Jr., R.D., 1995. *Structural Geology: principles, concepts and problems* (second edition).
1248 Prentice Hall. Englewood Cliffs, New Jersey
- 1249 Hebrand, M., Amark, M., 1989. Esker formation and glacier dynamics in eastern Skane and
1250 adjacent areas, southern Sweden. *Boreas* 18, 67-81.
- 1251 Hodgkins, R., Tranter, M., Dowdeswell, J.A., 2004. The characteristics and formation of a High-
1252 Arctic proglacial icing. *Geografiska Annaler* A86, 265-275.
- 1253 Hooke, R. Le B., Fastook, J., 2007. Thermal conditions at the bed of the Laurentide Ice Sheet in
1254 Maine during deglaciation: implications for esker formation. *Journal of Glaciology* 53, 646-
1255 658.
- 1256 Hopkins, O.B., 1923. Some structural features of the plains area of Alberta caused by Pleistocene
1257 glaciation. *Bulletin of the Geological Society of America* 34, 419-430.
- 1258 Hoppe, G., 1952. Hummocky moraine regions, with special reference to the interior of Norrbotten.
1259 *Geografiska Annaler* A34, 1-72.
- 1260 Howarth, P.J., 1971. Investigations of two eskers at eastern Breidamerkurjokull, Iceland. *Arctic and*
1261 *Alpine Research* 3, 305-318.
- 1262 Jennings, C.E., 2006. Terrestrial ice streams – a view from the lobe. *Geomorphology* 75, 100-124.
- 1263 Johnson, M.D., Clayton, L., 2003. Supraglacial landsystems in lowland terrain. In: Evans, D.J.A. (Ed.),
1264 *Glacial Landsystems*. Arnold, London, pp. 228-251.
- 1265 Johnston, W.A., Wickenden, R.T.D., 1931. Moraines and glacial lakes in southern Saskatchewan and
1266 southern Alberta, Canada. *Royal Society of Canada Transactions* 31, 81-95.
- 1267 Kehew, A.E., Lord, M.L., 1986. Origin and large scale erosional features of glacial lake spillways in the
1268 northern Great Plains. *Geological Society of America Bulletin* 97, 162-177.
- 1269 Kehew, A.E., Lord, M.L., 1987. Glacial lake outbursts along the midcontinent margins of the
1270 Laurentide ice sheet. In: Mayer, L., Nash, D. (Eds.), *Catastrophic Flooding*, Allen and Unwin,
1271 Boston, pp. 95-120.
- 1272 Kehew, A.E., Clayton, L., 1983. Late Wisconsinan floods and development of the Souris- Pembina
1273 spillway system in Saskatchewan, North Dakota and Manitoba. In: Teller, J.T., Clayton, L.
1274 (Eds.), *Glacial Lake Agassiz*, Geological Association of Canada, (Special Paper 26) pp. 187-209.
- 1275 Kehew, A.E., Kozlowski, A.L., 2007. Tunnel channels of the Saginaw Lobe, Michigan, USA. In:
1276 Johansson, P., Sarala, P. (eds.), *Applied Quaternary Research in the Central Part of Glaciated*
1277 *Terrain*. Geological Survey of Finland, Special Paper 46, pp. 69-78.
- 1278 Kjær, K.H., Larsen, E., van der Meer, J.J.M., Ingólfsson, Ó., Krüger, J., Benediktsson, Í.Ö., Knudsen,
1279 C.G., Schomacker, A., 2006. Subglacial decoupling at the sediment/bedrock interface: a new
1280 mechanism for rapid flowing ice. *Quaternary Science Reviews* 25, 2704-2712.
- 1281 Kjearsgaard, A.A., 1988. Reconnaissance soil survey of the Oyen map sheet – 72M. Alberta Soil
1282 Survey Report S-76-36.

1283 Knudsen, O., 1995. Concertina eskers, Bruarjökull, Iceland: an indicator of surge-type glacier
1284 behaviour. *Quaternary Science Reviews*, 14, 487-493.

1285 Krüger, J., 1995. Origin, chronology and climatological significance of annual moraine ridges at
1286 Myrdalsjökull, Iceland. *The Holocene* 5, 420–427.

1287 Kupsch, W.O., 1962. Ice-thrust ridges in western Canada. *Journal of Geology* 70, 582-594.

1288 Larsen, N.K., Piotrowski, J.A., Christoffersen, P., Menzies, J., 2006. Formation and deformation of
1289 basal till during a glacier surge; Elisebreen, Svalbard. *Geomorphology* 81, 217–234.

1290 Le Heron, D.P., Etienne, J.L., 2005. A complex subglacial clastic dyke swarm, Solheimajökull, southern
1291 Iceland. *Sedimentary Geology* 181, 25–37.

1292 Lelandais, T., Ravier, E., Pochat, S., Bourgeois, O., Clark, C.D., Mourgues, R., Strzeczynski, P., 2018.
1293 Modelled subglacial floods and tunnel valleys control the life cycle of transitory ice streams.
1294 *The Cryosphere* 12, 2759-2772.

1295 Lemieux, J-M., Sudicky, E.A., Peltier, W.R., Tarasov, L., 2008. Dynamics of groundwater recharge
1296 and seepage over the Canadian landscape during the Wisconsinian glaciation. *Journal of*
1297 *Geophysical Research* 113, F01011, doi:10.1029/2007JF000838, 2008

1298 Livingstone, S.J., Evans, D.J.A., Ó Cofaigh, C., Hopkins, J., 2010. The Brampton Kame Belt and Pennine
1299 Escarpment Meltwater Channel System (Cumbria, UK). *Morphology, Sedimentology and*
1300 *Formation. Proceedings of the Geologists' Association* 121, 423–443.

1301 Livingstone, S.J., Utting, D., Ruffell, A., Clark, C.D., Pawley, S., Atkinson, N., Fowler, A.C., 2016.
1302 Discovery of relict subglacial lakes and the mechanism and geometry of drainage. *Nature*
1303 *Communications* 7:11767, doi: 10.1038/ncomms11767

1304 Mandl, G., Harkness, R.M., 1987. Hydrocarbon migration by hydraulic fracturing. In: Jones, M.E.,
1305 Preston, R.M.F. (Eds.), *Deformation of Sediments and Sedimentary Rocks*. Geological Society
1306 of London, Special Publication, vol. 29, pp. 39–53.

1307 Margold, M., Stokes, C.R., Clark, C.D., 2015. Ice streams in the Laurentide Ice Sheet: Identification,
1308 characteristics and comparison to modern ice sheets. *Earth Science Reviews* 143, 117-146.

1309 Margold M., Stokes C.R., Clark C.D., 2018. Reconciling records of ice streaming and ice margin
1310 retreat to produce a palaeogeographic reconstruction of the deglaciation of the Laurentide
1311 Ice Sheet. *Quaternary Science Reviews* 189, 1-30.

1312 Mazzini, A., Svensen, H.H., Forsberg, C.F., Linge, H., Lauritzen, S-E., Haflidason, H., Hammer, Ø.,
1313 Planke, S., 2017. A climatic trigger for the giant Troll pockmark field in the northern North
1314 Sea. *Earth and Planetary Science Letters* 464, 24-34.

1315 Mokhtari Fard, A., 2002. Large dead-ice depressions in flat-topped eskers: evidence of a Preboreal
1316 jökulhlaup in the Stockholm area, Sweden. *Global and Planetary Change* 35, 273-295.

1317 Mollard, J.D., 2000. Ice-shaped ring-forms in Western Canada: their airphoto expressions and
1318 manifold polygenetic origins. *Quaternary International* 68–71, 187-198.

1319 Mooers, H.D., 1990. Ice-marginal thrusting of drift and bedrock: thermal regime, subglacial aquifers
1320 and glacial surges. *Canadian Journal of Earth Sciences* 27, 849-862.

1321 Moran, S.R., Clayton, L., Hooke, R., Fenton, M.M., Andriashek, L.D., 1980. Glacier-bed landforms of
1322 the prairie region of North America. *Journal of Glaciology* 25, 457-473.

1323 Mossop, G.D., Shetsen, I., 1994. *Geological Atlas of the Western Canada Sedimentary Basin*. Special
1324 Report. Canadian Society of Petroleum Geologists and Alberta Research Council, 510 pp.

1325 Mulligan, R.P.M., Eyles, C.H., Marich, A.S., 2019. Subglacial and ice-marginal landforms in south-
1326 central Ontario: implications for ice sheet reconfiguration during deglaciation. *Boreas* 48,
1327 635-657.

1328 Norris, S.L., Evans, D.J.A., Ó Cofaigh, C., 2018. Geomorphology and till architecture of terrestrial
1329 palaeo-ice streams of the southwest Laurentide Ice Sheet: A borehole stratigraphic
1330 approach. *Quaternary Science Reviews* 186, 186-214.

- 1331 Ó Cofaigh, C., 1996. Tunnel valley genesis. *Progress in Physical Geography* 20, 1-19.
- 1332 Ó Cofaigh, C., Evans, D.J.A., Smith, I.R., 2010. Large-scale reorganization and sedimentation of
1333 terrestrial ice streams during late Wisconsinan Laurentide ice sheet deglaciation. *Geological*
1334 *Society of America Bulletin* 122, 743-756.
- 1335 Parizek, R.R., 1969. Glacial ice-contact ridges and rings. *Geological Society of America Special Paper*
1336 123, 49-102.
- 1337 Patterson, C.J., 1994. Tunnel valley fans of the St Croix moraine, east-central Minnesota, USA. In:
1338 Warren, W.P., Croot, D.G. (eds.), *Formation and Deformation of Glacial Deposits*. Balkema,
1339 Rotterdam, pp. 69-87.
- 1340 Patterson, C.J., 1997. Southern Laurentide ice lobes were created by ice streams: Des Moines Lobe in
1341 Minnesota, USA. *Sedimentary Geology* 111, 249-261.
- 1342 Patterson, C.J., 1998. Laurentide glacial landscapes: the role of ice streams. *Geology* 26, 643-646.
- 1343 Paulen, R.C., McClenaghan, M.B., 2015. Late Wisconsin ice-flow history in the Buffalo Head Hills
1344 kimberlite field, north-central Alberta. *Canadian Journal of Earth Sciences* 52, 51-67.
- 1345 Perkins, A.J., Brennand, T.A., Burke, M.J., 2016. Towards a morphogenetic classification of eskers:
1346 implications for modelling ice sheet hydrology. *Quaternary Science Reviews* 134, 19-38.
- 1347 Peters, L. E., Anandakrishnan, S., Alley, R. B., Smith, A.M., 2007. Extensive storage of basal
1348 meltwater in the onset region of a major West Antarctic ice stream. *Geology* 35, 251-254.
- 1349 Pettapiece, W.W., 1986. *Physiographic Subdivision of Alberta*. Agriculture and Agri-
1350 Food Canada, Ottawa.
- 1351 Phillips, E., Evans, D.J.A., Atkinson, N., Kendall, A., 2017. Structural architecture and glaciectonic
1352 evolution of the Mud Buttes cupola hill complex, southern Alberta, Canada. *Quaternary*
1353 *Science Reviews* 164, 110-139.
- 1354 Phillips, E., Everest, J., Reeves, H., 2013. Micromorphological evidence for subglacial multiphase
1355 sedimentation and deformation during overpressurized fluid flow associated with
1356 hydrofracturing. *Boreas* 42, 395-427.
- 1357 Price, N.J., Cosgrove, J.W. 1990. *Analysis of Geological Structures*. Cambridge University Press,
1358 Cambridge.
- 1359 Price, R. J., 1969. Moraines, sandar, kames and eskers near Breiðamerkurjökull, Iceland. *Transactions*
1360 *of the Institute of British Geographers* 46, 17-43.
- 1361 Price, R.J., 1982. Changes in the proglacial area of Breiðamerkurjökull, southeastern Iceland: 1890-
1362 1980. *Jökull* 32, 29-35.
- 1363 Raymond, C. F., Johannesson, T., Pfeffer, T., Sharp, M., 1987. Propagation of a glacier surge into
1364 stagnant ice. *Journal of Geophysical Research*, 92, 9037-9049.
- 1365 Roberts, D.H., Yde, J., Long, A.J., Knudsen, N.T., Lloyd, J.M., 2009. Ice marginal dynamics during surge
1366 activity, Kuannersuit Glacier, Disko Island, West Greenland. *Quaternary Science Reviews* 28,
1367 209-222.
- 1368 Rose, J., 1989. Glacier stress patterns and sediment transfer associated with the formation of
1369 superimposed flutes. *Sedimentary Geology* 62, 151-176.
- 1370 Ross, M., Campbell, J.E., Parent, M., Adams, R.S., 2009. Palaeo-ice streams and the subglacial
1371 landscape mosaic of the North American mid-continental prairies. *Boreas* 38, 421-439.
- 1372 Russell A.J., Gregory A.G., Large A.R.G., Fleisher P.J., Harris T., 2007. Tunnel channel formation during
1373 the November 1996 jökulhlaup, Skeiðarárjökull, Iceland. *Annals of Glaciology* 45, 95-103.
- 1374 Russell, A.J., Knight, P.G., van Dijk, T.A.G.P., 2001b. Glacier surging as a control on the development
1375 of proglacial, fluvial landforms and deposits, Skeiðarársandur, Iceland. *Global and Planetary*
1376 *Change* 28, 163-174.
- 1377 Russell, A. J., Knudsen, Ó., Fay, H., Marren, P. M., Heinz, J., Tronicke, J., 2001a. Morphology and

1378 sedimentology of a giant supraglacial, ice-walled, jökulhlaup channel, Skeiðarársandur,
1379 Iceland. *Global and Planetary Change* 28, 203-226.

1380 Sauer, E.K., 1978. The engineering significance of glacier ice thrusting. *Canadian Geotechnical Journal*
1381 15, 457–472.

1382 Schomacker, A., Krüger, J., Kurth, K., 2006. Ice-cored drumlins at the surge-type glacier Bruarjökull,
1383 Iceland: a transitional-state landform. *Journal of Quaternary Science* 21, 85–93.

1384 Sharp, M.J., 1985a. “Crevasse-fill” ridges—A landform type characteristic of surging? *Geografiska*
1385 *Annaler* A67, 213-220.

1386 Sharp, M.J., 1985b. Sedimentation and stratigraphy at Eyjabakkajökull - an Icelandic surging glacier.
1387 *Quaternary Research* 24, 268-284.

1388 Shetsen, I., 1987. Quaternary geology, southern Alberta. Alberta Research Council, Alberta
1389 Geological Survey, Map 207, scale 1:500 000.

1390 Shetsen, I., 1990. Quaternary geology, central Alberta. Alberta Research Council, Alberta Geological
1391 Survey, Map 213.

1392 Siegfried, M. R., Fricker, H. A., Carter, S. P., Tulaczyk, S., 2016. Episodic ice velocity fluctuations
1393 triggered by a subglacial flood in West Antarctica. *Geophysics Research Letters* 43, 2640–
1394 2648.

1395 Sjogren, D.B., Rains, R.B., 1995. Glaciofluvial erosional morphology and sediments of the Coronation-
1396 Spondin scabland, east-central Alberta. *Canadian Journal of Earth Sciences* 32, 565–578.

1397 Slater, G., 1927. Structure of the Mud Buttes and Tit Hills in Alberta. *Bulletin of the Geological*
1398 *Society of America*, p. 38.

1399 Sookhan, S., Eyles, N., Arbelaez-Moreno, L., 2018. Converging ice streams: a new paradigm for
1400 reconstructions of the Laurentide Ice Sheet in southern Ontario and deposition of the Oak
1401 Ridges Moraine. *Canadian Journal of Earth Sciences* 55, 373-396.

1402 Sproule, J. C., 1939. The Pleistocene geology of the Cree Lake region, Saskatchewan. *Transactions of*
1403 *the Royal Society of Canada, Series 3*, 33, 101-7.

1404 Stalker, A.M., 1960. Ice-pressed drift forms and associated deposits in Alberta. *Bulletin* 57.
1405 *Geological Survey of Canada, Ottawa.*

1406 Stalker, A.M., 1961. Buried valleys in central and southern Alberta. *Bulletin* 15. *Geological Survey of*
1407 *Canada, Ottawa.*

1408 Stalker, A.M., 1973. [The large interdrift bedrock blocks of the Canadian Prairies. Geological Survey](#)
1409 [Canada, Paper 75-1A. 421–422.](#)

1410 Stalker, A.M., 1976. Megablocks, or the enormous erratics of the Albertan Prairies. *Geological Survey*
1411 *of Canada, Paper 76-1C*, 185-188.

1412 St-Onge, D.A., 1972. Sequence of glacial lakes in north-central Alberta. *Bulletin* 213. *Geological*
1413 *Survey of Canada, Ottawa.*

1414 Storrar, R.D., Stokes C.R., Evans, D.J.A., 2014a. Increased channelization of subglacial drainage during
1415 deglaciation of the Laurentide Ice Sheet. *Geology* 42, 239–242.

1416 Storrar, R.D., Stokes, C.R., Evans, D.J.A., 2014b. Morphometry and pattern of a large sample
1417 (>20,000) of Canadian eskers and implications for subglacial drainage beneath ice sheets.
1418 *Quaternary Science Reviews* 105, 1–25.

1419 Storrar, R.D., Evans, D.J.A., Stokes, C.R., Ewertowski, M., 2015. Controls on the location, morphology
1420 and evolution of complex esker systems at decadal timescales, Breiðamerkurjökull,
1421 southeast Iceland. *Earth Surface Processes and Landforms* 40, 1421–1438.

1422 Storrar, R.D., Ewertowski, M., Tomczyk, A., Barr, I.D., Livingstone, S.J., Ruffell, A., Stoker, B.J., Evans,
1423 D.J.A., in press. Equifinality and preservation potential of complex eskers. *Earth Surface*
1424 *Processes and Landforms.*

1425 Tsui, P.C., Cruden, D.M., Thomson, S., 1989. Ice thrust terrains and glaciotectonic settings in central

1426 Alberta. *Canadian Journal of Earth Sciences* 26, 1308-1318.

1427 Utting, D. J., Atkinson, N., Pawley, S.M., Livingstone, S.J., 2016. Reconstructing the confluence zone
 1428 between Late Wisconsinan Laurentide and Cordilleran ice along the Rocky Mountain
 1429 Foothills, Alberta. *Journal of Quaternary Science* 31, 769-787.

1430 van der Meer, J.J.M., Kjær, K.H., Krüger, J., Rabassa, J., Kilfeather, A.A., 2009. Under pressure: clastic
 1431 dykes in glacial settings. *Quaternary Science Reviews* 28, 708–720.

1432 Vaughan, D.G., Corr, H.F.J., Smith, A.M., Pritchard, H.D., Shepherd, A., 2008. Flowswitching and
 1433 water piracy between Rutford ice stream and Carlson inlet, west Antarctica. *Journal of*
 1434 *Glaciology* 54, 41-48.

1435 Wickenden, R.T.D., 1931. An area of little or no drift in southern Saskatchewan. *Transactions of the*
 1436 *Royal Society of Canada* 25, 45-47.

1437
 1438

1439 **Figure captions**

1440 Fig. 1: The palaeo-ice streams of the southern Canadian Prairies and summary of their related flow
 1441 sets mapped on SRTM digital elevation model (after Ó Cofaigh et al., 2010; Norris et al., 2018). CAIS
 1442 = Central Alberta Ice Stream; HPIS = High Plains Ice Stream.

1443

1444 Fig. 2: Location map and DEM showing place names referred to in text and major geomorphological
 1445 features of the study area and its regional context. Inset map of the surficial geology of the study
 1446 area (from Fenton et al., 2013) shows: E - aeolian deposits; LG - glaciallacustrine deposits; FG -
 1447 glacialfluvial deposits; M - undifferentiated moraine (diamict); MS - stagnation moraine; MF - fluted
 1448 moraine; MT - ice thrust moraine.

1449

1450 Fig. 3: Glacial geomorphology map of the Neutral Hills Upland area of southeast central Alberta. Grid
 1451 lines define bespoke co-ordinate system for ease of reference when using following figures.
 1452 Following figure captions use this co-ordinate system to identify the mid-point of the grid square in
 1453 which the landform examples occur (e.g., C7, F14, A5).

1454

1455 Fig. 4: Examples of major glacitectonic thrust masses: a) Nose Hill viewed from the southeast (C7);
 1456 b) Google Earth (Landsat 7 at 15 m resolution) oblique view of the west Neutral Hills with
 1457 Gooseberry Lake (3.4 km long) in the foreground (F7); c) exposure through the Mud Buttes cupola
 1458 hill, showing deformed bedrock strata (G4). Field truck (circled) for scale; d) exposure through
 1459 deformed bedrock ridge near Mushroom Lake (F14).

1460 Fig. 5: Examples of overprinted glacitectonic thrust masses: a) the Killarney Lake area (I11-12),
 1461 where three phases of deformation are apparent in the surface lineaments. Phase 1 involved the
 1462 lateral displacement of a mega-raft 25 km to the south near St Lawrence Lake. Location of sections
 1463 KL1 and KL2 are shown; b) stratigraphic exposures through the Killarney Lake thrust masses, showing
 1464 sediments and structures and clast macrofabrics for sections KL1 (upper) and KL2 (lower); c) LiDAR
 1465 extracts showing the area south of Sounding Lake (upper, F7) and the western Neutral Hills and the
 1466 Nose Hill/Ribstone Creek area (lower, C7).

1467 Fig. 6: Complex overprinting of thrust masses in the Misty Hills, Sharp Hills, Mud Buttes and Esther
 1468 uplands (G4). Area highlighted in green is the western block, which is the most recently displaced
 1469 part of the complex, deformed by easterly flowing ice, as documented by fluted till. The Grassy

1470 Island Moraine, indicative of widespread stagnant ice melt out, is also demarcated by orange dashed
1471 line.

1472 Fig. 7: Features associated with major thrust masses: a) LiDAR image of ridge-rimmed depressions or
1473 doughnuts, locally aligned to form discontinuous chains on the summit of the east Neutral Hills
1474 (chain examples are circled by black outline; I6). Also visible on the eastern end of the thrust mass is
1475 a fan-shaped assemblage of doughnut forms with a channel at its apex marked by a chain of ponds
1476 and an esker trending towards the east-northeast; b) isolated pit containing a small pond and cutting
1477 across the structural grain (ridges and furrows) of the west Neutral Hills; c) LiDAR image of large pits,
1478 some lying in chains, bounded by fault scarps and located on the distal slopes of the western Neutral
1479 Hills (F7); d) large mass movement feature resembling a retrogressive flow scar, located on the distal
1480 slope of the west end of the eastern Neutral Hills (H6).

1481
1482 Fig. 8: Examples of short lineaments and ridges: a) and b) LiDAR images of non-fluted MTR type 1
1483 corrugation ridges at the west end of the western Neutral Hills (C8) and near New Brigden (G/H3)
1484 respectively; c) LiDAR image of cross-cutting lineaments directly southeast of Nose Hill, displaying
1485 ridge fragmentation and dense pitting indicative of ice melt-out after tectonic grain development
1486 (C/D7). Lineaments run north-south and east-west; d) Semi-transparent Google Earth image draped
1487 over LiDAR DEM of MTR type 2 (recessional push moraines) south of Sedalia and near Sounding
1488 Creek (F-G, 1/2).

1489
1490 Fig. 9: LiDAR images of examples of areas overridden moraines and cupola hills: a) arcuate series of
1491 muted moraine ridges surrounding Coronation (A6/7), which likely originated as composite thrust
1492 ridges; b) streamlined cupola hill located NE of Sounding Lake, showing faint surface fluting (white
1493 lines), localised geometric ridge networks and surface pits indicative of ice melt-out (H7/8); c)
1494 overridden thrust masses (circled) exhibiting structural lineaments parallel to the direction of
1495 overriding ice flow as defined by flutings (white lines). Located south of the Sounding Creek
1496 depression (G1). Ice flow was towards the east.

1497
1498 Fig. 10: LiDAR imagery of examples of rubble terrain: a) elongate assemblage located southeast of
1499 Kirriemuir (I4) and containing Quaternary sediment, best illustrated at quarry outcrop marked by the
1500 "x" label (see Fig. 10e). Broken lines trace faint surface flutings; b) isolated rafts lying within an area
1501 of ice-walled lake plains and hummocky terrain in the Altario Moraine (H5); c) incipient, partially
1502 fragmented rafts (outlined) and their tear fault-bounded depressions located north of Little Gem
1503 (E4). Tear fault traces are marked by straight broken lines; d) "rubble stripes" located south of the
1504 eastern Neutral Hills (H6), with overridden and quarried thrust mass outlined; e) sedimentary and
1505 structural details and clast macrofabric from quarry exposure through Quaternary deposits in a
1506 single raft in the Kirriemuir elongate assemblage (see "x" on Fig. 10a).

1507
1508 Fig. 11: LiDAR images of examples of multiple parallel lineations (flutings) and groove features with
1509 mega rafts: a) NNW-SSE aligned flutings on the bed of the Central Alberta Ice Stream, south of
1510 Coronation (A5-6), showing a grooved terrain lying between relatively higher topography containing
1511 overridden composite thrust ridges, geometric ridge networks and/or fluvially eroded residual bars
1512 of the "Coronation-Spondin scabland". Inset shows a succession of hill-hole pairs in the grooved
1513 terrain; b) rubble stripes on the footprint of the Fabyan-Amisk palaeo-ice stream (demarcated by the

1514 black dashed lines; C-D, 11-15). Insets show that the fluting pattern is locally composed of linear
1515 mega-raft chains (outlined); c) groove and mega-raft pairs, illustrated by an example from the bed of
1516 the former easterly flowing Ice Stream 2A, north of Battle River (upper), and an example from
1517 overridden thrust moraines immediately northwest of the map area, where westerly flowing ice
1518 displaced a thin-skinned mega-raft.

1519

1520 Fig. 12: LiDAR images of examples of geometric ridge networks: a) the CAIS footprint around the
1521 town of Brownfield (B8), showing extensive geometric ridges as well as several zig-zag eskers; b) the
1522 footprint of the Prospect Valley lobe near Lloydminster (immediately northeast of the map area),
1523 showing the location of a sedimentary exposure through a ridge together with a section cliff image
1524 and clast macrofabric data.

1525

1526 Fig. 13: LiDAR images showing examples of eskers: a) large, flat-topped esker passing laterally into
1527 flat-topped hills (ice-walled lake plains) on the floor of the Sounding Lake-Eyehill Creek depression
1528 (E-H, 8-10), illustrating the torturous alignment of the main ridge and its circular deflection that
1529 forms a 180° change in direction. Note the increasingly wider flat-topped summit starting at the area
1530 of the circular deflection and then towards the northwest; b) flat-topped eskers and their tributary
1531 and distributary branches located 10 km south of Wainwright and in the area of Ribstone Lake (D-
1532 F13), illustrating a large flat-topped ridge that fans out and terminates at pitted outwash on the
1533 distal edge of the Prospect Valley composite thrust moraine belt. Dashed line delineates a chain of
1534 elongate depressions that are inferred to have resulted from collapse into a buried tunnel channel;
1535 c) tunnel channels near Kinsella (immediately northwest of the map area) within an area of
1536 hummocky terrain and flat-topped hills (ice-walled lake plains) and containing segments of flat-
1537 topped ridges that rise above the channels walls; d) hummocky terrain north of Hardisty (B13),
1538 containing flat-topped hills (ice-walled lake plains) and minor eskers and doughnut chains grading
1539 southeasterly into an area of complex and meandering esker ridges contained within channels of
1540 variable width and displaying arcuate cliff segments.

1541

1542 Fig. 14: LiDAR image of hummocky terrain north of Irma (A15), illustrating a range of landforms
1543 typical of this type of landscape, including eskers, contiguous doughnuts and doughnut chains and
1544 excellent examples of ridge-rimmed mounds or flat-topped hills (ice-walled lake plains). At the
1545 centre of the image is a prime example of an “unstable ice-walled lake plain” through which
1546 subglacial tunnel channels and muted hummocks can be detected.

1547

1548 Fig. 15: Examples of pitted and hummocky terrain interpreted as areas of formerly ice-cored
1549 glacial tectonic thrust mass: a) LiDAR image of an area located directly south of the western Neutral
1550 Hills thrust complex (D/E7) and containing substantial lakes with cliffed, often rectilinear or arcuate
1551 boundaries and details of a hummock exposure located at the yellow “X” symbol that show
1552 significant deformation, thrust faulting and diapirism of bedrock and Quaternary sediments; b)
1553 LiDAR image of an area of largely chaotically pitted Quaternary materials with discontinuous
1554 lineaments located immediately north of the western Neutral Hills (E9); c) LiDAR image of the “North
1555 Altario depression” (I6), with the main landforms annotated. The veneer of glacial lacustrine deposits
1556 linked to flat-topped hills is outlined by the dashed line.

1557

1558 Fig. 16: Examples of hummocky terrain: a) LiDAR image and ground photograph of the Veteran
1559 Moraine (D6) showing its component landforms of hummocks, flat-topped hills and eskers; b) details
1560 of an exposure through a typical hummock in the Veteran Moraine, showing clay-rich diamicton with
1561 sheared sand lenses; c) LiDAR image of the Altario Moraine (H5/6), showing contiguous doughnut
1562 mounds, short sinuous hummocky ridges, ice-walled lake plains, eskers and associated doughnut
1563 chains; d) LiDAR image showing locations of hummocky terrain exposures in the Viking Moraine
1564 around Kinsella (A15; see also Figs. 13d and 14) and annotated photographs of the stratigraphic
1565 details and clast macrofabrics. White dotted lines highlight thrust structures.

1566

1567 Fig. 17: LiDAR images of examples of erosional channels, large terraces and cliffs: a) prominent
1568 channels with cliffed margins in the area around Hardisty, west of the Battle River (A10-14), which
1569 occupies the large trench on the bottom right of the image. The reticulate pattern, which isolates
1570 polygonal-shaped areas of prairie surface containing overridden thrust mass lineaments (MTR Type
1571 1); b) probable subglacial tunnel channels identifiable as sinuous chains of elongate lakes partially
1572 obscured by glacial depositional landforms and in places (i.e. Wilkins Lake) aligned with eskers (i =
1573 C11; ii = G10; iii = I9); c) spillway channel networks, illustrated by the Loyalist Creek and Monitor
1574 Creek channels (left; F-G5) incised through glacitectonic thrust masses on the west side of the
1575 Monitor Creek basin and by Sounding Creek (right; H-I, 2-5), which is incised through the Misty
1576 Hills/Esther Uplands thrust moraine complex and then through the pitted glacialfluvial deposits of the
1577 Grassy Island Moraine.

1578

1579 Fig. 18: Summary maps (annotated on the regional DEM) of: a) the major glacial landform
1580 components and landsystem imprints, showing the inset arcuate assemblages of moraine arcs that
1581 demarcate the repeat surging of the ice lobes of "eastern" provenance flowing south-southwesterly
1582 into the eastern margin of the CAIS and alternating with the CAIS-derived flow set 4 footprint; and b)
1583 palaeo-ice stream extents, flow sets and relative event chronology for the map area and immediate
1584 environs based on the distribution of landsystems and their cross-cutting relationships. Note that
1585 the large esker network of the Eyehill Creek-Sounding Lake depression is highlighted as an example
1586 of reversed drainage back into and through stagnating ice, in this case the ice that was responsible
1587 for the Flow set 4 footprint.

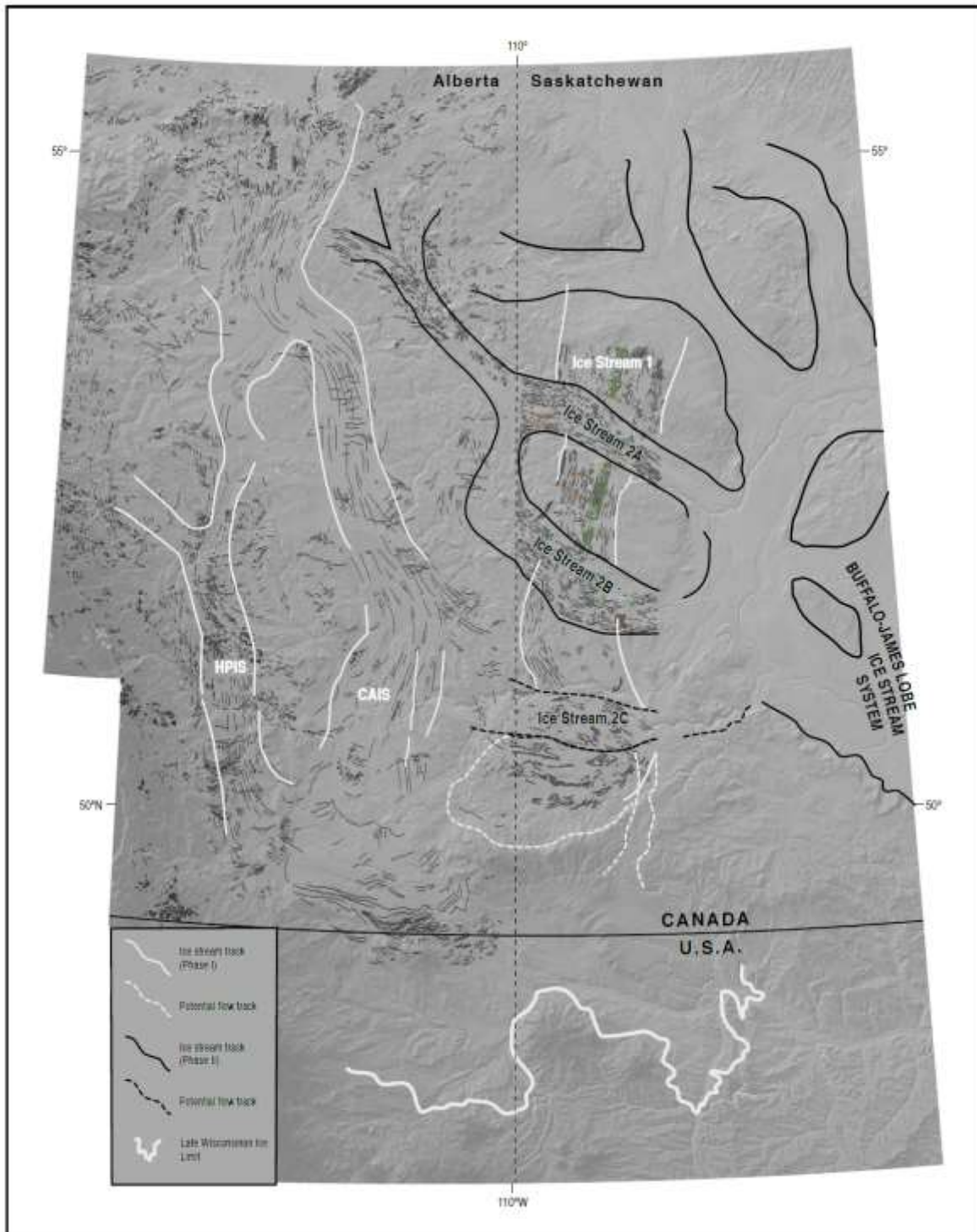
1588

1589 Fig. 19: Details of the Event 5 lobate ice stream surge in the Lloydminster/Prospect Valley area: i) to
1590 iii) LiDAR images of the main landsystem components identified on an extract from the
1591 geomorphology map in Fig. 3; b) oblique aerial photograph of a modern analogue for the ice-cored
1592 surge moraine, Skeiðarárjökull foreland, Iceland. Note that this moraine still contains significant
1593 buried snout ice but ongoing melt-out has initiated the fragmentation and pitting of inset linear
1594 ridges related to folds and thrust slices. Esker ridges can also be seen emerging through the
1595 downwasting landform complex.

1596 Fig. 20: Conceptual model of the landsystem signature produced by surging into areas of stagnant
1597 ice lying over Cretaceous bedrock on the Canadian prairies, with example figures of typical
1598 landforms labelled: a) Phase A shows ice sheet marginal downwasting and recession during which
1599 large areas of ice may get buried by glacialfluvial outwash. 1 = ice sheet margin, 2 = meltwater
1600 drainage pathways with 2a representing earlier tunnels and 2b the later stage of englacial drainage
1601 adjusting to aggrading outwash fans, 3 = aggrading glacialfluvial outwash comprising regional

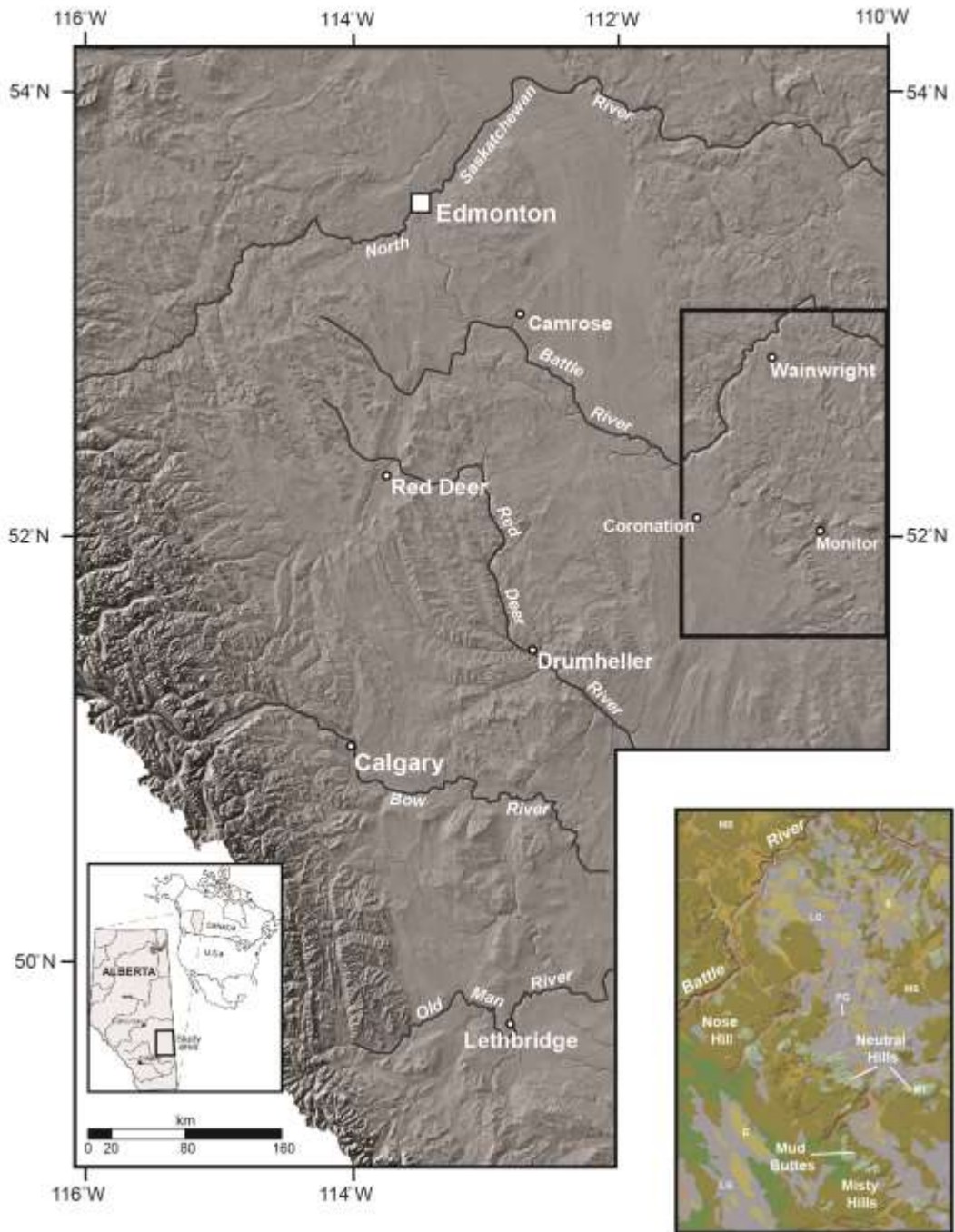
1602 northeasterly-directed drainage along the ice margin (3a) and proglacial/supraglacial ice-contact
1603 fans (3b), and 4 = sub-marginal till wedges; b) Phase B shows the advanced stages of local ice
1604 stagnation, where buried glacier ice (1) contains an extensive karst network from which ice-walled
1605 lake plains, eskers and kame and kettle topography emerge (2). Englacial to subglacial drainage
1606 networks have by this time been developed by northeasterly draining meltwater (i.e. reversed
1607 drainage), in which eskers, doughnut chains and till eskers form. Extensive areas of doughnuts (4)
1608 also form due to subglacial squeezing of till into cavities beneath thin ice and/or blow-out or de-
1609 gassing through the glacial sediment cover; c) Phase C shows the surge of the ice sheet margin
1610 (1) and its construction of a composite thrust moraine due to glacial tectonic disruption of Cretaceous
1611 bedrock (2), which is then pushed into the area of stagnating glacier ice (3). The ice is dislocated into
1612 thrust masses and its englacial material is consequently deformed. The area of former outwash lying
1613 distal to the stagnant ice is also compressed in the proglacial stress field (4). Large melt-out pits and
1614 retrogressive slumps gradually evolve in the ice-cored thrust mass. Pressurised aquifers create
1615 hydrofractures and blow-out features (doughnuts) in the composite thrust moraine. Crevasse
1616 squeeze ridges are developed on the proximal slopes of the proglacial thrust complex and subglacial
1617 surface due to intensive surge-related crevassing.

1618



1619

1620



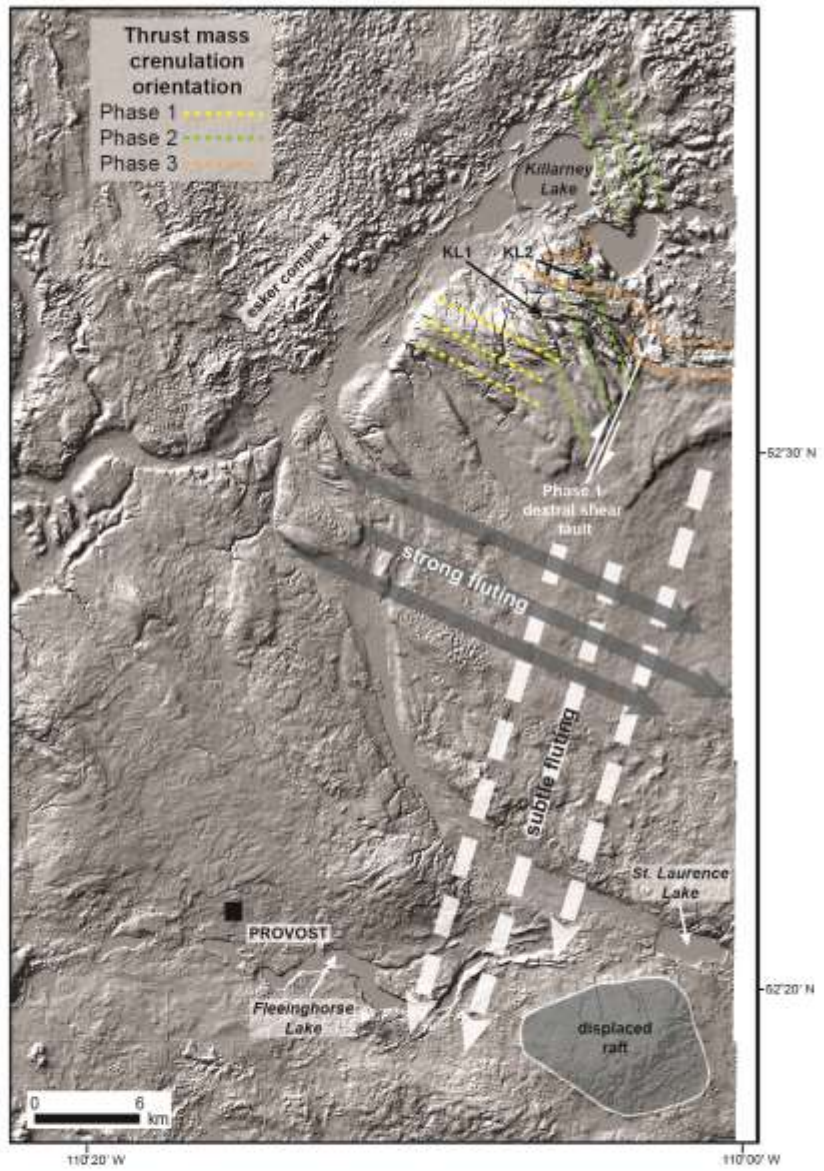
1621

1622



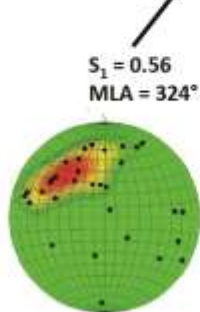
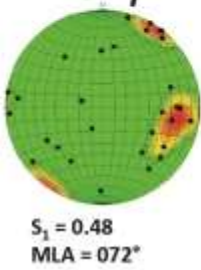
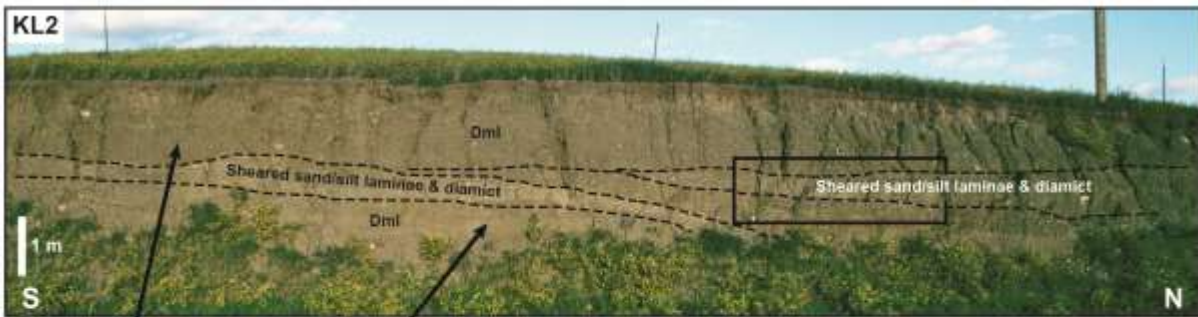
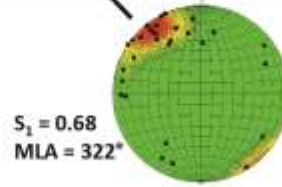
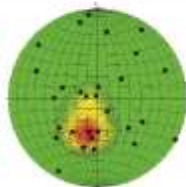
1625

1626



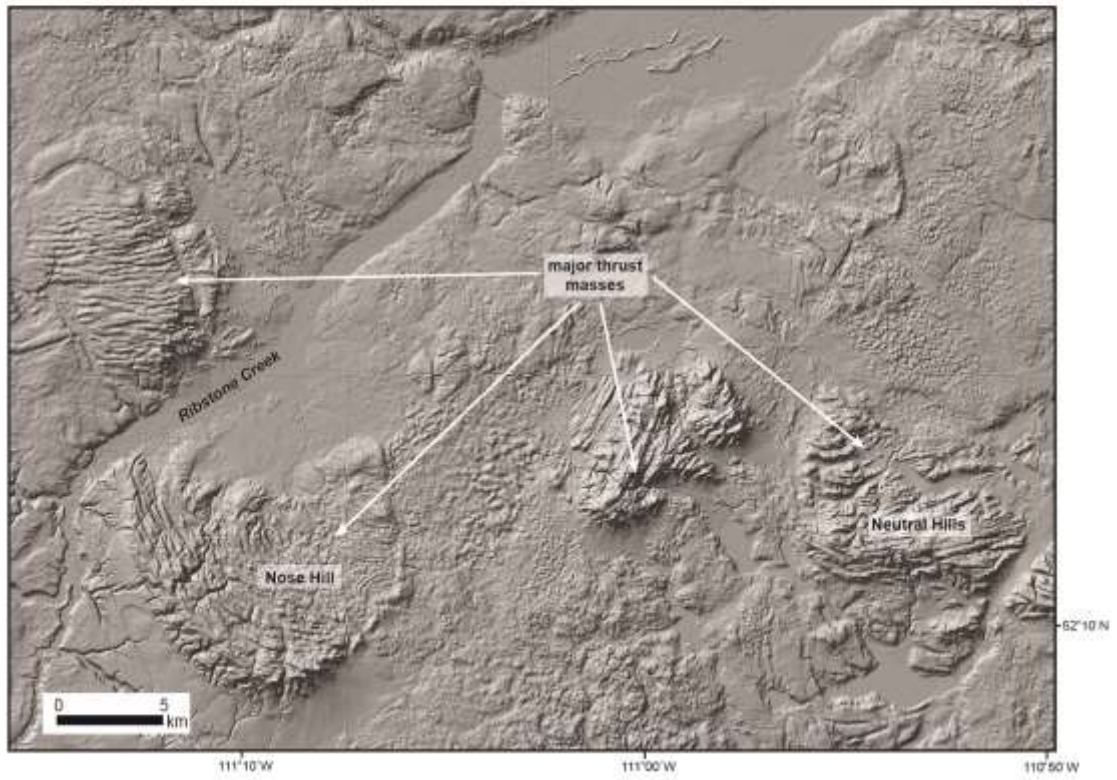
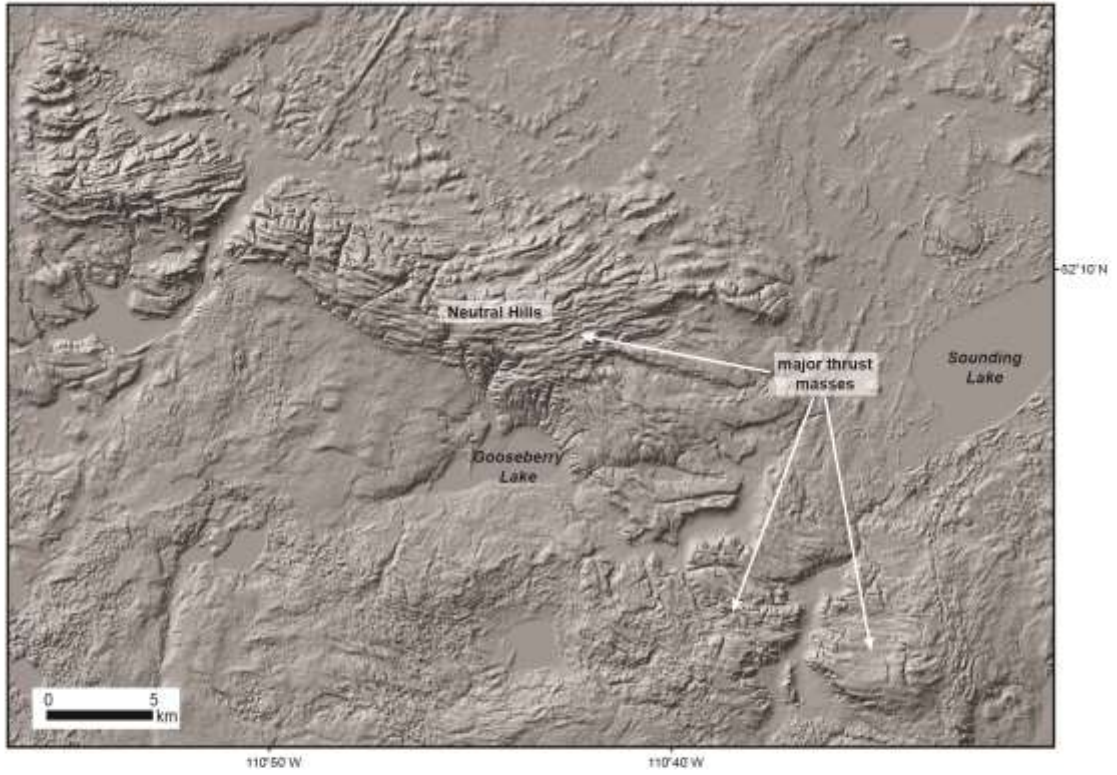
1627

1628



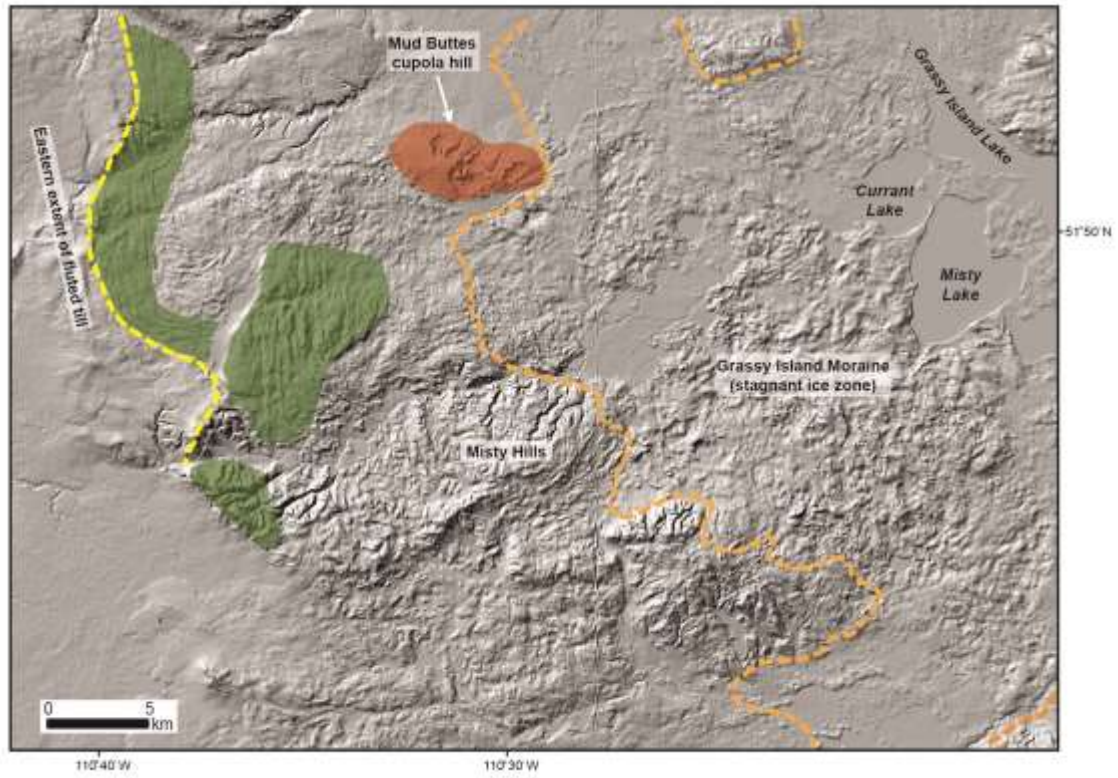
1629

1630



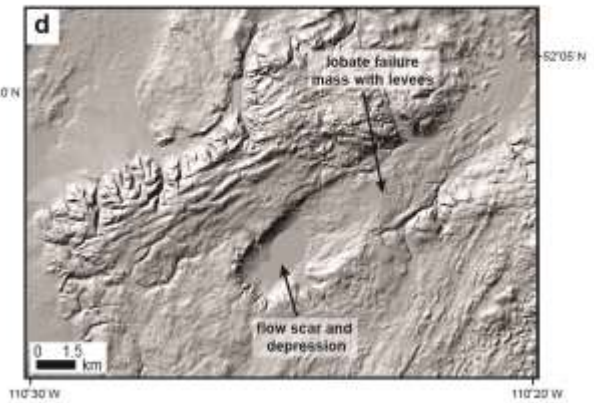
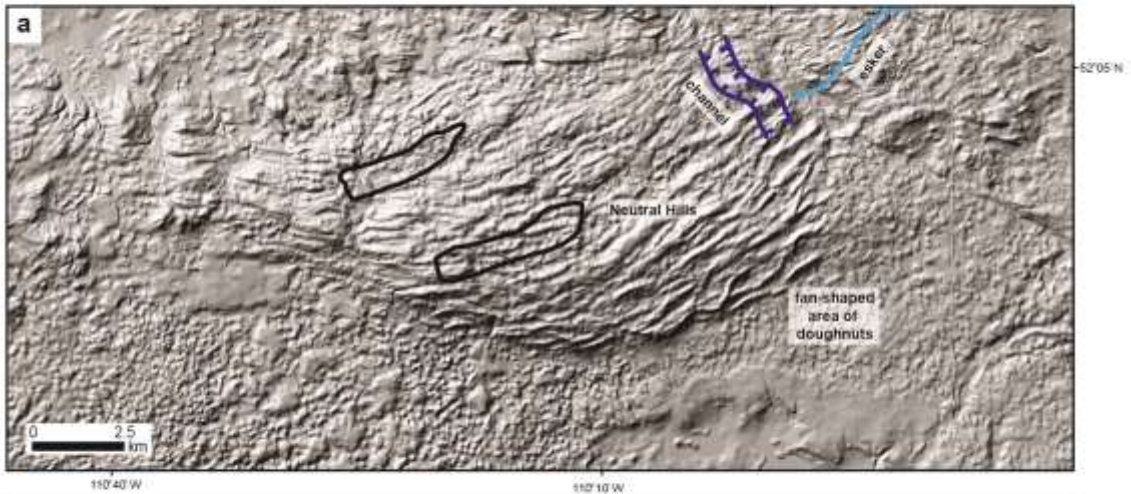
1631

1632



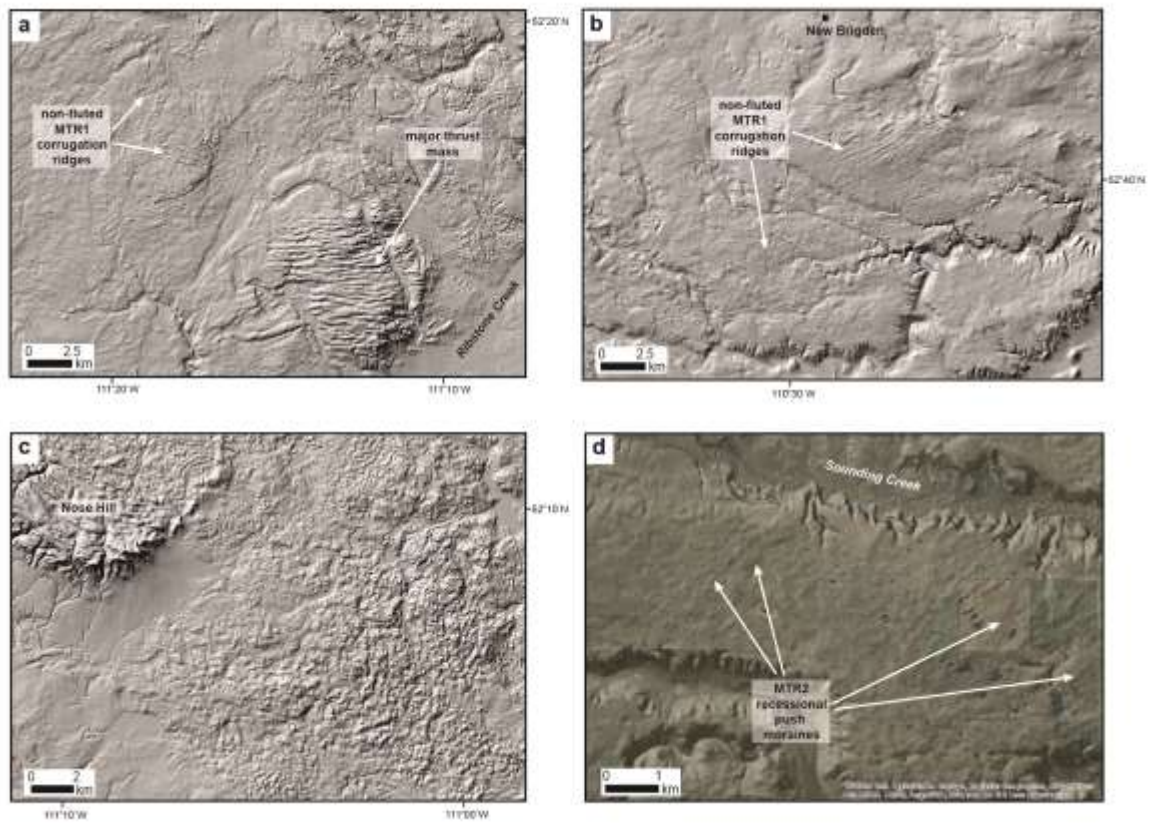
1633

1634



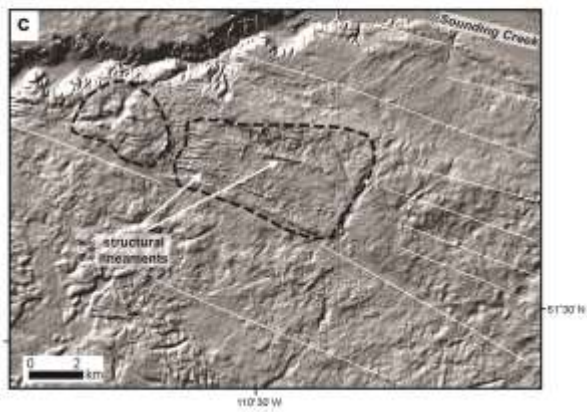
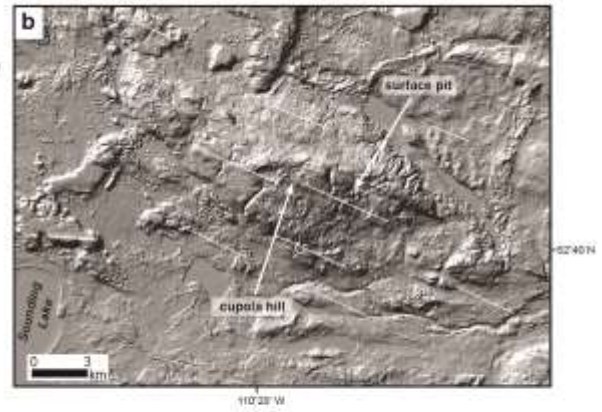
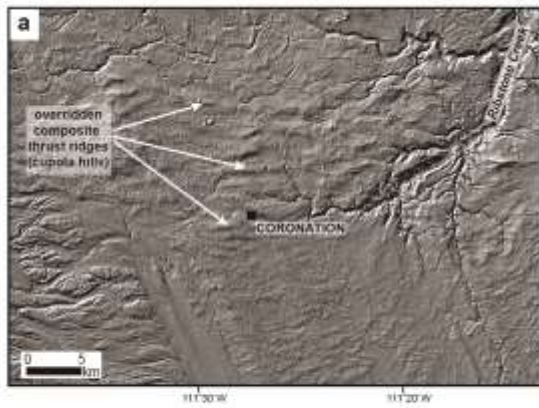
1635

1636



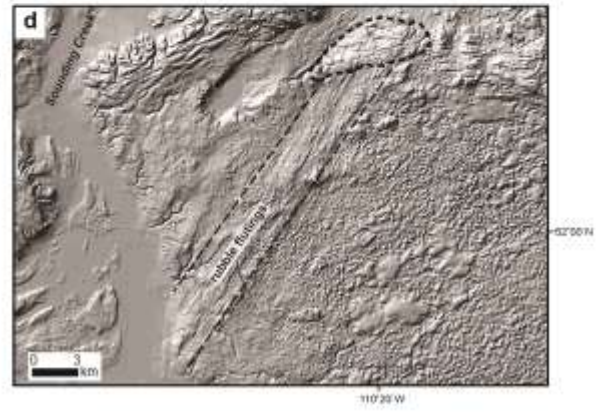
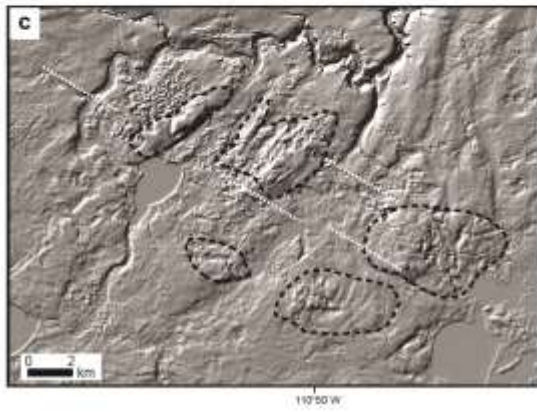
1637

1638



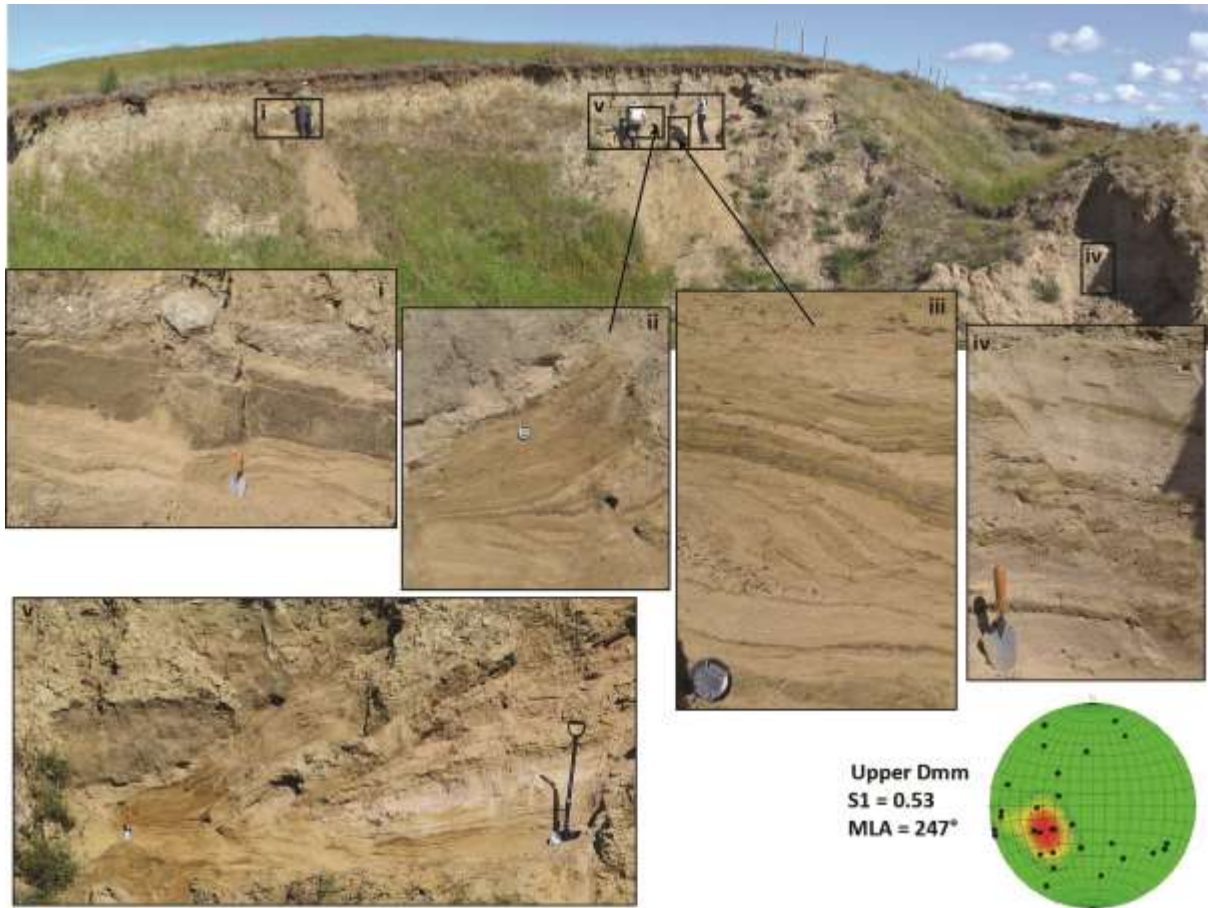
1639

1640



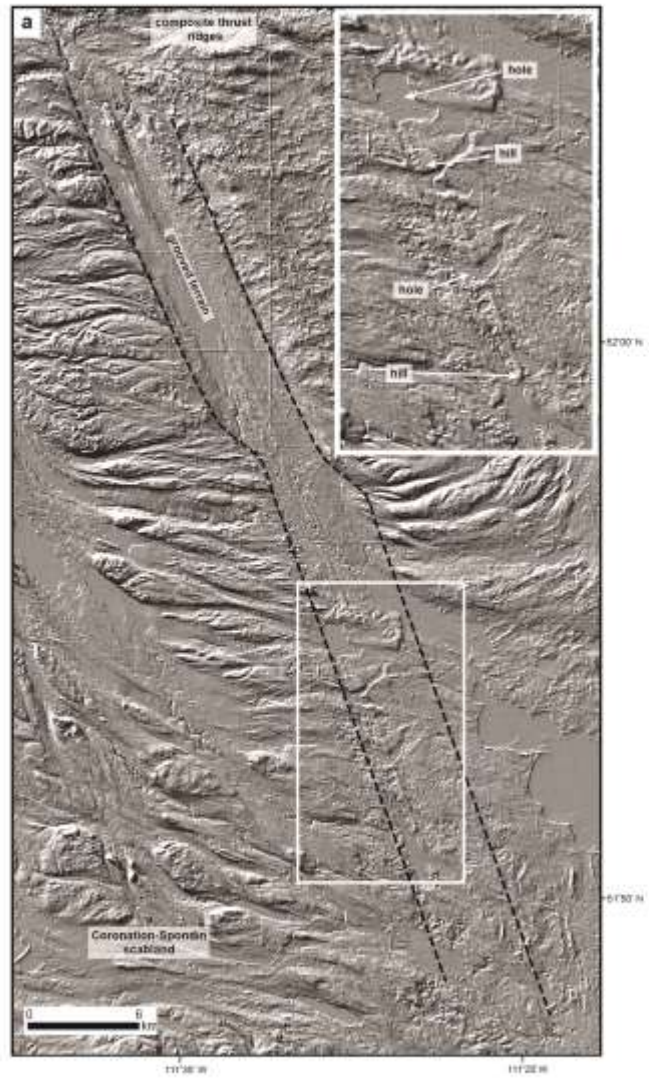
1641

1642



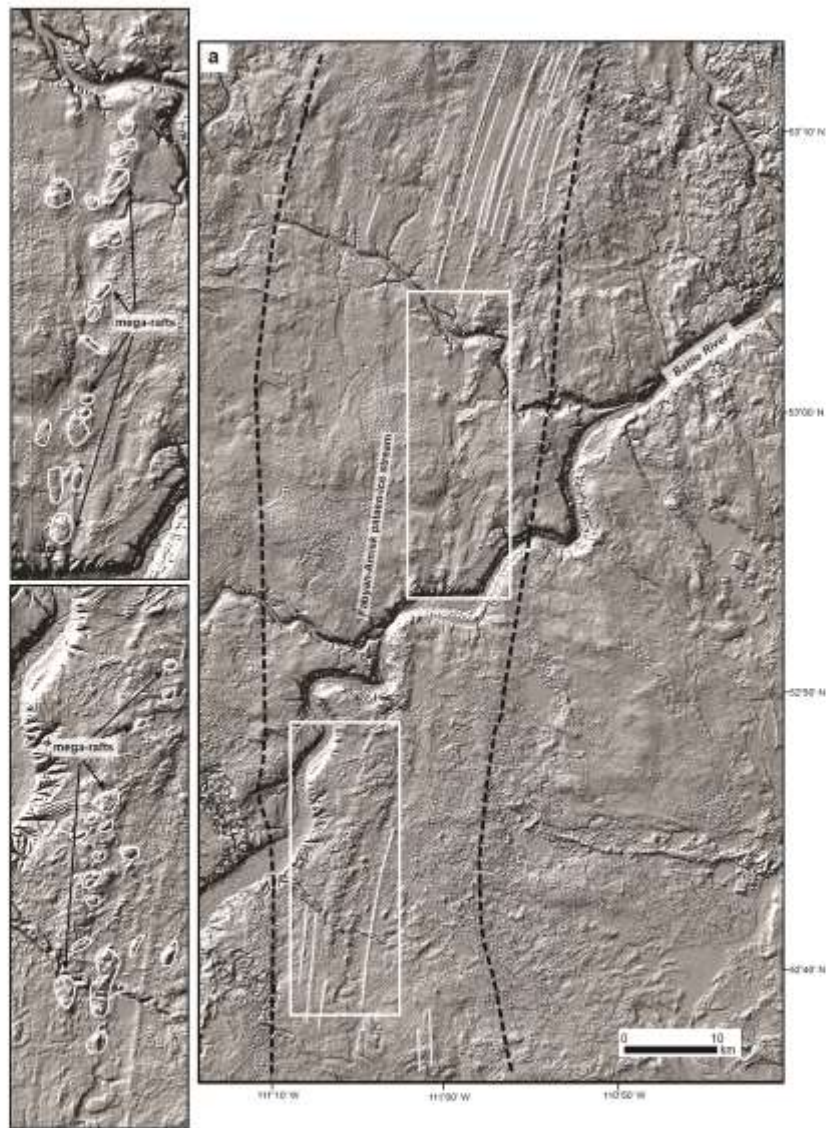
1643

1644



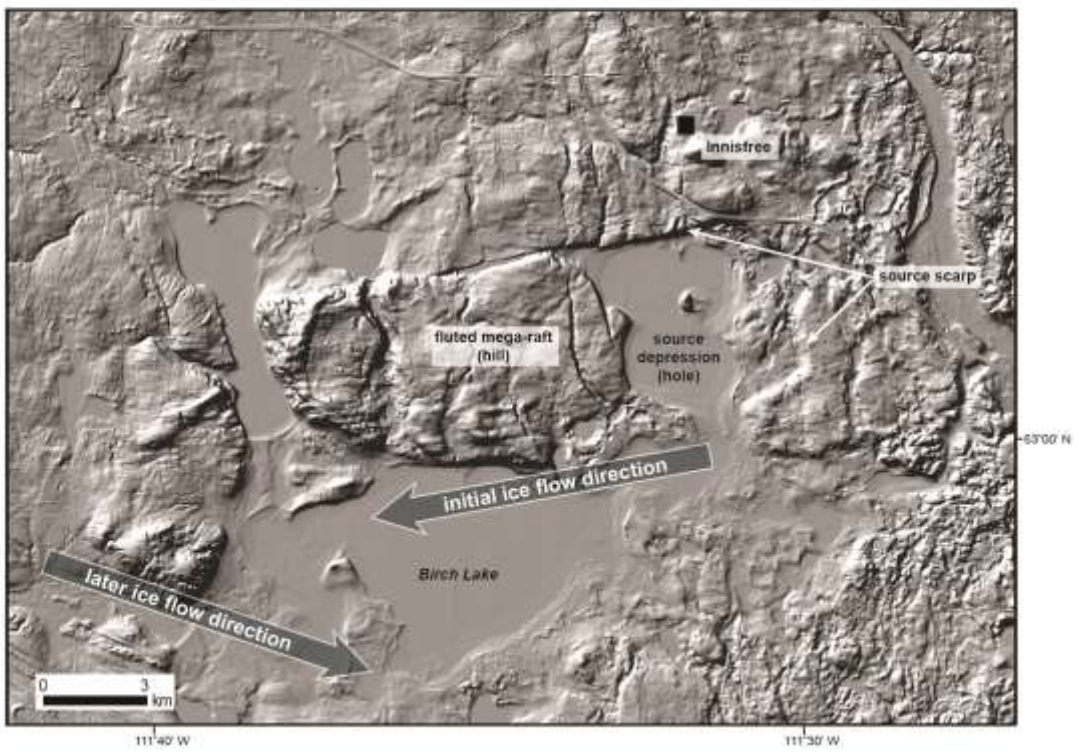
1645

1646



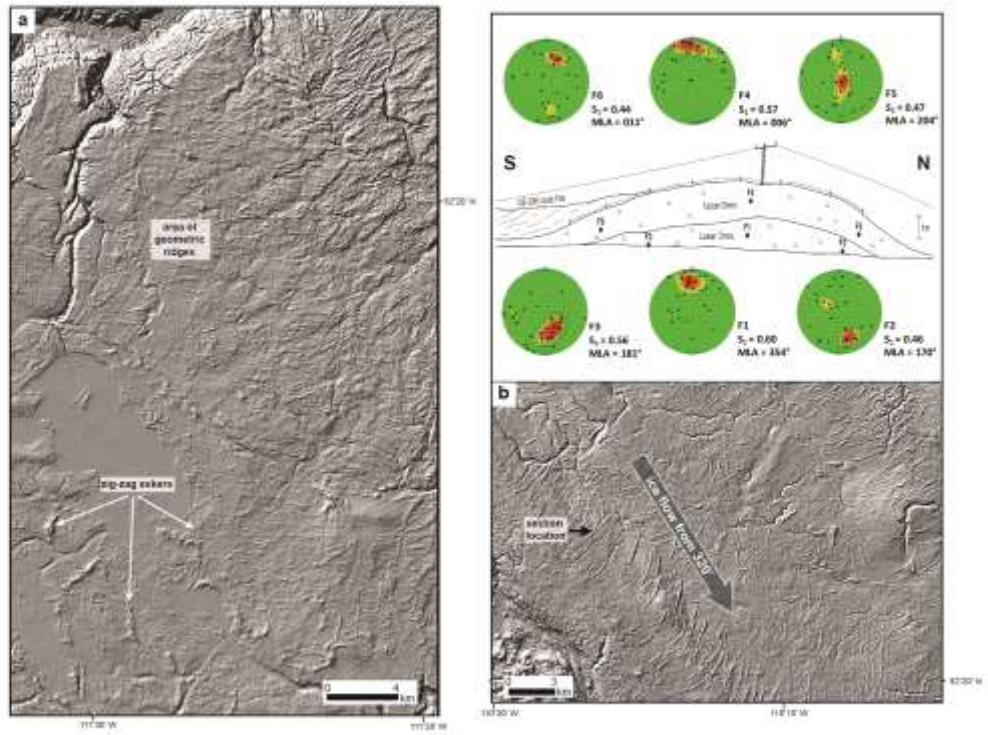
1647

1648



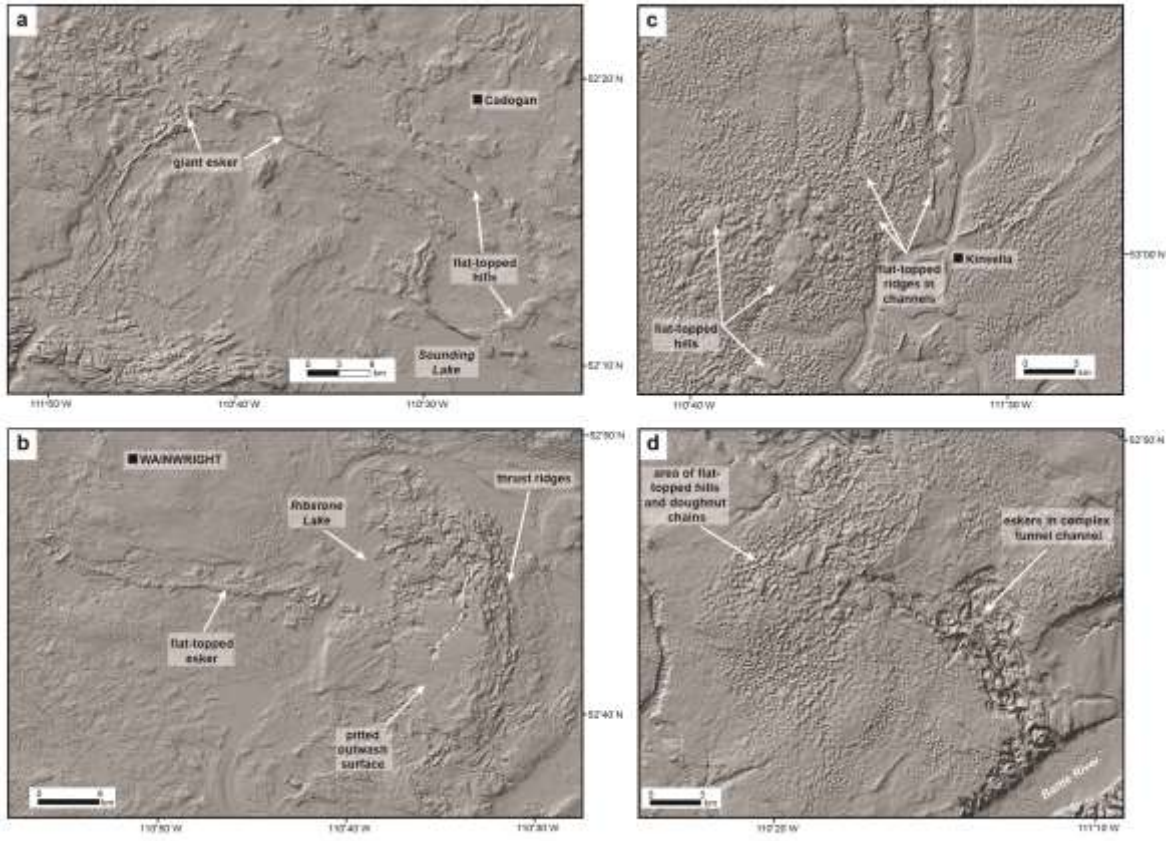
1649

1650



1651

1652



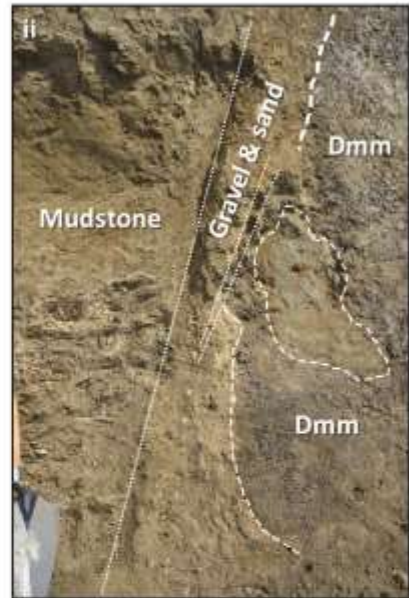
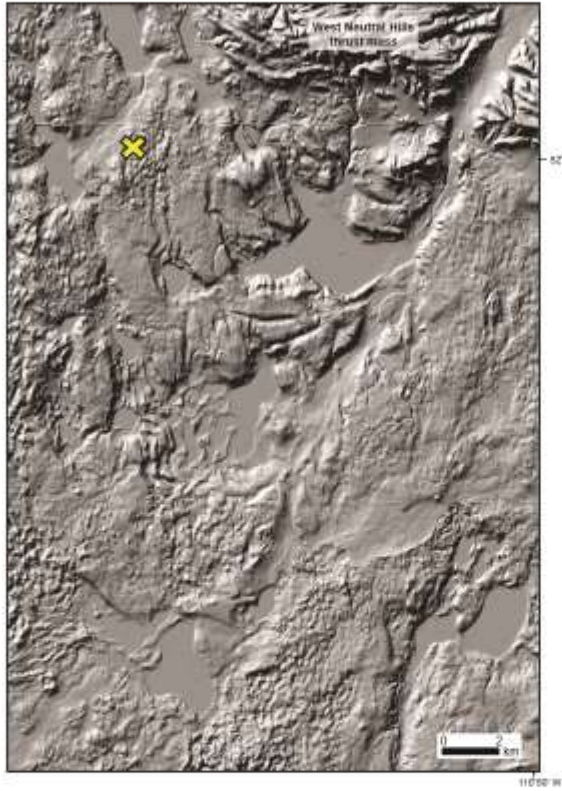
1653

1654



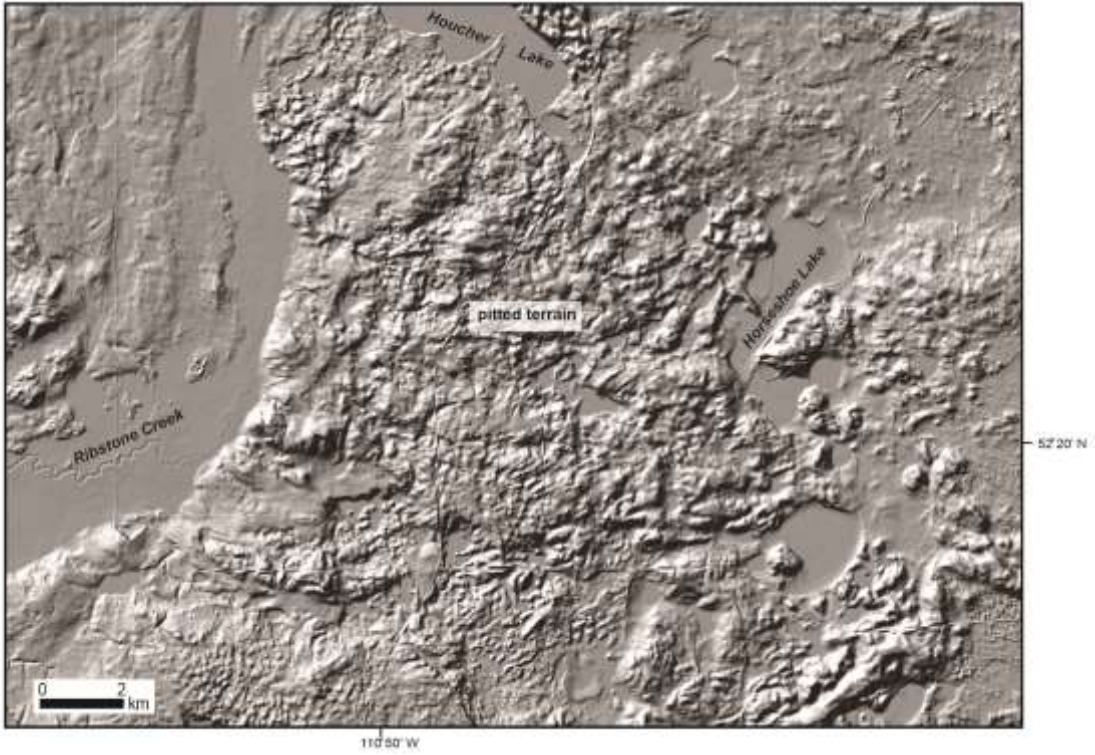
1655

1656



1657

1658

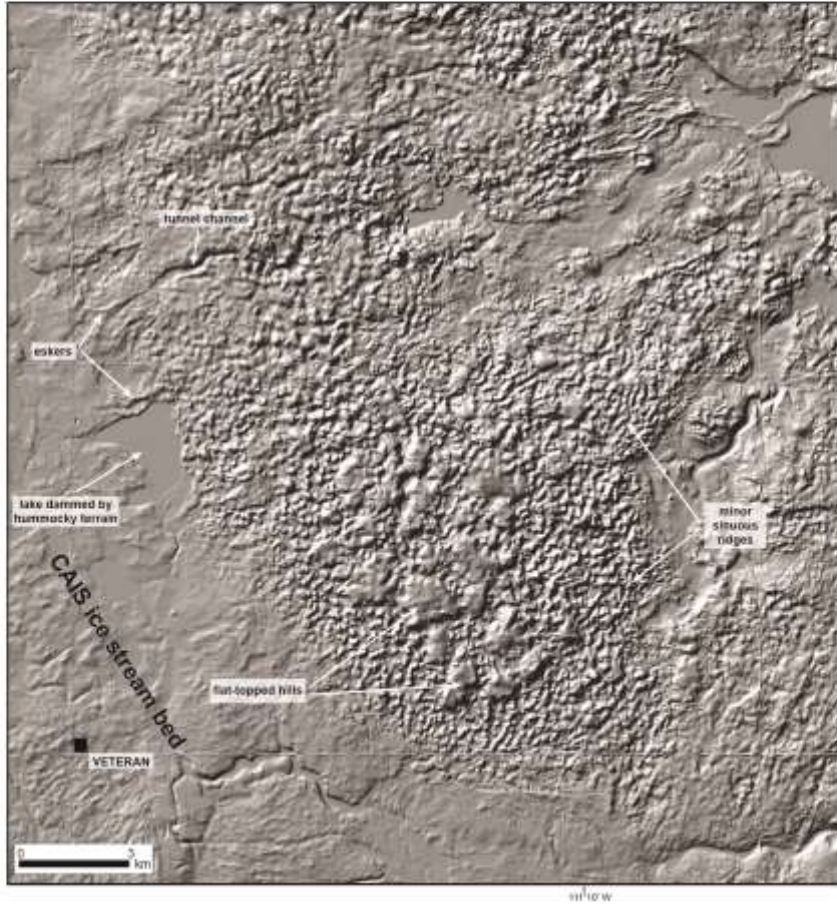


1659



1660

1661



1662

1663

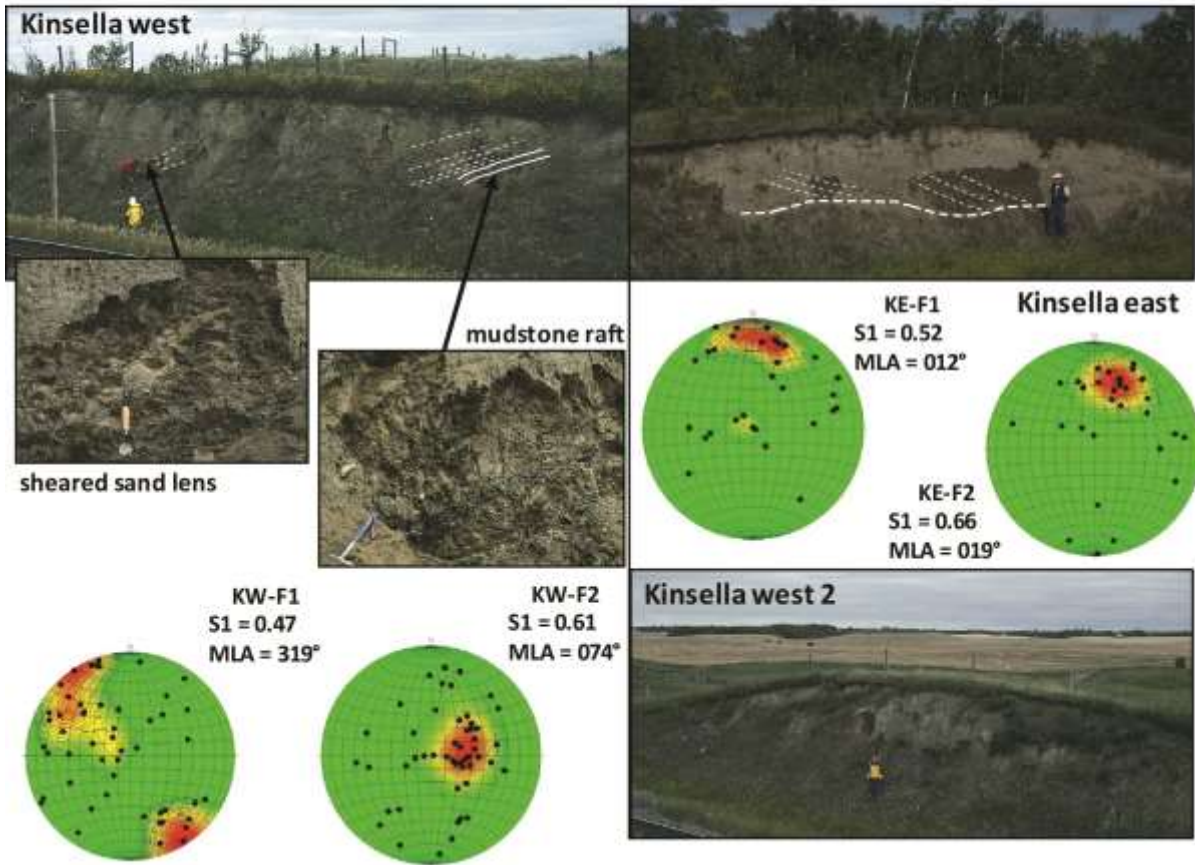
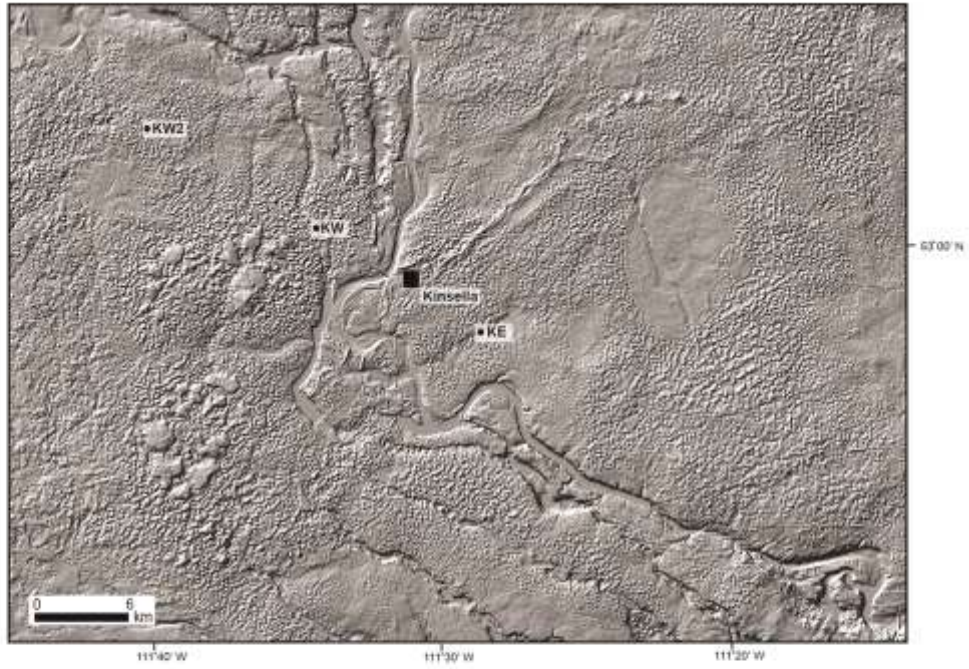


1664



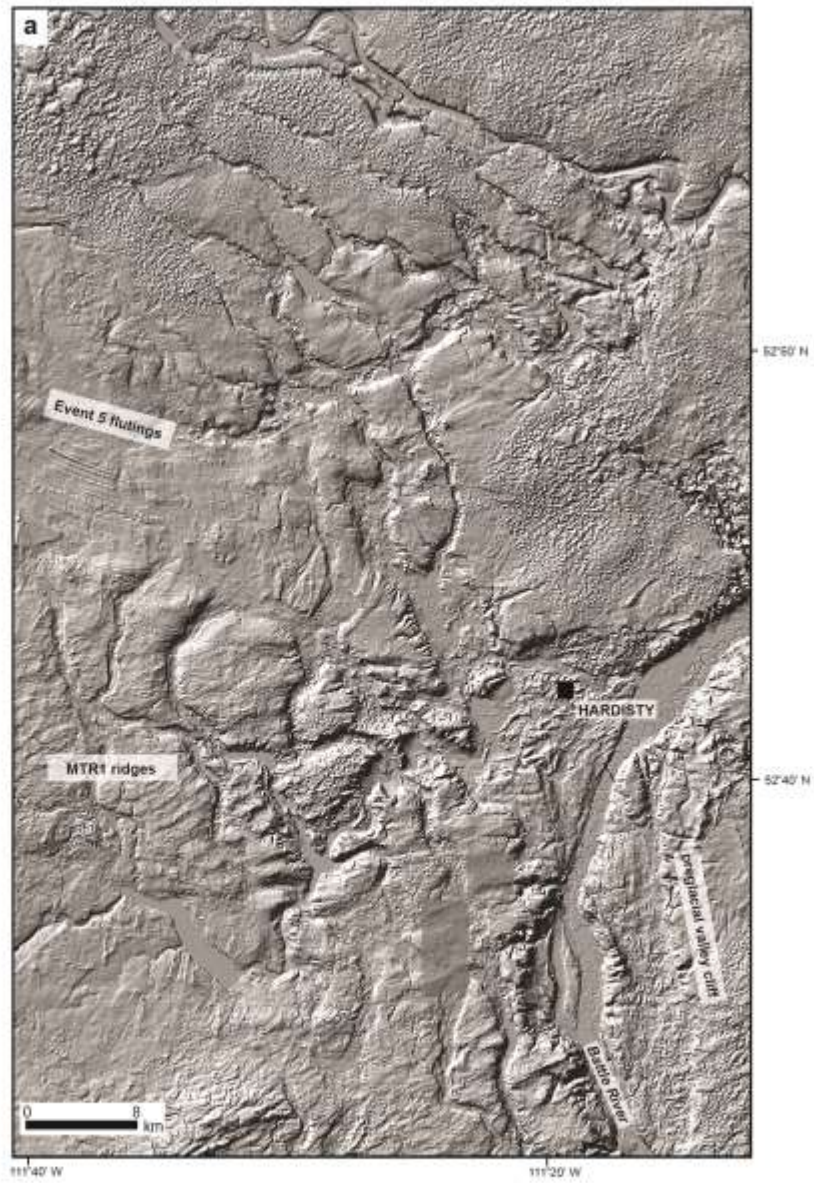
1665

1666



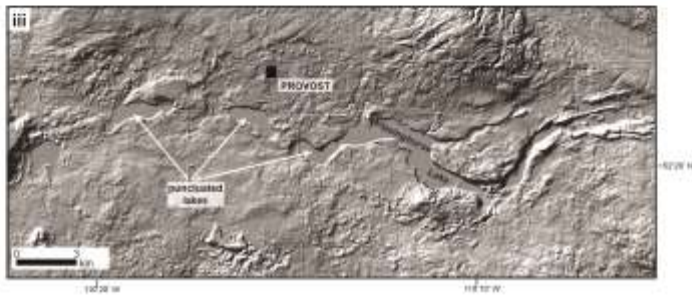
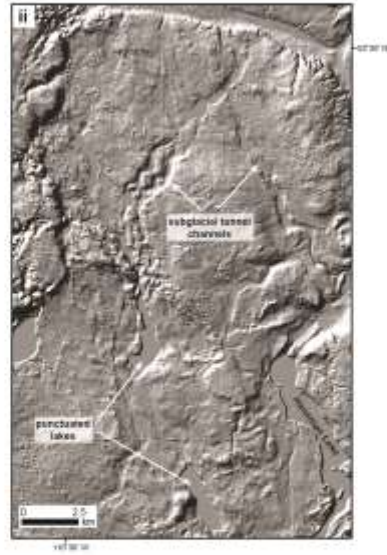
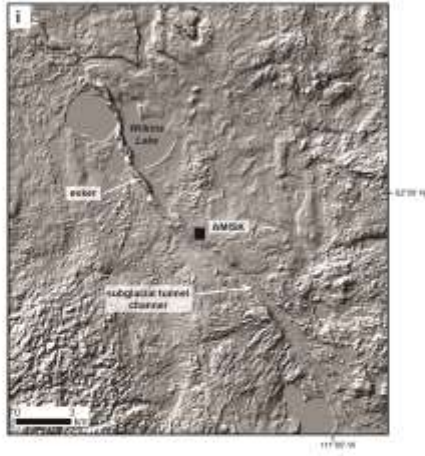
1667

1668



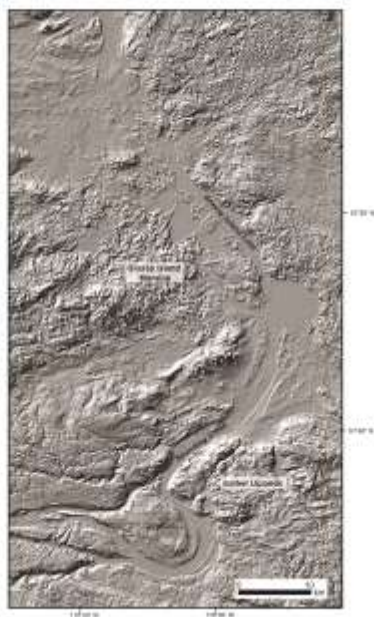
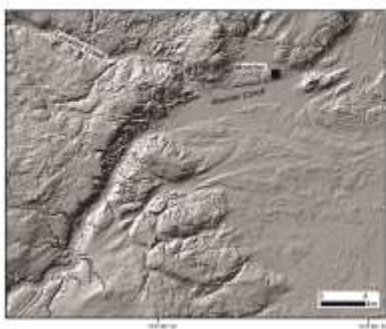
1669

1670



1671

1672



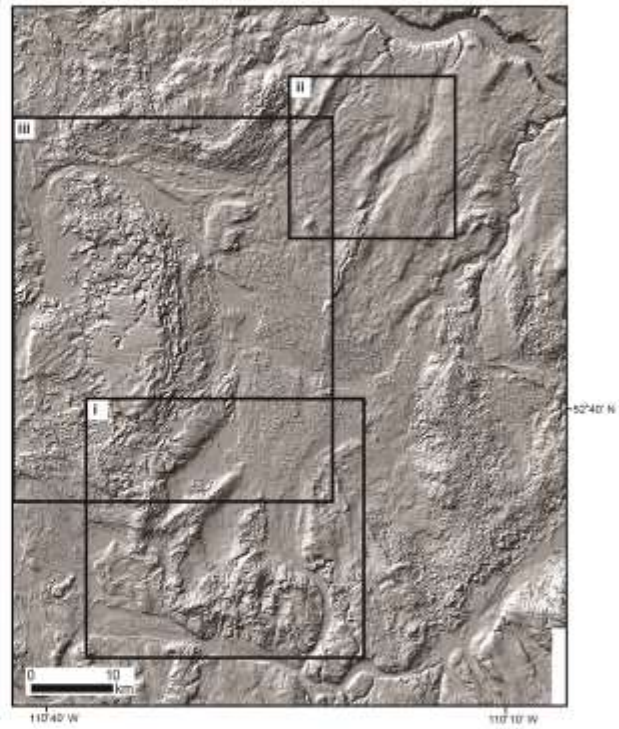
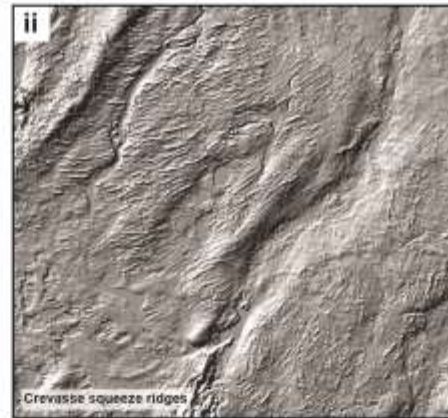
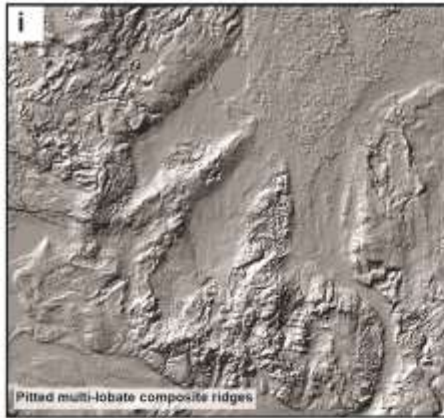
1673

1674



1677

1678



1679

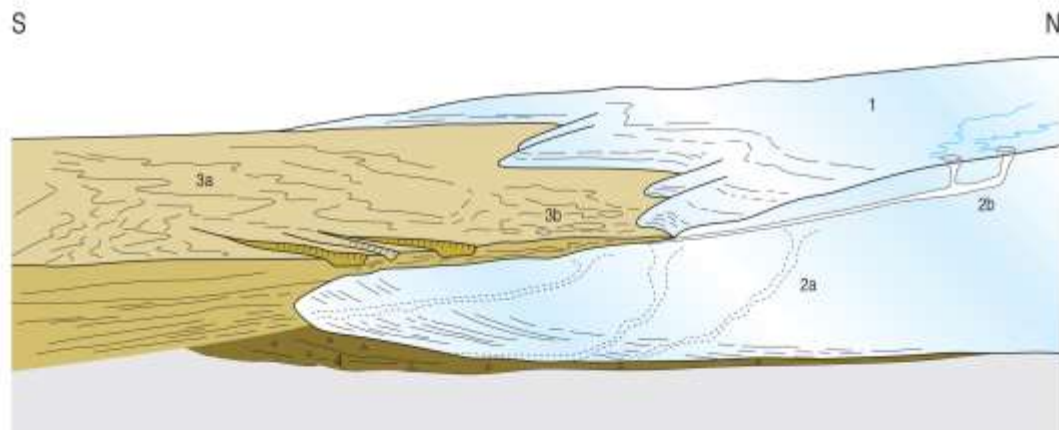
1680



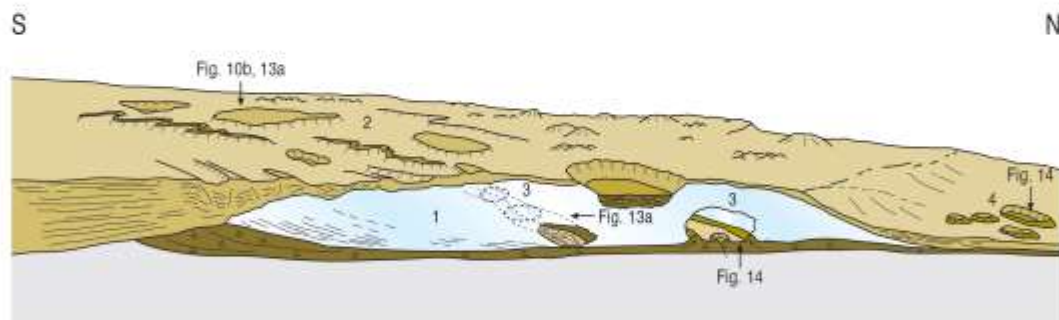
1681

1682

PHASE A - ice sheet marginal recession



PHASE B - localised ice stagnation (Fig. 6, 13, 16c)



PHASE C - ice lake surge (Fig.5 19a)

